

Polyhydroxyalkanoate-based thin films: characterization and optimization for calcium phosphate crystallization

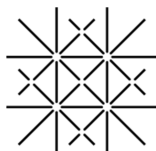
Inauguraldissertation

zur

Erlangung der Würde eines Doktors der Philosophie
vorgelegt der
Philosophische-Naturwissenschaftlichen Fakultät
der Universität Basel

von

Agnieszka Maria Jagoda
aus Tychy, Polen



UNI
BASEL

Ruda Śląska, 2013

Original document stored on the publication server of the University of Basel

edoc.unibas.ch



This work is licenced under the agreement „Attribution Non-Commercial No Derivatives

– 2.5 Switzerland“. The complete text may be viewed here:

creativecommons.org/licenses/by-nc-nd/2.5/ch/deed.en



Attribution-Noncommercial-No Derivative Works 2.5 Switzerland

You are free:



to Share — to copy, distribute and transmit the work

Under the following conditions:



Attribution. You must attribute the work in the manner specified by the author or licensor (but not in any way that suggests that they endorse you or your use of the work).



Noncommercial. You may not use this work for commercial purposes.



No Derivative Works. You may not alter, transform, or build upon this work.

- For any reuse or distribution, you must make clear to others the license terms of this work. The best way to do this is with a link to this web page.
- Any of the above conditions can be waived if you get permission from the copyright holder.
- Nothing in this license impairs or restricts the author's moral rights.

Your fair dealing and other rights are in no way affected by the above.

This is a human-readable summary of the Legal Code (the full license) available in German:
<http://creativecommons.org/licenses/by-nc-nd/2.5/ch/legalcode.de>

Disclaimer:

The Commons Deed is not a license. It is simply a handy reference for understanding the Legal Code (the full license) — it is a human-readable expression of some of its key terms. Think of it as the user-friendly interface to the Legal Code beneath. This Deed itself has no legal value, and its contents do not appear in the actual license. Creative Commons is not a law firm and does not provide legal services. Distributing of, displaying of, or linking to this Commons Deed does not create an attorney-client relationship.

Genehmigt von der Philosophisch-Naturwissenschaftlichen Fakultät der Universität

Basel auf Antrag von

Prof. Dr. Wolfgang Meier

und

Prof. Dr. Andreas Taubert

Basel, den 13. November 2012

Prof. Dr. Jörg Schibler

Dekan

TABLE OF CONTENTS

| | |
|--|-----------|
| ACKNOWLEDGEMENTS | 2 |
| ABSTRACT..... | 4 |
| ABBREVIATIONS AND SYMBOLS..... | 7 |
| 1. INTRODUCTION | 9 |
| 1.1. Biomaterials | 10 |
| 1.2. Polyhydroxyalkanoates (PHAs)..... | 15 |
| 1.2.1. General overview | 15 |
| 1.2.2. PHA-based materials | 17 |
| 1.2.3. Langmuir monolayers and interfacial behavior of PHAs | 19 |
| 1.3. Calcium phosphate and template-directed crystallization | 23 |
| 1.4. References..... | 28 |
| 2. MOTIVATION AND CONCEPT..... | 34 |
| 3. RESULTS AND DISCUSSION..... | 36 |
| 3.1. PHUE monolayers | 37 |
| 3.2. PHUE-lipid mixed films | 47 |
| 3.3. PHUE and PHUE-lipid film mineralization | 63 |
| 4. CONCLUSIONS AND OUTLOOK | 79 |
| 5. APPENDIX | 82 |
| 5.1. Polymer molar mass optimization | 82 |
| 5.1.1. One-component films | 82 |
| 5.1.2. PHUE3k-DOPS mixed films | 84 |
| 5.1.3. Mineralization of PHUE3k-DOPS films | 85 |
| 5.2. Langmuir-Blodgett transfers..... | 87 |
| CURRICULUM VITAE | 90 |

Acknowledgements

First of all, I want to thank my PhD supervisor *Dr. Katarzyna Kita-Tokarczyk*. Even though we communicated mostly via emails or Skype, she is the one from whom I learned the most during my PhD study. She gave me not only useful scientific advice, but also a trust and freedom in performing the research. I am very thankful for her time and patience in correcting my manuscripts, all the good words, which motivated me to go on, and help also with non-research related issues.

I thank *Prof. Dr. Wolfgang Meier* for the opportunity to perform my PhD research in his laboratories, in an atmosphere of freedom and trust. I thank *Prof. Dr. Manfred Zinn* and *Dr. Roland Hany* for discussions and suggestions related to the investigated polymers. *Empa St.Gallen* is acknowledged for providing the polymers. The *Swiss National Science Foundation* is gratefully acknowledged for the financial support.

Also, I thank *Prof. Dr. Andreas Taubert* for his interest in my research and co-refereeing my PhD thesis. *Prof. Dr. Edwin Constable* is acknowledged for being a chairman during my PhD exam.

I also thank *Prof. Dr. Patrycja Dynarowicz-Łątka* and *Dr. Katarzyna Hąc-Wydro*, my Master thesis supervisors, who recommended me for this PhD project.

The Center for Microscopy (ZMB), University of Basel, is acknowledged for the access to electron microscopy facilities. In particular, I thank *Gianni Morson* for his help with TEM imaging and his everlasting smile, *Eva Bieler* for her time and help with SEM/EDXS measurements, and *Vesna Olivieri* for providing me the TEM grids always in the quantities I needed.

During my PhD, I supervised five Nanoscience project students, *Michael Gerspach*, *Andreas Spielhofer*, *Benjamin Banusch*, *Stefan Winkler*, and *Simona Hübner*. I appreciate their help with the experiments.

I also thank all people from the administrative and technical staff of the University of Basel for their assistance in research and non-research related problems.

Many thanks go to all my office mates (especially, *Dr. Serena Belegriou*, *Dr. Nico Bruns*, *Justyna Kowal*, *Fabian Ite*, *Dalin Wu*, *Dr. Marzena Kocik*, *Satrajit Chakrabarty*, *Martin Rother*, *Dr. Adrian Dinu*, *Dr. Anja Car*, *Dr. Thomas Schuster*, *Christoph Edlinger*) for a great atmosphere in the offices we shared.

During my PhD time I made many friendships, which are lasting despite of long distances.

I thank in particular *Dr. Marek Orzechowski*- for helping me to accommodate in Basel, *Dr. Sindhu Menon*- for discussions and listening about life/research problems, *Dr. Marta Mumot*- for her support, whenever needed, *Dr. Jarosław Szymczak* and *Aneliia Shchyrba* for our “coffee times” and lots of fun we had together.

I thank my Mother- *Maria*, brothers- *Dawid* and *Robert*, and grandparents- *Genowefa* and *Jan*, for accepting my life choices, believing in me, and giving me the strength in everything I do.

A big thank you goes to my boyfriend *Krzysztof Tajchert*, who encouraged me when I had moments of doubts, for his patience, tolerance, enjoying my successes with me and many more...

Abstract

Novel polymer-inorganic composites attract scientific and commercial attention as potential biomaterials for orthopedic applications, due to the fact that currently used materials have still many drawbacks, e.g. problems with cell attachment or degradation products toxicity. Furthermore, scientific research progressively focuses on mimicking the structure and function of the body's organs. For example, bone is a natural composite of an organic matrix (collagen) and inorganic crystals (calcium phosphate). Such a combination of two components, which alone have disadvantages like poor load bearing of collagen and brittleness of calcium phosphate, enables bone to accept high load and fulfill its functions in the body. Thus, by combining components with complementary properties, materials with improved or novel properties could be produced. In tissue engineering, such materials are then processed into three-dimensional (3D) structural supports, scaffolds for cells, which can be seeded either before implantation to the patient or the patient's body may serve as a 'bioreactor'.

Most of the currently used scaffolds have been prepared via top-down strategies, using for example bulk materials with additives or by blending inorganic and organic components. Since any foreign material introduced to the body is recognized by its surface, tissue engineering research turns towards controlled assembly of inorganic components at the nanoscale, directed by molecularly organized polymer scaffolds, by a so-called bottom-up approach. One advantage of this strategy is the control and tuning of the scaffold's surface properties, which enhance the interfacial compatibility between the implant and cells, and consequently may decrease the probability of the implant rejection.

Among others, polyhydroxyalkanoates (PHAs), natural microbial polyesters, are very interesting candidates for biomedical applications, due to their biocompatibility and

biodegradability. However, PHA-based materials reported so far have been prepared using top-down strategies, without detailed analysis and control of the polymer surface properties.

The aim of this thesis was to prepare PHA-based composite materials with potential future applications in orthopedic applications, using the bottom-up approach and to understand i) the scaffold formation, ii) its interactions with most abundant cell membrane components (phospholipids), and iii) templating mechanisms for calcium phosphate crystallization. Poly([R]-3-hydroxy-10-undecenoate) (PHUE), a representative of medium-chain-length PHAs, was investigated. Due to its elastomeric properties the polymer can form a flexible matrix for calcium phosphate crystals, similarly to collagen in bone.

PHUE scaffolds were prepared using the Langmuir monolayer technique, which enabled a control over the polymer molecular organization, and produced stable two-dimensional (2D) films on the air-water interface. Interactions of the polymer with biologically important molecules, cell membrane lipids, in mixed Langmuir films were evaluated – this approach is a simple method to model the behavior of living cells in the presence of a synthetic (implant) material. The interactions were highly reliant on the lipid head group size and orientation at the free water surface, and are interpreted considering intra- and intermolecular forces between lipid and polymer molecules.

The organic-inorganic composite materials were obtained by using one-component (polymer or lipid) and mixed (polymer-lipid) monomolecular films as templates influencing the growth of calcium phosphate. Crystal size and size distribution, morphology, and composition depend on the nature of organic film-forming molecules and interactions between them. Organic-inorganic composite materials with various properties were achieved by using different lipids and lipid/polymer ratios in the films,

and the crystal growth conditions (mineralization time, ions concentration). Briefly, good control of calcium phosphate crystallization was achieved with films containing negatively charged lipid and higher excess of the lipid (for anionic and zwitterionic lipids).

This thesis presents the first thorough analysis of PHAs surface properties, which may be helpful to better understand already used PHA-based biomaterials. The study of PHA interactions with lipids provides additional insights for development of e.g. polymer-lipid coating materials. Last, but not least, calcium phosphate crystallization beneath PHAs and its mixed films with lipids may inspire new developments in bone tissue engineering using naturally synthesized polymers. In the broader context, the outcome of this work may have impact not only on PHA-based materials, but also on the understanding of other polyester-based biomaterials. Furthermore, the results may be also of interest for applications where properties of thin, molecularly organized films are crucial for the product design and performance, such as sensors.

Abbreviations and symbols

| | |
|----------|--|
| 2D | two-dimensional |
| 3D | three-dimensional |
| ACP | amorphous calcium phosphate |
| AFM | atomic force microscopy |
| BAM | Brewster angle microscopy |
| DOPC | 1,2-dioleoyl- <i>sn</i> -glycero-3-phosphocholine |
| DOPE | 1,2-dioleoyl- <i>sn</i> -glycero-3-phosphoethanolamine |
| DOPS | 1,2-dioleoyl- <i>sn</i> -glycero-3-phospho-L-serine |
| DPPE | 1,2-dipalmitoyl- <i>sn</i> -glycero-3-phosphocholine |
| EDX | energy dispersive X-ray spectroscopy |
| FDA | Food and Drug Administration |
| HAP | hydroxyapatite |
| HEPES | 4-(2-hydroxyethyl)piperazine-1-ethanesulfonic acid |
| LB | Langmuir-Blodgett transfer/ film |
| lcl-PHAs | long-chain-length polyhydroxyalkanoates |
| LE | liquid expanded |
| LS | Langmuir-Schaefer transfer/ film |
| mcl-PHAs | medium-chain-length polyhydroxyalkanoates |
| MVs | matrix vesicles |
| P(3HB) | poly([R]-3-hydroxybutyrate) |
| P(4HB) | poly([R]-4-hydroxybutyrate) |
| P(3HH) | poly([R]-3-hydroxyhexanoate) |
| P(3HN) | poly([R]-3-hydroxynonanoate) |
| P(3HO) | poly([R]-3-hydroxyoctanoate) |

| | |
|------------------|--|
| P(3HV) | poly([R]-3-hydroxyvalerate) |
| PBS | phosphate buffer saline |
| PC | phosphatidylcholine |
| PCL | poly(caprolactone) |
| PDI | polydispersity index |
| PE | phosphatidylethanolamine |
| PEG | poly(ethylene glycol) |
| PGA | poly(glycolic acid) |
| PHA(s) | polyhydroxyalkanoate(s) |
| PHUE | poly([R]-3-hydroxy-10-undecenoate) |
| PLA | poly(lactic acid) |
| PLLA | poly(L-lactide) |
| PMOXA-PDMS-PMOXA | poly(2-methyloxazoline)-block-poly(dimethylsiloxane)- block-poly(2-methyloxazoline) |
| PS | phosphatidylserine |
| RGD | cell adhesive ligand: arginine-glycine-aspartic acid |
| SAM | self-assembled monolayer |
| scl-PHAs | short-chain-length polyhydroxyalkanoates |
| SEM | scanning electron microscopy |
| TE | tissue engineering |
| TEM | transmission electron microscopy |
| TR | transfer ratio |
| UV | ultraviolet |

1. Introduction

Tissue engineering (TE) is a field which “aims to regenerate damaged tissues, instead of replacing them, by developing biological substitutes that restore, maintain or improve tissue function”.^[1] The biological substitutes are obtained by combining cells with a scaffold, which serves as a 3D template for the tissue formation or regeneration. Scaffolds may be prepared by numerous fabrication techniques using a variety of biomaterials, as briefly described in section 1.1. For many years, TE research was focused on studying and fabricating one-component materials, mostly metal alloys, polymers, or ceramics. However, none of these alone can fully serve the tissue replacement purpose, thus nowadays TE focuses more on complex materials. Such composite materials are of particular interest for the formation of structural tissues like bone, which is a complex material of organic matrix- collagen, responsible for the bone ductility and toughness, and inorganic- calcium phosphate in the form of hydroxyapatite (HAP), providing high mechanical stiffness.^[2] A similar type of a combination of a polymer-based matrix with an inorganic is applied in this thesis to generate novel composite materials, using a biodegradable polymer from the group of polyhydroxyalkanoates (PHAs, section 1.2) and its mixtures with phospholipids to template the growth of calcium phosphate (section 1.3). Such composite materials could be further used as implant coatings in orthopedic applications.

1.1. Biomaterials

A biomaterial, according to the European Society for Biomaterials, is defined as a “material intended to interface with biological systems to evaluate, treat, augment or replace any tissue, organ or function of the body”.^[1] The scaffold needs to provide a microenvironment for cells, which will enable their attachment, proliferation, and differentiation.^[3-4] To achieve these functions, scaffolds made from biomaterials, regardless of the tissue type, should fulfill many requirements, the most important ones are briefly described below.

Biodegradability. TE aims for the scaffolds to be replaced over time by the body’s own newly regenerated tissue. For that reason, scaffolds have to be degradable, and products of that biodegradation should be non-toxic and able to leave the body without harming other tissues. Ideally, the rate of scaffold degradation and a new tissue formation should be equal.^[3]

Biocompatibility (interfacial compatibility) of any material depends on the scaffold shape, porosity, surface properties, degradation products and the environment where it is incorporated.^[5] Most mammalian cells proliferate only when they are attached to a surface, thus the scaffold’s surface should promote their adhesion and further normal growth and function.^[6] This can be induced by optimization of material’s surface chemistry (charge, composition) and physics (topography, roughness, hydrophilicity/hydrophobicity, surface energy),^[7-9] considering that cells favor hydrophilic surfaces^[10-11] with micro-level surface topography.^[12] Surfaces should also induce cellular healing response: the best way to achieve this is to cover or functionalize a well-controlled scaffold surface with biological (bio-mimicking) components (e.g. cell adhesive ligands RGD, arginine-glycine-aspartic acid).^[13-14] By taking into consideration material properties, both physico-chemical and biological, one can obtain a synergy in non-

specific and specific interactions,^[15-16] resulting in the formation of surfaces 'attractive' to cells.

Biomaterial processing requires a deep understanding of molecular interactions taking place between a biomaterial and cells, and, in the case of composite materials, between cells and individual material components.^[7] However, these interactions have been rarely studied, particularly for polymeric biomaterials.^[17-19] Also, little is known about early cell-biomaterial interactions in bone, comparing for example to those in cardiovascular system and soft tissues,^[20] which constitutes challenges in the development of successful bone implant materials.

Mechanical properties. Mechanical properties are specific for a tissue and thus should also be considered in the scaffold development. In particular, it is challenging for orthopedic applications, where the scaffold has to maintain its mechanical integrity from the implantation time till the end of the restoration process.^[8]

Scaffold architecture. Scaffolds should be highly porous with interconnecting pores, which enables cells migration, tissue vascularization, and improves nutrients diffusion and removal of degradation products.^[1, 6] The pore size is a critical parameter, which varies with tissues; for example for skin materials pores should be in the range between 20 – 125 μm .^[21] Regarding the bone implant materials, there are two levels of porosity, macroporosity (pore size 100 - 500 μm)^[21-22] and microporosity (pore size < 10 μm)^[23], Figure 1. Macroporosity is intentionally introduced to materials, in order for the material to be penetrative to cells, while microporosity, helpful in distribution of body fluids, results mainly from the fabrication technique used to create macroporosity.^[24]

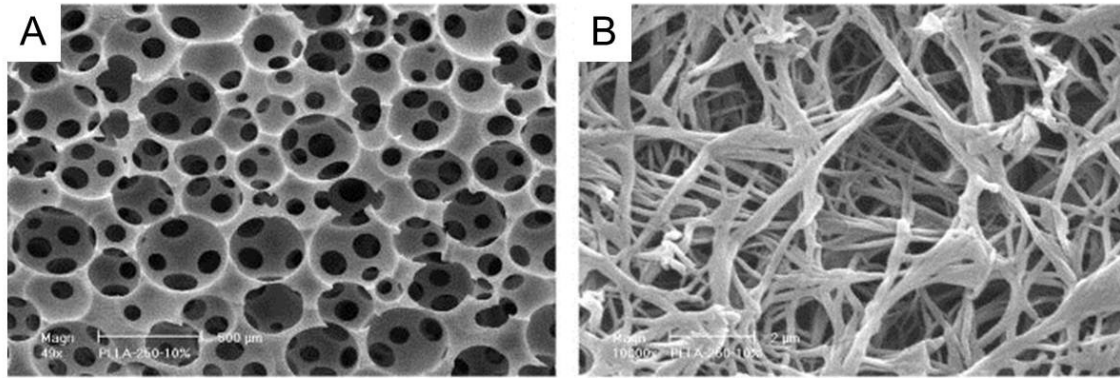


Figure 1. SEM images of macroporous (A) and nanofibrous (B) poly(L-lactid) (PLLA) 3D scaffolds at low (x50) and high (x10,000) magnifications.^[25]

A versatile method to produce 3D porous matrices of ultrafine fibers is electrospinning. Fibers may be produced from various compounds, synthetic and natural polymers, or ceramics, and with a wide range of diameters,^[4] without using organic solvents. Although, there is a large variety of fabrication methods, designing porous structures with good mechanical properties is still a major difficulty, due to the fact that the fracture toughness decreases almost linearly with porosity increase.^[26-28] For that reason, nowadays TE focusses on combining different fabrication techniques and various biomaterials. For example, Li et al. prepared electrospun nanofibers from poly(lactic-co-glycolic acid) (PLGA) and poly(caprolactone) (PCL) and then placed them at the angle, while concentrated simulated body fluid (SBF) was provided from the top on the bottom edge of the mats.^[29] Such tilted orientation of electrospun fibers mats resulted in the formation of calcium phosphate gradient (Figure 2), which gradually influenced material stiffness and activity of pre-osteoblast cells.

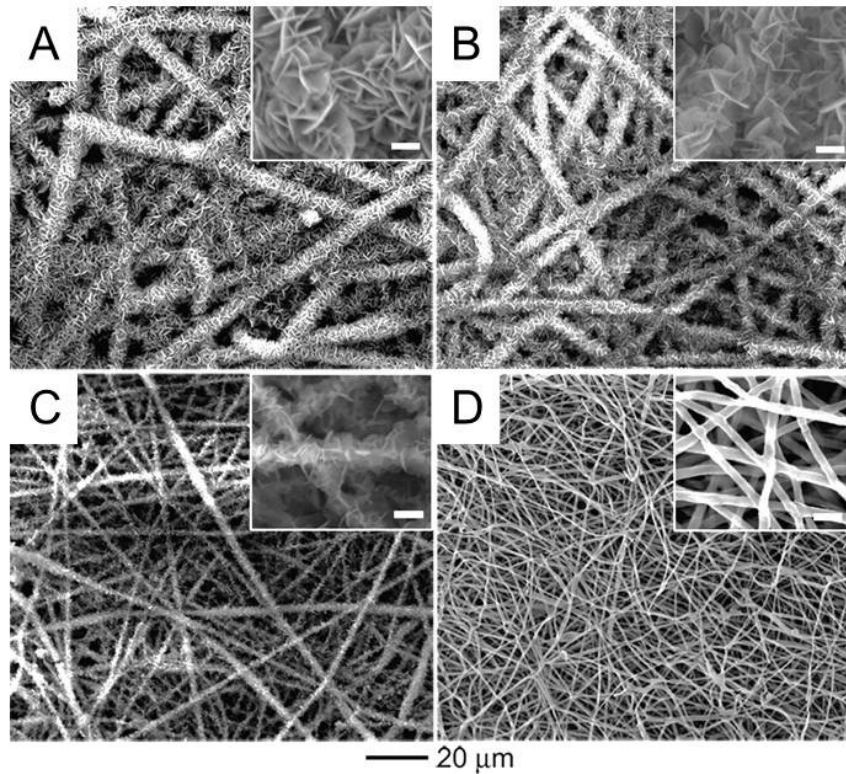


Figure 2. SEM images of calcium phosphate coatings on a plasma-treated nonwoven mat of PLGA nanofibers. The images were taken from different regions, with d (distance from the bottom edge of the substrate) corresponding to: (a) 0, (b) 6, (c) 9, and (d) 11 mm. The scale bars in the insets are 2 μm .^[29]

Additionally, biomaterials should fulfill tissue-specific requirements. A ‘good’ material for bone implants should be: (i) osteoinductive- capable of stimulating the progenitor cells to differentiate and begin the osteogenesis process, (ii) osteoconductive- to support bone growth on the implant surface, and (iii) capable of osseointegration, defined as an ‘intimate (structural and functional) contact’ between bone and implant.^[30-31]

Depending on the intended tissue application, different materials can be used, which then dictate also the choice of the scaffold preparation technique. Regarding the orthopedic applications, there are generally three groups of biomaterials used for scaffolds preparation:

- **metal alloys** (e.g. titanium, cobalt-chromium, platinum, stainless steel)^[7]- provide superior mechanical properties, but lack of biodegradation. They also often corrode and release metal ions, which can be toxic or induce allergy.
- **ceramics**- including the most frequently investigated calcium phosphate (mostly tricalcium phosphate and hydroxyapatite),^[32] the main bone component. Generally ceramics are characterized by brittleness, high mechanical stiffness, and very low elasticity, and thus it is difficult to process them into highly porous scaffolds.^[33] However, their advantage is excellent osteoconductivity and biocompatibility, due to similarity to the native bone minerals.^[1]
- **polymers** (synthetic and natural)- are more flexible than materials from previous groups, which simplifies their processing, but limits the use in load-bearing applications. The main characteristic of naturally derived polymers (e.g. collagen) is their similarity to the materials in the body and biodegradability, which is still a drawback of many synthetic equivalents.^[1, 34] On the other hand, the composition and structure of synthetic polymers (with the most used: poly(caprolactone) (PCL), poly(L-lactide) (PLLA), poly(lactic acid) (PLA), poly(glycolic acid) (PGA), and their copolymers)^[4, 35-37] can be easily tuned during the synthesis, to obtain desired material properties and degradation profiles. However, most polymers are hydrophobic and lack bioactive ligands, which make their surfaces unfavorable for cells to adhere.^[8, 38] Although they are biodegradable, there is still no clear answer regarding the toxicity of their degradation products.^[4, 39] Improvements in this area concentrate on, for example, copolymerization with more hydrophilic and/or biodegradable compounds (e.g. polysaccharides or poly(ethylene glycol)),^[40]

functionalization with cellular signaling ligands (i.a. RGD, fibronectin),^[41] or coating with calcium phosphate.^[42] These examples reflect a current trend in TE with focus on composite materials.

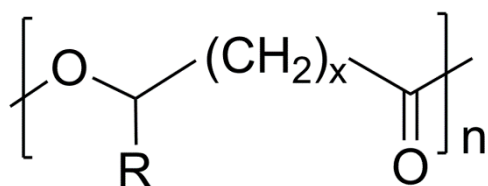
In the field of bone implants, a great number of biomaterials and scaffold fabrication methods have been already thoroughly studied, which consequently leads to many feasible material/ processing combinations. By choosing appropriate components one can obtain materials with improved or novel properties.^[3, 43] For example, polymer coatings of metal alloys were shown to increase the metal corrosion resistance,^[44] ceramic coatings (in particular, calcium phosphate) of metal alloys improved the strength of a bone bonding to the implant,^[45] while combination of polymers with ceramics offers a favorable equilibrium between the material biocompatibility and mechanical properties, and improved osteogenic properties.^[42, 46] Herein, novel composite materials based on polyhydroxyalkanoates polymers and calcium phosphate are proposed and studied. The properties of these two materials are briefly described in the subsequent sections.

1.2. Polyhydroxyalkanoates (PHAs)

1.2.1. General overview

Polyhydroxyalkanoates (PHAs) are a large class of thermoplastic polyesters, which are naturally synthesized by various microorganisms and genetically modified plants.^[47-49] Their general structure is shown in Figure 3. PHAs are stored as water-insoluble inclusions within the cytoplasm of cells, serving as energy and carbon source.^[50-52] They are biocompatible and biodegradable, and thus gained an increased

interest, especially for biomedical applications.^[53-54] PHA's are divided in three groups: (i) short-chain-length PHAs (**scl-PHAs**)- built up from monomers of C3 to C5 in length; (ii) medium-chain-length PHAs (**mcl-PHAs**)- contain monomers with 6 to 14 carbon atoms, and (iii) long-chain-length PHAs (**lcl-PHAs**)- with monomers containing more than 14 carbon atoms.^[55-56] Most frequently investigated are scl-PHAs, due to their availability and low production costs.



R = alkyl groups (C1-C13)
x = 1-3
n = 100-30000

Figure 3. General structure of polyhydroxyalkanoates.

Depending on the synthesis substrate (e.g. hydrocarbons, sugars, fatty acids, waste materials), the growth medium (type of bacteria strains or transgenic plants), and conditions used for PHAs synthesis, one can tune the monomer chain length to obtain tailor-made polymers.^[57-58] The polymer size in turn influences their degradation profile^[6] and physicochemical properties.^[59]

Mcl-PHAs are elastomers, with low crystallinity and tensile strength, but high elongation to break.^[5] During the polymer biosynthesis, fatty acids (substrates) degrade with removal of a C2 unit in each cycle in the form of acetyl-CoA, in the so-called β -oxidation cycle.^[49] For that reason, all mcl-PHAs are copolymers of monomers with two carbon atoms less than the carbon source in the bioreactor.^[60] In particular, poly([R]-3-hydroxyundecenoate) (PHUE), which was used in this thesis, was obtained by feeding

bacteria with 10-undecenoic acid (C11), and contains randomly distributed [R]-3-hydroxy-6-heptenoate (C7), [R]-3-hydroxy-8-nonenoate (C9), and [R]-3-hydroxy-10-undecenoate (C11) monomers; Figure 4.

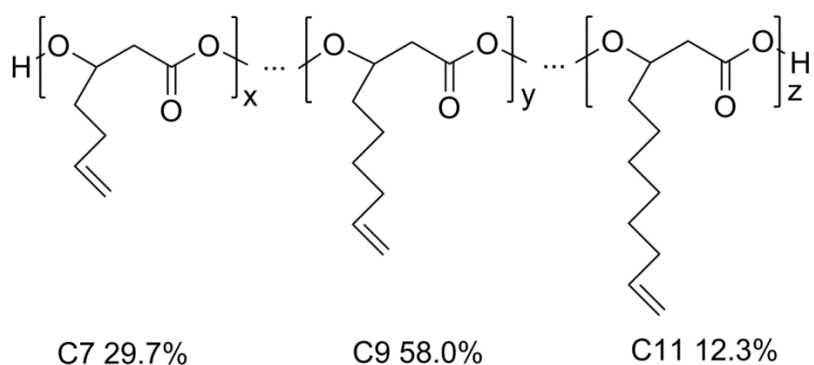


Figure 4. Chemical structure of PHUE containing randomly distributed C7, C9, and C11 monomers; x, y, z correspond to the number of monomers, respectively.

Biosynthetic route, from which PHAs are produced, generates hydrophobic polymers, with limited use in some applications, for example, drug delivery. That limitation may be overcome by either blending with other (more hydrophilic) polymers^[59, 61] or by feeding bacteria with functionalized substrates. As a result, PHAs with the same functionalities in side chains will be produced^[55, 59] and can be then further chemically modified.^[55, 62] A great diversity of substrates as well as biosynthetic and chemical modifications of PHAs offers a possibility for tuning the polymer properties, and thus expanding the number of their potential applications.

1.2.2. PHA-based materials

PHAs have been already successfully applied in various applications, including packaging, textile, printing and photographic materials.^[50] They have also been shown useful as a new type of a biofuel^[63] or as starting materials for the development of fine

chemicals, e.g. vitamins, antibiotics, or pheromones.^[64-65] Moreover, due to their biocompatibility and biodegradability, they have been used in biomedical applications, for example in drug delivery,^[66] wound management (surgical meshes, wound dressings, repair patches, sutures, skin substitutes),^[59, 67-68] or implants for the cardiovascular system (vascular grafts, heart valves, stents).^[67-69] A crucial step for PHA-based materials in biomedical applications was achieved in 2007, when the United States Food and Drug Administration (FDA) approved the first PHA polymer- poly([R]-4-hydroxybutyrate), P(4HB), for suture applications. PHAs have been also considered for orthopedic materials, which are of a particular interest for this thesis.

PHA research on load-bearing applications, such as bone tissue engineering, usually focuses on scl-PHAs (mainly poly([R]-3-hydroxybutyrate), P(3HB)). However, because of their crystalline nature and thus also slow degradation rate, scl-PHAs have to be copolymerized or blended with other polymers or compounds that ensure better flexibility and degradation profile.^[43] In contrast, elastomeric mcl-PHAs, due to their low tensile strengths, have to be used together with other compounds improving their load-bearing capacity.

Investigations on PHA feasibility for orthopedic applications shows that P(3HB)-based materials had high in vitro bioactivity, improved mechanical properties (comparing to the pure polymer before reinforcing with HAP),^[70-71] good healing response,^[72-73] and showed bone tissue formation close to the implant with no inflammatory response.^[74-77] Regarding mcl-PHAs, so far only a poly([R]-3-hydroxyhexanoate)-co-poly([R]-3-hydroxybutyrate), P(3HH)-P(3HB) was studied and showed stimulating bone growth^[78] and better performance on cells attachment, proliferation and differentiation, comparing to pure P(3HB).^[79-81] Due to these favorable properties, P(3HB)-based materials have

been used to produce, for example, bone graft substitutes, scaffolds for bone and cartilage repair, spinal cages or internal fixation devices (screws).^[43, 59]

The development of successful biomaterials largely relies on understanding the material surface properties, however PHA-based materials have been so far prepared from bulk polymers using top-down strategies (e.g. salt leaching or blending with other components). In none of these, the material surface properties, very important for further interfacial compatibility of an implant with the body, have been studied and precisely controlled – such a control could, however, improve the materials behavior in the presence of cells. To study surface properties of synthetic materials in the asymmetric environments, such as in the body, very useful are thin molecular films prepared at the air-water interface (so-called Langmuir monolayers).

1.2.3. Langmuir monolayers and interfacial behavior of PHAs

Langmuir monolayers are two-dimensional (2D) monomolecular thin films, formed by spreading water-insoluble (and preferentially surface active) molecules at the air-water interface. Such a thin layer can be compressed on the aqueous surface by movable barriers of a Langmuir trough (Figure 5), to lead to a decrease in the surface tension of water depending on the molecular film's orientation and organization. Conventionally, surface pressure (a difference between the surface tension of a clean subphase and the subphase covered with a monolayer) is plotted versus mean molecular area as a surface pressure-area (π -A) isotherm, from which one can evaluate physicochemical properties of a thin film, such as molecular organization,^[82-83] molecular area, film elasticity,^[84] or stability.^[85] The films can be also visualized during compression by using a Brewster angle microscope (BAM),^[86-87] Figure 5. Apart from relative film thickness, this method provides information about film morphology on the

micrometer length scale to allow a detailed investigation of Langmuir film phase behavior.^[88]

Thin films have often been used to understand biomembrane formation and functions, since they constitute half of a bilayer.^[89] Moreover, they may provide information about interactions and thermodynamics of mixing in multicomponent systems.^[90] They can also be transferred (vertically or horizontally) to solid supports forming Langmuir-Blodgett (LB)^[91] or Langmuir-Schaefer (LS)^[92] films, respectively.

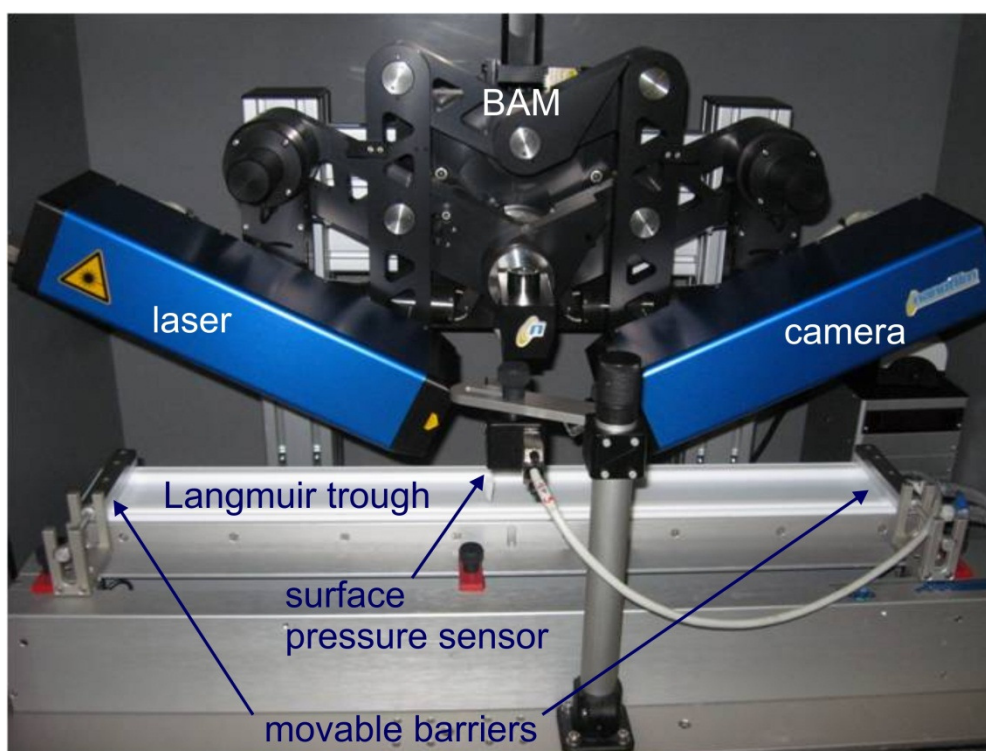


Figure 5. Experimental set-up: Langmuir trough and Brewster angle microscope (BAM).

Even though the monolayer approach is experimentally relatively uncomplicated, PHAs interfacial behavior has not been studied in much detail. There exist only a few reports, which focus mainly on scl-PHAs.

Nobes et al. studied the spreading behavior of P(3HB) and its copolymers with poly([R]-3-hydroxyvalerate), P(3HV) (at different molar ratios) at the air-water interface,

in order to understand the nascent structure of PHAs inclusions.^[93] The investigated polymers formed reproducible monolayers and were concluded to have affinity for water, which was hydrogen bonded and responsible for a non-crystalline state of nascent PHAs granules.

P(3HB) monolayers were also investigated by Lambeek et al.,^[94] who performed more detailed analysis (including e.g. change in the experimental conditions, monolayer stability and hysteresis). It was pointed out that P(3HB) monolayer undergoes a phase transition during the compression, forms crystalline domains and collapses at a relatively high surface pressure (around 65 mN/m). Additionally, P(3HB) transferred on solid supports was found to be crystalline and in a helical conformation.

The Langmuir monolayer technique was further used by Jo et al. to compare the degradation kinetics of P(3HB) and poly(L-lactide) (PLLA).^[95] It was shown that hydrophobic P(3HB) degraded on both, enzymatic and alkaline subphases, at higher surface pressures, contrary to more hydrophilic PLLA, which degraded at lower surface pressures.

One conference report compares the monolayer behavior of bacterial and synthetic scl- and mcl-PHAs (represented by P(3HH), poly([R]-3-hydroxyoctanoate) (P(3HO)), poly([R]-3-hydroxynonanoate) (P(3HN))).^[96] The authors observed that surface pressures vary with the polymer composition. Briefly, mcl-PHAs reach lower surface pressures than scl-PHAs at similar packing densities, which was related to the more elastomeric character of mcl-PHAs comparing with the crystalline scl-PHAs. Furthermore, monolayers from synthetic scl-PHAs and mcl-PHAs were easily transferred on various solid supports (including mica, glass, and silicon wafers), while bacterial scl-PHAs multilayers were not so efficiently transferred. It was postulated that bacterial scl-PHAs

do not retain their molecular organization during the transfer, but there was no further explanation as to the reason for this behavior.

The properties of the polymers (and when applicable also solid supports) were hardly taken into account in discussion sections of the above reports. For example, Lambeek et al. have not considered a large polydispersity index (PDI) of their polymer, which could explain the irreversible behavior of the compression cycles in the hysteresis experiments. Compression could induce dissolution of the shorter polymer chains in the aqueous subphase, leading to the observed isotherm shift to lower mean molecular areas. Jo et al. have not discussed the large (five-fold) difference in the molar mass of P(3HB) and PLLA, which could lead to differences in degradation rates, while Nobes et al. have not provided the molar mass and/or PDI values at all. It is clear that the studies on PHA surface properties were not investigated and interpreted carefully.

As the polymer monolayer behavior is known to be highly dependent on the polymer properties, the full PHUE monolayer characterization was first performed in this thesis (chapter 3.1), including additional results on the influence of the polymer molar mass and LB transfers on various substrates (Appendix, chapters 5.1 and 5.2). The monolayer method was further used to investigate if and how calcium phosphate crystal growth is influenced by the PHUE and PHUE-lipid films at the air-water interface. Langmuir monolayers have previously been used as templates for controlled growth of two most important biological crystals, calcium carbonate^[97-100] and calcium phosphate.^[101-108] In this work, we were particularly interested in calcium phosphate as a major bone component.

1.3. Calcium phosphate and template-directed crystallization

Calcium phosphate occurs in many phases, which differ in properties (e.g. solubility, elasticity, or compressive strength), resulting from different molar ratio of Ca/P. This last parameter was therefore introduced to classify calcium phosphate phases. Generally, the lower the Ca/P ratio, the more acidic and thus more soluble in water is the calcium phosphate.^[109] Properties of amorphous calcium phosphate and hydroxyapatite, the two calcium phosphate phases most important for this thesis, are summarized in Table 1.

Table 1. Properties of selected calcium phosphate phases.

| Calcium phosphate phase | Chemical formula | Ca/P (molar ratio) | Solubility | Compressive strength, MPa |
|-----------------------------------|--|------------------------------|-------------------|----------------------------------|
| Amorphous calcium phosphate (ACP) | $\text{Ca}_x(\text{PO}_4)_y \cdot n\text{H}_2\text{O}$ | 1.2-2.2 | - | 15 |
| Hydroxyapatite (HAP) | $\text{Ca}_{10}(\text{PO}_4)_6(\text{OH})_2$ | 1.67 | 116.8 | 100 |

HAP is the least soluble and the most stable phase of calcium phosphate, however it is rarely found in Nature in its pure form. More often, it lacks calcium while orthophosphate ions are replaced by carbonate ions. This form is called carbonated hydroxyapatite and is the most abundant inorganic component in the mammalian bones. HAP has enormous compressive strength (100 MPa), but is very brittle. The vast load-bearing capacity of bone results from HAP combination with organic, flexible component (collagen), which improves mechanical properties of the bone.

In cells, ‘matrix vesicles’ (MVs) are one of the most important structures for calcium phosphate mineralization. MVs membrane is mainly composed of lipids (phosphatidylserine, PS) and calcium-selective channel proteins (Annexin V).^[110] Calcium, supplied to the phosphate-rich interior of MVs, is then bound by negatively

charged PS, which results in precipitation of calcium phosphate (in its amorphous form, ACP).^[111] In cells, these crystals are growing, disrupting the vesicles, and finally they merge with other ACP crystals, which are then converted to HAP, the most stable form of calcium phosphate.

Human-made organic-inorganic composite materials are normally generated by so-called organic matrix-mediated mineralization.^[112] The templating organic molecules should be amphiphilic, with appropriate hydrophilic-hydrophobic ratio, which on the one hand will protect the templates from dissolution in water (hydrophobic block) and on the other hand, will allow interactions with ions (hydrophilic part).^[112] For that reason, very interesting appear to be polymers,^[34-36] whose hydrophilic-hydrophobic ratio can be tuned during the synthesis, or which can be cross-linked (in the case of hydrophilic polymers) to form insoluble species.

There are mainly two ways in which templates direct the nucleation. Firstly, crystals formation may results from initial ions interacting with functional organic molecules. For example, Zhang et al. showed that negatively charged monolayers from arachidic acid attracted first calcium ions, forming a positively charged layer, which then was a driving force to concentrate phosphate ions, and afterwards the nucleation of calcium phosphate was initiated.^[105] On the other hand, templates may induce heterogeneous nucleation- the mineral nucleates primarily at the template's surface, because the activation energy for nucleation is lowered due to the reduction of the interfacial energy,^[113] in this way also the nucleation induction time is meaningfully reduced.^[114] Template-directed inorganic mineralization mainly uses self-assemblies from organic molecules, e.g. vesicles, self-assembled monolayers or thin films (Langmuir monolayers).^[112, 115]

Self-assembled monolayers (SAMs) may be produced using molecules with different functional groups and various solid substrates, and these are the most important factors influencing crystals size, shape, orientation, and phases.^[116-117] For example, Löbbicke et al. used thiol-functionalized SAMs prepared on gold surfaces for synthesis of polymer brushes with different charges.^[118] It was shown that despite the difference in calcium phosphate crystals morphology (related to the charge of the polymer) both calcium phosphate-polymer hybrid materials showed improved cell viability (comparing to the polymer brushes not coated with the mineral).

The main advantage of templates prepared by the Langmuir monolayer technique is the possibility to easily control distances between molecules, and thus crystals in different phases may be obtained. Orientation of these phases is determined by the charge density and arising from that electrostatic, structural, and stereochemical matching with surfactant head groups.^[112, 115] The properties of the resulting hybrid organic-inorganic materials can be tailored by the organic film-forming material(s) and crystal growth parameters (e.g. ionic strength, pH, temperature, stirring rate, additives). So far, calcium phosphate growth was controlled by monolayers prepared from fatty acids,^[101-104] a phospholipid (DPPC),^[105] and polymers.^[106-108]

Regarding the polymer monolayers, only films from charged synthetic polymers have been investigated in the crystallization templating context. Casse et al. used the monolayers prepared from polyanionic poly(n-butylacrylate)-block-poly(acrylic acid) to control the growth of calcium phosphate, and found that mineralization strongly depends on the ions concentrations, the subphase pH, and the stirring rate of the subphase.^[106] Briefly, mineralization was best controlled at high pH values (when the polymer was highly negatively charged) and at low (2 mM) ions concentration. Contrary to Casse et al., Junginger et al. analyzed the templating properties of polycationic monolayers from

poly(n-butyl methacrylate)-block-(poly[2-(dimethylamino)ethyl methacrylate] for calcium phosphate mineralization.^[107] Depending on the subphase pH, the monolayer was highly (low pH) or slightly (high pH) charged, which in turn influenced the morphology of the calcium phosphate crystals; smaller and more densely packed crystals were formed at low pH, comparing with the large and less defined crystals obtained at pH 8. Comparing with the results from Casse et al., it appears that for the good control of calcium phosphate crystallization, the film-forming polymer should be charged (regardless if positively or negatively), which attracts then the counter- ions (phosphate or calcium, respectively) and induces the calcium phosphate nucleation.

Additionally, Junginger et al. investigated the effect of an oscillating polymer film from (poly(butadiene)-block-poly[2-(dimethylamino)ethyl methacrylate]) on calcium phosphate crystallization.^[108] Similarly to the previous study,^[107] the polymer was highly positively charged at low pH, which caused also low stability of that film when comparing with the high pH. The increase in mineralization time led to the formation of more uniform crystals when the monolayer was slightly charged (pH 8), whereas when the film was charged, different crystal morphologies were observed depending on the mineralization time. Such different behavior comparing with the previous study was attributed to difference in the hydrophilic-hydrophobic block ratio in the polymer. Briefly, polymers with a large hydrophilic block and high degree of charge lead to the formation of uniform crystals of calcium phosphate.

Summarizing, it is clear from the literature that static as well as dynamic soft polymeric films prepared at the air-water interface direct mineralization of calcium phosphate to form crystals with various morphologies and sizes. Nevertheless, the studied so far polymer monolayers were prepared from non-biocompatible and non-biodegradable synthetic polymers. In this thesis, emphasis is put on the biodegradable,

naturally synthesized polymer, PHUE. It is hydrophobic, however by addition of lipids at various molar ratios one can change the film properties (e.g. amphiphilicity, elasticity), which led to the first reports on how mixed monomolecular films template calcium phosphate crystallization.

1.4. References

1. O'Brien, F., *Mater. Today* **2011**, *14* (3), 88.
2. Viguet-Carrin, S.; Garnero, P.; Delmas, P., *Osteoporosis Int.* **2006**, *17* (3), 319.
3. Ma, P. X., *Adv. Drug Deliv. Rev.* **2008**, *60* (2), 184.
4. Kim, T. G.; Shin, H.; Lim, D. W., *Adv. Funct. Mater.* **2012**, *22* (12), 2446.
5. Rai, R.; Keshavarz, T.; Roether, J. A.; Boccaccini, A. R.; Roy, I., *Mater. Sci. Eng. R Rep.* **2011**, *72* (3), 29.
6. Williams, S. F.; Martin, D. P.; Horowitz, D. M.; Peoples, O. P., *Int. J. Biol. Macromol.* **1999**, *25* (1-3), 111.
7. Williams, D. F., *Biomaterials* **2008**, *29* (20), 2941.
8. Hutmacher, D. W., *Biomaterials* **2000**, *21* (24), 2529.
9. Brunette, D. M., *Int. J. Oral Maxillofac. Implants* **1988**, *3* (4), 231.
10. Arima, Y.; Iwata, H., *Biomaterials* **2007**, *28* (20), 3074.
11. Yang, C. Y.; Huang, L. Y.; Shen, T. L.; Yeh, J. A., *Eur. Cell. Mater.* **2010**, *20*, 415.
12. Wilkinson, C. D. W.; Riehle, M.; Wood, M.; Gallagher, J.; Curtis, A. S. G., *Mat. Sci. Eng. C* **2002**, *19* (1), 263.
13. Ruoslahti, E.; Pierschbacher, M. D., *Science* **1987**, *238* (4826), 491.
14. Chung, I. M.; Enemchukwu, N. O.; Khaja, S. D.; Murthy, N.; Mantalaris, A.; Garcia, A. J., *Biomaterials* **2008**, *29* (17), 2637.
15. Drotleff, S.; Lungwitz, U.; Breunig, M.; Dennis, A.; Blunk, T.; Tessmar, J.; Gopferich, A., *Eur. J. Pharm. Biopharm.* **2004**, *58* (2), 385.
16. Place, E. S.; Evans, N. D.; Stevens, M. M., *Nature Mater.* **2009**, *8* (6), 457.
17. Tribet, C., *Biochimie* **1998**, *80* (5-6), 461.
18. Kita-Tokarczyk, K.; Itef, F.; Grzelakowski, M.; Egli, S.; Rossbach, P.; Meier, W., *Langmuir* **2009**, *25* (17), 9847.
19. Berkovich, A. K.; Lukashev, E. P.; Melik-Nubarov, N. S., *Biochim. Biophys. Acta* **2012**, *1818* (3), 375.
20. Thomsen, P.; Ericson, L. E., Inflammatory Cell Response to Bone Implant Surfaces. In *The bone-biomaterial interface*, Davies, J. E., Ed. University of Toronto Press: Toronto, 1991; pp 153-169.
21. Chen, P. Y.; McKittrick, J.; Meyers, M. A., *Prog. Mater. Sci.* **2012**, *57* (8), 1492.
22. Murphy, C. M.; Haugh, M. G.; O'Brien, F. J., *Biomaterials* **2010**, *31* (3), 461.

23. Hing, K. A.; Annaz, B.; Saeed, S.; Revell, P. A.; Buckland, T., *J. Mater. Sci. - Mater. Med.* **2005**, *16* (5), 467.
24. Dorozhkin, S. V., *Biomaterials* **2010**, *31* (7), 1465.
25. Wei, G.; Ma, P. X., *J. Biomed. Mater. Res. Part A* **2006**, *78A* (2), 306.
26. Suchanek, W.; Yoshimura, M., *J. Mater. Res.* **1998**, *13* (01), 94.
27. Le Huec, J. C.; Schaefferbeke, T.; Clement, D.; Faber, J.; Le Rebeller, A., *Biomaterials* **1995**, *16* (2), 113.
28. Tricoteaux, A.; Rguiti, E.; Chicot, D.; Boilet, L.; Descamps, M.; Leriche, A.; Lesage, J., *J. Eur. Ceram. Soc.* **2011**, *31* (8), 1361.
29. Li, X.; Xie, J.; Lipner, J.; Yuan, X.; Thomopoulos, S.; Xia, Y., *Nano Lett.* **2009**, *9* (7), 2763.
30. Albrektsson, T.; Johansson, C., *Eur. Spine J.* **2001**, *10*, S96.
31. Stevens, M. M., *Mater. Today* **2008**, *11* (5), 18.
32. LeGeros, R. Z., *Adv. Dent. Res.* **1988**, *2* (1), 164.
33. Wang, M., *Biomaterials* **2003**, *24* (13), 2133.
34. Place, E. S.; George, J. H.; Williams, C. K.; Stevens, M. M., *Chem. Soc. Rev.* **2009**, *38* (4), 1139.
35. Puppi, D.; Chiellini, F.; Piras, A. M.; Chiellini, E., *Prog. Polym. Sci.* **2010**, *35* (4), 403.
36. Shoichet, M. S., *Macromolecules* **2009**, *43* (2), 581.
37. Park, H.; Temenoff, J. S.; Mikos, A. G., Biodegradable Orthopedic Implants. In *Engineering of Functional Skeletal Tissues*, 1st ed.; Bronner, F.; Farach-Carson, M. C.; Mikos, A. G., Eds. Springer-Verlag: London, 2007; Vol. 3, pp 55-68.
38. Agrawal, C. M.; Ray, R. B., *J. Biomed. Mater. Res.* **2001**, *55* (2), 141.
39. Athanasiou, K. A.; Niederauer, G. G.; Agrawal, C. M., *Biomaterials* **1996**, *17* (2), 93.
40. Oh, J. K., *Soft Matter* **2011**, *7* (11), 5096.
41. Marklein, R. A.; Burdick, J. A., *Adv. Mater.* **2010**, *22* (2), 175.
42. Choong, C.; Triffitt, J. T.; Cui, Z. F., *Food Bioprod. Process.* **2004**, *82* (2), 117.
43. Misra, S. K.; Valappil, S. P.; Roy, I.; Boccaccini, A. R., *Biomacromolecules* **2006**, *7* (8), 2249.
44. Feng, W.; Patel, S. H.; Young, M. Y.; Zunino, J. L.; Xanthos, M., *Adv. Polym. Tech.* **2007**, *26* (1), 1.

45. Alzubaydi, T.; AlAmeer, S.; Ismaeel, T.; AlHijazi, A.; Geetha, M., *J. Mater. Sci. - Mater. Med.* **2009**, *20* (0), 35.
46. Kim, I.-A.; Kim, H. J.; Kim, H.-M., *J. Biomed. Mater. Res., Part B* **2010**, *93B* (1), 113.
47. Kim do, Y.; Kim, H. W.; Chung, M. G.; Rhee, Y. H., *J. Microbiol.* **2007**, *45* (2), 87.
48. Kose, G. T.; Korkusuz, F.; Korkusuz, P.; Purali, N.; Ozkul, A.; Hasirci, V., *Biomaterials* **2003**, *24* (27), 4999.
49. Sudesh, K.; Abe, H.; Doi, Y., *Prog. Polym. Sci.* **2000**, *25* (10), 1503.
50. Chen, G. Q., *Chem. Soc. Rev.* **2009**, *38* (8), 2434.
51. Williamson, D. H.; Wilkinson, J. F., *J. Gen. Microbiol.* **1958**, *19* (1), 198.
52. Steinbüchel, A.; Valentin, H. E., *FEMS Microbiol. Lett.* **1995**, *128* (3), 219.
53. Brandl, H.; Bachofen, R.; Mayer, J.; Wintermantel, E., *Can. J. Microbiol.* **1995**, *41* (13), 143.
54. Brandl, H.; Gross, R. A.; Lenz, R. W.; Fuller, R. C., *Adv. Biochem. Eng./Biotechnol.* **1990**, *41*, 77.
55. Hazer, D. B.; Kilicay, E.; Hazer, B., *Mat. Sci. Eng. C* **2012**, *32* (4), 637.
56. Lee, S. Y., *Trends Biotechnol.* **1996**, *14* (11), 431.
57. Hartmann, R.; Hany, R.; Geiger, T.; Egli, T.; Witholt, B.; Zinn, M., *Macromolecules* **2004**, *37* (18), 6780.
58. Hartmann, R.; Hany, R.; Pletscher, E.; Ritter, A.; Witholt, B.; Zinn, M., *Biotechnol. Bioeng.* **2006**, *93* (4), 737.
59. Zinn, M.; Witholt, B.; Egli, T., *Adv. Drug Deliv. Rev.* **2001**, *53* (1), 5.
60. Gross, R. A.; DeMello, C.; Lenz, R. W.; Brandl, H.; Fuller, R. C., *Macromolecules* **1989**, *22* (3), 1106.
61. Nguyen, S.; Marchessault, R. H., *Macromol. Biosci.* **2004**, *4* (3), 262.
62. Hazer, B.; Steinbüchel, A., *Appl. Microbiol. Biotechnol.* **2007**, *74* (1), 1.
63. Zhang, X.; Luo, R.; Wang, Z.; Deng, Y.; Chen, G. Q., *Biomacromolecules* **2009**, *10* (4), 707.
64. Ruth, K.; Grubelnik, A.; Hartmann, R.; Egli, T.; Zinn, M.; Ren, Q., *Biomacromolecules* **2007**, *8* (1), 279.
65. Ren, Q.; Ruth, K.; Thony-Meyer, L.; Zinn, M., *Appl. Microbiol. Biotechnol.* **2010**, *87* (1), 41.
66. Koosha, F.; Muller, R. H.; Davis, S. S., *Crit. Rev. Ther. Drug* **1989**, *6* (2), 117.

67. Williams, S. F.; Martin, D. P., Applications of Polyhydroxyalkanoates (PHA) in Medicine and Pharmacy. In *Biopolymers Online*, Wiley-VCH Verlag GmbH & Co. KGaA: 2005.
68. Valappil, S. P.; Misra, S. K.; Boccaccini, A. R.; Roy, I., *Expert Rev. Med. Devices* **2006**, 3 (6), 853.
69. Martin, D. P.; Williams, S. F., *Biochem. Eng. J.* **2003**, 16 (2), 97.
70. Boeree, N. R.; Dove, J.; Cooper, J. J.; Knowles, J.; Hastings, G. W., *Biomaterials* **1993**, 14 (10), 793.
71. Ni, J.; Wang, M., *Mater. Sci. Eng. C* **2002**, 20 (1–2), 101.
72. Kose, G. T.; Korkusuz, F.; Korkusuz, P.; Hasirci, V., *Tissue Eng.* **2004**, 10 (7-8), 1234.
73. Kose, G. T.; Korkusuz, F.; Ozkul, A.; Soysal, Y.; Ozdemir, T.; Yildiz, C.; Hasirci, V., *Biomaterials* **2005**, 26 (25), 5187.
74. Doyle, C.; Tanner, E. T.; Bonfield, W., *Biomaterials* **1991**, 12 (9), 841.
75. Shishatskaya, E. I.; Khlusov, I. A.; Volova, T. G., *J. Biomater. Sci. Polym. Ed.* **2006**, 17 (5), 481.
76. Luklinska, Z. B.; Schluckwerder, H., *J. Microsc.* **2003**, 211 (Pt 2), 121.
77. Luklinska, Z. B.; Bonfield, W., *J. Mater. Sci. Mater. Med.* **1997**, 8 (6), 379.
78. Wang, Y.; Bian, Y. Z.; Wu, Q.; Chen, G. Q., *Biomaterials* **2008**, 29 (19), 2858.
79. Cool, S. M.; Kenny, B.; Wu, A.; Nurcombe, V.; Trau, M.; Cassady, A. I.; Grøndahl, L., *J. Biomed. Mater. Res. Part A* **2007**, 82A (3), 599.
80. Wang, Y. W.; Wu, Q.; Chen, G. Q., *Biomaterials* **2004**, 25 (4), 669.
81. Yang, M.; Zhu, S.; Chen, Y.; Chang, Z.; Chen, G.; Gong, Y.; Zhao, N.; Zhang, X., *Biomaterials* **2004**, 25 (7-8), 1365.
82. Dynarowicz Łątka, P.; Kita, K.; Milart, P.; Dhanabalan, A.; Cavalli, A.; Oliveira, O. N., Jr., *J. Colloid Interface Sci.* **2001**, 239 (1), 145.
83. Ferreira, M.; Dynarowicz-Łątka, P.; Miñones, J.; Caetano, W.; Kita, K.; Schalke, M.; Lösche, M.; Oliveira, O. N., *J. Phys. Chem. B* **2002**, 106 (40), 10395.
84. Haefele, T.; Kita-Tokarczyk, K.; Meier, W., *Langmuir* **2005**, 22 (3), 1164.
85. Dynarowicz-Łątka, P.; Dhanabalan, A.; Oliveira Jr, O. N., *Adv. Colloid Interface Sci.* **2001**, 91 (2), 221.
86. Hoenig, D.; Moebius, D., *J. Phys. Chem.* **1991**, 95 (12), 4590.
87. Henon, S.; Meunier, J., *Rev. Sci. Instrum.* **1991**, 62 (4), 936.

88. Dynarowicz-Łatka, P.; Miñones, J.; Kita, K.; Milart, P., The utility of Brewster angle microscopy in evaluating the origin of the plateau in surface pressure/area isotherms of aromatic carboxylic acids. *Trends in Colloid and Interface Science XVI*. Miguel, M.; Burrows, H. D., Eds. Springer Berlin / Heidelberg: 2004; Vol. 123, pp 152-155.
89. Eaman, M.; Deleu, M., *Biotechnol. Agron. Soc. Environ* **2010**, *14* (4), 719.
90. Dynarowicz Łatka, P.; Kita-Tokarczyk, K., *Adv. Colloid Interface Sci.* **1999**, *79* (1), 1.
91. Schwartz, D. K., *Surf. Sci. Rep.* **1997**, *27* (7–8), 245.
92. Langmuir, I.; Schaefer, V. J., *J. Am. Chem. Soc.* **1938**, *60* (6), 1351.
93. Nobes, G. A. R.; Holden, D. A.; Marchessault, R. H., *Polymer* **1994**, *35* (2), 435.
94. Lambeek, G.; Vorenkamp, E. J.; Schouten, A. J., *Macromolecules* **1995**, *28* (6), 2023.
95. Jo, N.-J.; Iwata, T.; Lim, K. T.; Jung, S.-H.; Lee, W.-K., *Polym. Degrad. Stabil.* **2007**, *92* (7), 1199.
96. Nobes, G. A. R.; Orts, W. J.; Glenn, G. M., Orientation studies of microbial polyesters at the air-water interface. In *From Annual Technical Conference - Society of Plastics Engineers* 1999; Vol. 57, pp 2185-2189.
97. Chen, Y.; Xiao, J.; Wang, Z.; Yang, S., *Langmuir* **2009**, *25* (2), 1054.
98. DiMasi, E.; Patel, V. M.; Sivakumar, M.; Olszta, M. J.; Yang, Y. P.; Gower, L. B., *Langmuir* **2002**, *18* (23), 8902.
99. Stripe, B.; Uysal, A.; Lin, B. H.; Meron, M.; Dutta, P., *Langmuir* **2012**, *28* (1), 572.
100. Loste, E.; Díaz-Martí, E.; Zarbakhsh, A.; Meldrum, F. C., *Langmuir* **2003**, *19* (7), 2830.
101. Xu, G.; Aksay, I. A.; Groves, J. T., *J. Am. Chem. Soc.* **2001**, *123* (10), 2196.
102. Lu, H. B.; Ma, C. L.; Cui, H.; Zhou, L. F.; Wang, R. Z.; Cui, F. Z., *J. Cryst. Growth* **1995**, *155* (1-2), 120.
103. Ma, C. L.; Lu, H. B.; Wang, R. Z.; Zhou, L. F.; Cui, F. Z.; Qian, F., *J. Cryst. Growth* **1997**, *173* (1-2), 141.
104. Dey, A.; Bomans, P. H.; Muller, F. A.; Will, J.; Frederik, P. M.; de With, G.; Sommerdijk, N. A., *Nature Mater.* **2010**, *9* (12), 1010.
105. Zhang, L. J.; Liu, H. G.; Feng, X. S.; Zhang, R. J.; Zhang, L.; Mu, Y. D.; Hao, J. C.; Qian, D. J.; Lou, Y. F., *Langmuir* **2004**, *20* (6), 2243.

106. Casse, O.; Colombani, O.; Kita-Tokarczyk, K.; Mueller, A. H. E.; Meier, W.; Taubert, A., *Faraday Discuss.* **2008**, *139*, 179.
107. Junginger, M.; Kita-Tokarczyk, K.; Schuster, T.; Reiche, J.; Schacher, F.; Muller, A. H. E.; Colfen, H.; Taubert, A., *Macromol. Biosci.* **2010**, *10* (9), 1084.
108. Junginger, M.; Bleek, K.; Kita-Tokarczyk, K.; Reiche, J.; Shkilnyy, A.; Schacher, F.; Muller, A. H. E.; Taubert, A., *Nanoscale* **2010**, *2* (11), 2440.
109. Dorozhkin, S. V.; Epple, M., *Angew. Chem. Int. Ed.* **2002**, *41* (17), 3130.
110. Merolli, A.; Santin, M., *Molecules* **2009**, *14* (12), 5367.
111. Wuthier, R. E.; Rice, G. S.; Wallace, J. E., Jr.; Weaver, R. L.; LeGeros, R. Z.; Eanes, E. D., *Calcif. Tissue Int.* **1985**, *37* (4), 401.
112. Mann, S., *Biomaterialization Principles and Concepts in Bioinorganic Materials Chemistry*. Oxford University Press: Oxford, 2001.
113. Mann, S., Biomaterialization and Biomimetic Materials Chemistry. In *Biomimetic Materials Chemistry*, Mann, S., Ed. VCH Publishers: New York, 1996.
114. Heywood, B. R., Template-Directed Nucleation and Growth of Inorganic Materials. In *Biomimetic Materials Chemistry*, Mann, S., Ed. VCH Publishers: New York, 1996.
115. Xu, A.-W.; Ma, Y.; Colfen, H., *J. Mater. Chem.* **2007**, *17* (5), 415.
116. Balz, M.; Barriau, E.; Istratov, V.; Frey, H.; Tremel, W., *Langmuir* **2005**, *21* (9), 3987.
117. Toworfe, G. K.; Composto, R. J.; Shapiro, I. M.; Ducheyne, P., *Biomaterials* **2006**, *27* (4), 631.
118. Löbbicke, R.; Chanana, M.; Schlaad, H.; Pilz-Allen, C.; Günter, C.; Möhwald, H.; Taubert, A., *Biomacromolecules* **2011**, *12* (10), 3753.

2. Motivation and concept

Presently, a few polymers are used in the bone tissue engineering, mainly poly(lactic acid) (PLA) and poly(glycolic acid) (PGA), however, they are not free from numerous drawbacks, for example problems regarding cell attachment, inflammation reactions or poor mechanical properties. Very interesting materials with potential to overcome these disadvantages are polyhydroxyalkanoates (PHAs), microbial polyesters, frequently studied in the context of biomedical applications and also cited as candidates for orthopedic applications. However, hardly anything is known about their molecular behavior at interfaces, which determines further interfacial compatibility of the material with cells, and especially about their interactions with biologically relevant molecules, including cell membrane components and inorganics.

The aim of this thesis was to study the interfacial behavior of polyhydroxyalkanoates as potential candidates for orthopedic applications, to understand the principles of the polymer scaffold formation and template-directed inorganic precipitation, Figure 5. We used poly([R]-3-hydroxy-10-undecenoate) (PHUE) as a representative of mcl-PHA family, and the Langmuir monolayer technique was applied to prepare insoluble monolayers at the air-water interface, in order to mimic the polymer behavior in asymmetric environments (scheme A, Figure 5). Langmuir film morphology was directly visualized with Brewster angle microscopy. Such an experimental approach generated detailed information about the films' molecular organization, orientation, monolayer thickness, elasticity, and stability. Additionally, the Langmuir monolayer technique was applied to investigate mutual interactions between PHUE and lipids, most abundant cell membrane components (scheme B, Figure 6) – this may enable modeling of living cells' behavior in the presence of a synthetic material.

In the next step, one- and two-component films were used as scaffolds to investigate the growth control of calcium phosphate (scheme C, Figure 5). Calcium phosphate crystallization was also studied in dependence of the monolayer properties (composition, charge and charge density, elasticity) and mineralization conditions (time, ions concentration). The formed crystals were characterized with electron microscopy techniques (transmission and scanning) and energy-dispersive X-ray spectroscopy.

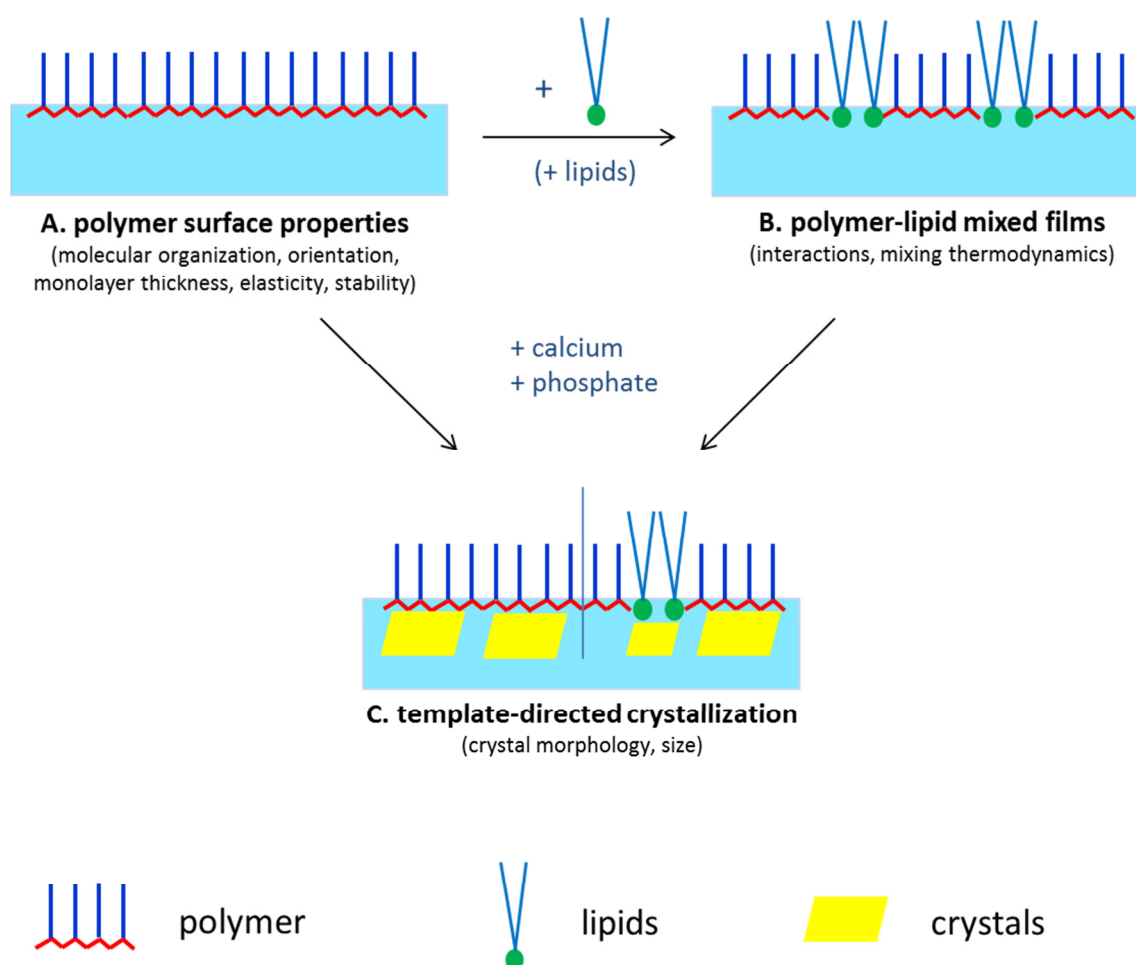


Figure 6. Schematic representation of the thesis objectives.

3. Results and discussion

The results and discussion part is presented as three publications. The first one contains a detailed analysis of pure PHUE monolayers and the method optimization for a mixed PHUE-lipid systems, using the most abundant cell membrane phospholipid, 1,2-dioleoyl-*sn*-glycero-3-phosphocholine (DOPC).

A thorough study of polymer-lipid mixed films is presented in the second paper. Here, two lipids (1,2-dioleoyl-*sn*-glycero-3-phospho-L-serine (DOPS) and 1,2-dioleoyl-*sn*-glycero-3-phosphoethanolamine (DOPE)) having the same hydrophobic part, but different hydrophilic head groups, were investigated. These results are compared with those from the PHUE-DOPC systems, allowing a deeper understanding of the lipid head group influence on the lipid interactions with the polymer.

The mixed films of PHUE with DOPS and DOPE served then as templates for calcium phosphate mineralization, which is described in the third paper. Additionally, templating properties of pure DOPS and DOPE for calcium phosphate crystallization are reported here for the first time. For pure and mixed films various experimental conditions were studied, such as mineralization time, ion concentration, and polymer-lipid molar ratio for mixed films.

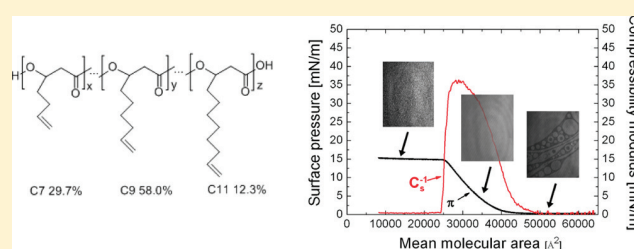
3.1. PHUE monolayers

Results were published in: “Interactions of biodegradable poly([R]-3-hydroxy-10-undecenoate) with DOPC lipid: a monolayer study”, *Langmuir*, **2011**, 27 (18), 10878-10885, A. Jagoda, P. Ketikidis, M. Zinn, W. Meier, K. Kita-Tokarczyk.

Interactions of Biodegradable Poly([R]-3-hydroxy-10-undecenoate) with 1,2-Dioleoyl-*sn*-glycero-3-phosphocholine Lipid: A Monolayer StudyAgnieszka Jagoda,[†] Pantelis Ketikidis,^{†,‡} Manfred Zinn,[‡] Wolfgang Meier,[†] and Katarzyna Kita-Tokarczyk^{*,†,§}[†]Department of Chemistry, University of Basel, Klingelbergstrasse 80, 4056 Basel, Switzerland[‡]Laboratory for Biomaterials, Swiss Federal Laboratories for Materials Science and Technology (Empa), Lerchenfeldstrasse 5, 9014 St. Gallen, Switzerland

S Supporting Information

ABSTRACT: Polyhydroxyalkanoates (PHAs) are biodegradable, biocompatible polyesters and very attractive candidates for biomedical applications as materials for tissue engineering. They have a hydrophobic character, but some are able to spread at the air–water interface to form monomolecularly thin films (Langmuir monolayers). This is a very convenient model to analyze PHA self-assembly in two dimensions and to study their molecular interactions with other amphiphilic compounds, which is very important considering compatibility between biomaterials and cell membranes. We used the Langmuir monolayer technique and Brewster angle microscopy to study the properties of poly([R]-3-hydroxy-10-undecenoate) (PHUE) films on the free water surface in various experimental conditions. Moreover, we investigated the interactions between the polymer and one of the main biomembrane components, 1,2-dioleoyl-*sn*-glycero-3-phosphocholine (DOPC). The addition of lipid to a polymer film does not change the monolayer phase behavior; however, the interactions between these two materials are repulsive and fall in two composition-dependent regimes. In summary, this is the first systematic study of the monolayer behavior of PHUE, thus forming a solid basis for a thorough understanding of material interactions, in particular in the context of biomaterials and implants.



1. INTRODUCTION

Polyhydroxyalkanoates (PHAs) are natural, aliphatic polyesters produced by a wide variety of microorganisms under specific growth conditions¹ and accumulated intracellularly. They are preferentially prepared via bacterial synthesis in continuous culture,² while the polymer composition is controlled by the nutrients and growth conditions, eventually leading to tailor-made materials with regard to chemical constitution.² PHAs possess many favorable properties which are required for development of medical devices (they are biodegradable, biocompatible thermoplastic elastomers). For example, a trileaflet heart valve scaffold was constructed using poly([R]-3-hydroxyoctanoate-*co*-3-hydroxyhexanoate) (PHO), which was then successfully implanted in the pulmonary position of lambs showing full functionality for 120 days.³ Due to these, PHAs are of great interest as materials for tissue engineering and for development of medical devices.^{4–6}

Physicochemical properties of PHAs can be tuned already upon biosynthesis or by further chemical modifications.⁷ Depending on the polymer structure and the bulk material form (fibers, surface coatings, and composites), different biocompatibility and cell viability properties can also be expected.^{7–9} Apart from biologically and medically relevant applications, PHAs are also interesting for materials science. For example, nanocomposites of different PHAs with single-wall carbon nanotubes were prepared by Yun et al.¹⁰ These authors found that the polymer

structure and crystallinity have an important effect on dispersibility of the nanotubes and thus on the mechanical properties of the composite. Unsaturated PHAs are also of interest since they can be modified via light-induced reactions: this was demonstrated for poly(3-hydroxy-10-undecenoate) (PHUE) which cross-links upon UV irradiation in the absence of any photoinitiators.¹¹ Moreover, the double bonds can be used for graft polymerization, preparation of organic–inorganic hybrid polymers, or covalent linkage of functional groups,¹² e.g., antifouling coatings.^{13–15}

Short-range organization in PHA bulk materials and blends was probed by small-angle neutron scattering.^{11,16} It was shown that a high degree of order exists in solvent-cast films from poly(3-hydroxyoctanoate)-*block*-polyethylene oxide, most likely due to the lamellar organization of the polymer and, in particular, due to its crystalline domains. The organization of polymer chains can be modulated depending on the polymer size, which offers a bottom-up approach for the preparation of surface-supported self-assembled structures.

When biomedical applications of PHAs are considered, interfacial interactions play a crucial role. For this reason, it appears that asymmetric interfaces are an environment to explore when

Received: May 4, 2011

Revised: July 6, 2011

Published: July 12, 2011

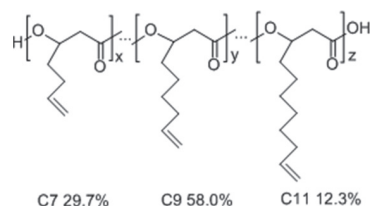
studying the behavior of these polymers. This is especially true because the polymers tend to self-organize, due to their hydrophobic nature and some amphiphilic character. In particular, by analyzing insoluble polymer monolayers at the air–water interface, one can study not only the surface activity of the amphiphilic material but also molecular organization in the film,¹⁷ monolayer stability,¹⁸ compressibility, and film morphology.^{19,20} These physicochemical parameters are crucial to understanding material behavior at the molecular level. From measurements of spread mixed monolayers at the air–water interface we learn about molecular interactions between polymers and lipids, for example,²¹ and the system thermodynamics. Additionally, with regard to biomedical applications of PHAs, mixed spread films from polymers and lipids provide a simple model to investigate the mutual affinity of the synthetic and natural materials. Here, we present results on the behavior and mixing energetics of films from PHUE and DOPC (a major biomembrane component) at various molar compositions, as the first approach to help understanding the interactions between a polymeric material and phospholipids at the molecular level.

Organized, thin films from PHAs have hardly been studied so far and reports exist from three research groups only. Nobes et al.²² investigated poly([R]-3-hydroxybutyrate) (PHB), and copolyesters of 3-hydroxybutyric acid with 3-hydroxyvaleric acid. These polymers can be spread from chloroform to form monolayers on the free water surface. For PHB, collapse pressures of approximately 20 mN/m were achieved at 18 °C, corresponding to packing densities of 0.15 nm²/repeating unit. No difference was observed by using slightly acidic or alkaline subphases, indicating that protonation/deprotonation of the polymers does not take place. The authors suggested that the polymer arranges on the surface as a random or partially ordered helical coil, where all monomers remain in contact with water.

However, a later study by Lambeek et al.²³ postulates that during compression the number of hydrated monomers is decreasing. These authors observed a transition at about 14 mN/m in the surface pressure–area isotherms from PHB and related it to a phase transition in the monolayer. While, at large areas, PHB films showed expanded monolayer behavior, they turned crystalline upon compression. Contrary to Nobes et al.,²² these authors suggested an expanded, noncrystalline monolayer model for large molecular areas. Hysteresis experiments supported this interpretation, as the compression–expansion cycles remained reversible when the maximum surface pressure to which the film was compressed laid below the transition pressure. If compressed further, however, the compression and expansion isotherms did not overlap anymore. This also might have resulted from very slow expansion kinetics of densely compressed polymer, where a 10 min pause after each cycle may not have been long enough for respreading of the film. Langmuir–Blodgett multilayers were crystalline and oriented in a way that suggested the helical PHB conformation; however, Brewster angle microscopy would be helpful to confirm the presence of a bilayer of helices at the air–water interface versus a multilayered, collapsed crystalline film above 14 mN/m.

Finally, a monolayer approach has proven very useful to investigate degradation kinetics of polyesters.²⁴ In this study, subphases with different alkalinity and with the presence of enzymes were used, and monolayer destabilization was monitored at different surface pressures. The monolayer packing seemed to be very different for poly(L-lactide) (PLLA) and PHB: both disintegrate quite similarly under alkaline conditions.

Scheme 1. PHUE Structure Containing [R]-3-Hydroxy-6-heptenoate (C7), [R]-3-Hydroxy-8-nonoate (C9), and [R]-3-Hydroxy-10-undecenoate (C11) in a Random Distribution



However, high surface pressures (packing densities) with PHB favored very fast enzymatic degradation in contrast to PLLA.

In conclusion, it is clear from the literature that only a little attention has been devoted to studying PHA behavior at the air–water interface. In this paper we aim at filling this gap: we first present a systematic study of monolayers from PHUE and their behavior depending on various experimental conditions. As this material finds applications in biomedical research, we further investigate and rationalize its interactions with the main cell membrane components, namely, phospholipids. This could serve as a simplified model to evaluate interfacial compatibility between tissue cells and biomaterials (or more generally synthetic materials, and polymers in particular).^{25–27} We have chosen the mixed Langmuir monolayer model to analyze the affinity of PHUE to a lipid, DOPC, as the major cell membrane component. The thermodynamic data allow evaluating the effect of a lipid on the properties of mixed films. Apart from biological implications, the mixed, complex monolayers may also be of interest to materials research (e.g., for novel implant coatings).

2. MATERIALS AND METHODS

Polymer Synthesis, Extraction, and Purification. To obtain PHUE, the bacterial strain *Pseudomonas putida* GPo1 (*P. putida*) was grown in a chemostat at a dilution rate of 0.1 1/h using 10-undecenoic acid as a single carbon source.² Collected cells were centrifuged and the pellets lyophilized (12 °C, 0.5 mbar, 72 h). Dry cell biomass was suspended in ethyl acetate (60 g/L), the suspension was stirred for at least 2 h, filtered, and concentrated by solvent distillation in a vacuum dryer until it became viscous (40 °C, 240 mbar). The polymer was then precipitated in cold methanol (4 °C), vacuum-dried for 2 days (40 °C, 30 mbar), and stored at –20 °C. It has to be noted that the biosynthesis route, from which PHUE originates, is an excellent means to control the polymer properties, yet it renders random polymers that contain a certain amount of shorter chains. This is, however, intrinsic to the synthesis due to β -oxidation and cannot be avoided.²⁸ As a result, the investigated polymer is a random terpolymer (Scheme 1).

Polymer Characterization. The molecular weight of PHUE was determined by gel permeation chromatography (GPC, Viscotek/Trisec Model 302). For analysis, typically 50 mg of purified polymer was dissolved in 10 mL of tetrahydrofuran (THF, Fisher Scientific, analytical grade) and filtered with a nylon filter (Titan2, 0.45 μ m). The monomer composition was determined by gas chromatography (GC) using a method developed by Furrer et al.²⁹ and confirmed by NMR. ¹H and ¹³C NMR experiments in solution were performed on a Bruker AV-400 spectrometer at 297 K using a 5 mm broad-band probe.^{14,29}

Lipids. DOPC (mass, 786 g/mol) was purchased from Avanti Polar Lipids, Inc. (Alabaster, AL, USA) as chloroform solution, 20 mg/mL. To avoid lipid oxidation, the stock solution was stored in a freezer under

argon. For monolayer experiments, diluted solutions were used (1 mg/mL in chloroform).

Langmuir Monolayers. Monolayer measurements were carried out on a KSV Inc. (Espoo, Finland) Langmuir Teflon trough (area: 420 cm²), equipped with two symmetric barriers. Surface pressure was recorded with the Wilhelmy plate method (ashless filter paper; width, 10 mm; accuracy, ± 0.1 mN/m). Before every measurement, the trough was cleaned twice with either ethyl acetate (Fluka, $\geq 99.9\%$ grade) or chloroform (HPLC-grade, Sigma-Aldrich), and ethanol (Fluka, grade $\geq 99.8\%$). Hydrophilic (Delrin) barriers were cleaned with ethanol and rinsed with bidistilled water. After several measurements, warm water (approximately 50 °C) was poured on the trough to help remove the remaining polymer.

Bidistilled water was used as subphase; its purity was checked by measuring the surface pressure changes during compression without a polymer film and monitoring the water surface by Brewster angle microscopy.

A polymer solution (in ethyl acetate or chloroform; concentration approximately 0.3 mg/mL) was spread on the water surface (approximately 60 μ L), using a gastight Hamilton syringe. Before spreading, syringes were rinsed a few times with an appropriate solvent. After spreading, the solvent was allowed to evaporate for approximately 10 min (unless otherwise specified), and then the monolayer was compressed, usually at 10 mm/min (unless otherwise specified). Apart from the temperature dependence experiments, all isotherms were recorded at 20 °C. Each measurement was repeated at least three times.

Brewster Angle Microscopy. A Brewster angle microscope (EP³SW system, Accurion, Göttingen, Germany) equipped with a Nd:YAG laser (532 nm), Nikon 20 \times long distance objective, and a monochrome CCD camera was used for investigations of the monolayer morphology. Brewster angle microscopy (BAM) images correspond to dimensions of 220 \times 250 μ m², with 1 μ m resolution.

3. RESULTS AND DISCUSSION

PHUE Analysis. Polymer composition was determined by GC and NMR, from which we obtained the structure shown in Scheme 1. The 3-hydroxyalkenoate monomers (C7, C9, C11) are distributed randomly along the backbone, and x , y , z correspond to the number of monomers containing C7, C9, and C11 side chains, respectively. These values are, however, difficult to calculate due to the large molar mass of the polymer (and the large error of mass determination). The percentages indicated in Scheme 1 denote molar proportions of the monomers.

From GPC, we obtained $M_w = 294\,600$ g/mol, $M_n = 165\,600$ g/mol, and the polydispersity index (PDI) of 1.8, which is a low value for polymers produced by bacteria. Differential scanning calorimetry (DSC) showed the glass transition temperature of -48.9 °C and no melting temperature.

PHUE Spreading Solutions. According to results from Terada and Marchessault,³⁰ we chose ethyl acetate as a solvent for PHUE. However, when stored in the freezer for a few months, the polymer tended to crystallize, and ethyl acetate was unable to dissolve the small crystals. Thus, we changed the solvent to chloroform. Surface pressure–area isotherms from PHUE, spread from either ethyl acetate or chloroform, were identical. On the one hand, this means that the spreading solvent does not influence monolayer behavior. On the other hand, dense patches of undissolved polymer were visible with BAM when the monolayers were spread from ethyl acetate. Although these patches were still small enough not to influence the isotherm, we chose to work with chloroform, from which we always obtained homogeneous films.

Due to the polymer organization kinetics and the tendency to crystallize at low temperatures, all solutions were prepared 2 days before planned experiments and stored at room temperature

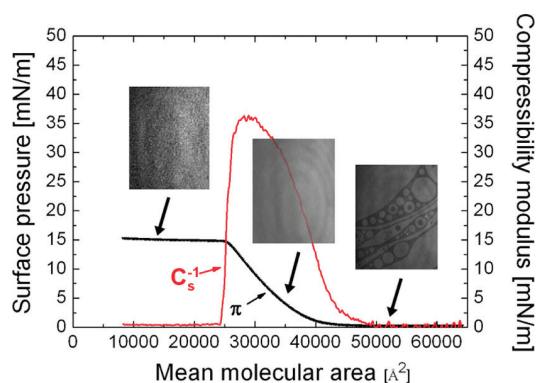


Figure 1. Surface pressure–area (π – A) isotherm, compressibility modulus (C_s^{-1}), and BAM images ($220 \times 250 \mu\text{m}^2$) of the PHUE monolayer.

(RT). Vortexing was used to mix the solutions, as sonication may be too invasive and break the longer chains.

Because PHUE side chains are terminated with double bonds, which may be easy to cross-link,³¹ we protected polymer solutions from light by wrapping the vials in aluminum foil and storing them in the dark. Under such conditions (RT, aluminum foil), solutions could be stored up to 3 months and give reproducible surface pressure isotherms.

PHUE Monolayers. Although PHUE has more of a hydrophobic than an amphiphilic character, it forms monolayers at the air–water interface. In Figure 1, BAM images show that at high mean molecular areas (surface pressure, 0 mN/m), gas and liquid monolayer phases coexisted (black regions, gas phase; gray, liquid domains). During the film compression, as the mean area available for a polymer molecule decreased, the PHUE film became more organized, and at about 40 000 \AA^2 /molecule, the surface pressure started to increase. From that point on, we observed a smooth monolayer with BAM. Further compression led to the surface pressure increase, but no changes of the monolayer behavior were visible with BAM. When 25 000 \AA^2 /molecule was reached (at about 15 mN/m), the polymer film collapsed, which was demonstrated by discontinuity of the isotherm and the formation of very reflective, crystalline structures.

The investigated PHUE is a statistical mixture of three different monomers, the only difference between these being the length of the hydrocarbon side chains (C7, C9, C11). It was shown before^{32,33} that, when considering mixed monolayers from small insoluble amphiphiles with chains of the same chemistry and small length difference, their mixing properties show ideal or almost ideal mixing behavior. This means the interactions in the film do not change with the addition of slightly shorter/longer chains, and therefore the monolayer morphology should not change, either. Thus we are convinced that different monomers do not influence PHUE monolayer behavior.

Regarding the PHUE orientation on the water surface, we can expect the PHUE side chains to be exposed toward air, and the backbone to face water. Even though only weakly hydrophilic, the backbone is still far more polar than carbon chains—the dipole moment of the ester group is ca. 1.8 D.³⁴ This orientation appears thus most energetically favorable. We should exclude two-dimensional organization of the polymer to produce domains, surface micelles, and so on, as these were not observed by BAM and grazing incidence X-ray diffraction (GIXD; data not shown). The organization of the film can be evaluated by GIXD if long-range ordering in the film existed. Unfortunately, this is not

the case with PHUE, as we have not observed any meaningful signal intensity. Moreover, with infrared reflection–absorption spectroscopy (IRRAS; not shown) we only observed a typical change of intensity of the water peak with surface pressure, which means, as expected, that water is expelled from the film during compression. The spectrum did not show surface pressure-dependent differences of intensities corresponding to any groups within the polymer and therefore suggests that no changes in molecular orientation take place during the film compression, apart from, obviously, tighter packing due to the decrease of the available area. The monolayer structure is therefore determined by the space-limiting, weakly hydrophilic backbone.

Surface pressure–area data were used to calculate the compressibility modulus values, C_s^{-1} (Figure 1). C_s^{-1} is calculated as $-A(\partial\pi/\partial A)_T$, and the values indicate the monolayer phases.³⁵ We observed only one maximum, which suggested that only one phase existed during the monolayer compression. The maximum value of C_s^{-1} (36 mN/m) indicated that at approximately 30 000 Å²/molecule the PHUE monolayer was in a liquid expanded state.³⁵

The isotherms were reversible upon several compression–expansion cycles (Figure S1, Supporting Information); no hysteresis was observed, which indicates that the PHUE did not dissolve in water and its monolayer behavior was elastic. We noticed only a small (about 1000 Å²/molecule) difference between the compression isotherm from the first cycle and the following ones. This was probably due to the slow expansion kinetics of the polymer (despite 30 min waiting time after expansion), and we may have been compressing already pre-organized domains of the polymer film in the second and the following cycles, instead of single molecules as during the first compression.

Monolayer stability was verified by monitoring the surface pressure change at constant area (28400 Å²/molecule, Figure S2, Supporting Information). The PHUE monolayer maintained its surface pressure for over 1 h, which indicated very high film stability. This result is highly relevant for enzymatic degradation studies and experiments that involve film transfer to solid surfaces, for example.

Monolayers from some amphiphilic compounds³⁶ are very sensitive to even small changes in experimental conditions. Since PHUE behavior at the air–water interface has not been investigated before, we checked the influence of various experimental conditions on the monolayer formation (Figure 2).

We observed no change in the isotherm shape and position, when the monolayer was compressed at various rates (from 2 to 100 mm/min; Figure 2A). This suggests that despite its large size, the polymer quickly organized at the air–water interface. This is rare for materials such as PHUE, which are not classical amphiphiles with distinctly different hydrophobic and hydrophilic parts. Moreover, PHUE isotherms were identical when 5, 10, or 30 min were allowed for the solvent to evaporate before starting film compression (Figure 2B). It appears that 5 min was long enough for both ethyl acetate and chloroform to evaporate from the water surface and that the film did not contain any plasticizing solvent. PHUE monolayers behaved in exactly the same way when the same number of molecules (6.5×10^{13}) were spread from solutions of different concentrations (between 0.3 and 1.1 mg/mL; Figure 2C). For “good” monolayer-forming materials, this should always be the case. However, for very hydrophobic molecules and large polymers, differences are sometimes observed due to material clustering and hampered

spreading when a concentrated solution is placed on the water surface.

The experimental parameters that only slightly influenced PHUE monolayers were the number of spread molecules and temperature. When the number of molecules at the interface was varied (from 5.0×10^{13} to 9.3×10^{13} , using different volumes of the same spreading solution at 0.3 mg/mL), a weak trend was observed (Figure 2D). With increasing spreading volume, the isotherms were slightly shifted to lower mean molecular areas. This occurs because as more molecules are spread on the same surface area, spreading is limited and clustering of molecules takes place already at 0 mN/m. This effect, however, did not lead to large clusters or domains, at least not of the size that would be detected by Brewster angle microscopy (above 1 μm).

Figure 2E shows how the subphase temperature (between 16 and 35 °C) influenced the PHUE isotherms. Contrary to what is commonly observed,^{37–39} the increase of water temperature shifted the isotherms to lower mean molecular areas. This is probably due to the increased solubility of the shorter polymer chains in warmer water. We also observed a decrease in collapse pressure with increasing temperature, indicating that the monolayers became less stable due to thermal motions, making them collapse earlier.

As a model for interactions of PHUE with cell membranes, we studied a simplified system of mixed monolayers composed of the polymer, and phospholipid DOPC, one of the main biomembrane components. At various polymer–lipid molar ratios, we could identify the extent of miscibility and the corresponding interaction energies.

Mixed Monolayers from PHUE and DOPC. PHUE was mixed with DOPC which, on its own, forms more condensed monolayers³⁰ than the polymer. DOPC monolayers have a higher collapse pressure (about 48 mN/m), and a higher compressibility modulus ($C_s^{-1}_{\max} = 92$ mN/m at 80 Å²/molecule). This value corresponds to a condensed liquid film.³⁵

Figure 3 shows the surface pressure–area isotherms from PHUE mixtures with DOPC, at different molar ratios—from 0.01 to 0.09 PHUE, in steps of 0.02 (Figure 3A), and from 0.1 to 0.9, in steps of 0.2 (Figure 3B). The reason for measuring isotherms from films of very small polymer molar ratios (Figure 3A) is the following: when we consider, in a relatively simple approximation, a cell attached to a polymer surface and assume that (1) the cell radius is in the range of 5–10 μm, (2) the polymer and the cell are in good contact, and (3) the cell membrane is made only from lipid molecules, the resulting molecular proportion of PHUE to lipid will be ca. 1:99. Therefore, to model this situation, we analyzed polymer–lipid films with very asymmetric composition. Cell attachment to biomaterials is regulated mostly by proteins; however, if a polymer happens to interact with cell membrane lipids, these interactions should not be strongly attractive, as this would lead to destruction of the cell membrane. On the other hand, the complete lack of affinity (repulsion) may disturb cell attachment, an important step for biomaterial integration.

As expected, the isotherms from the mixtures lay between the isotherms from pure PHUE and DOPC. The collapse pressures of mixed films (ca. 15 mN/m) did not differ much from the collapse pressure of the PHUE monolayer, which is indicative of poor miscibility between the two components.⁴⁰ Since the surface pressure after collapse slightly increased, we supposed that there might be a second collapse, corresponding to the lipid collapse pressure. Such behavior is observed for immiscible

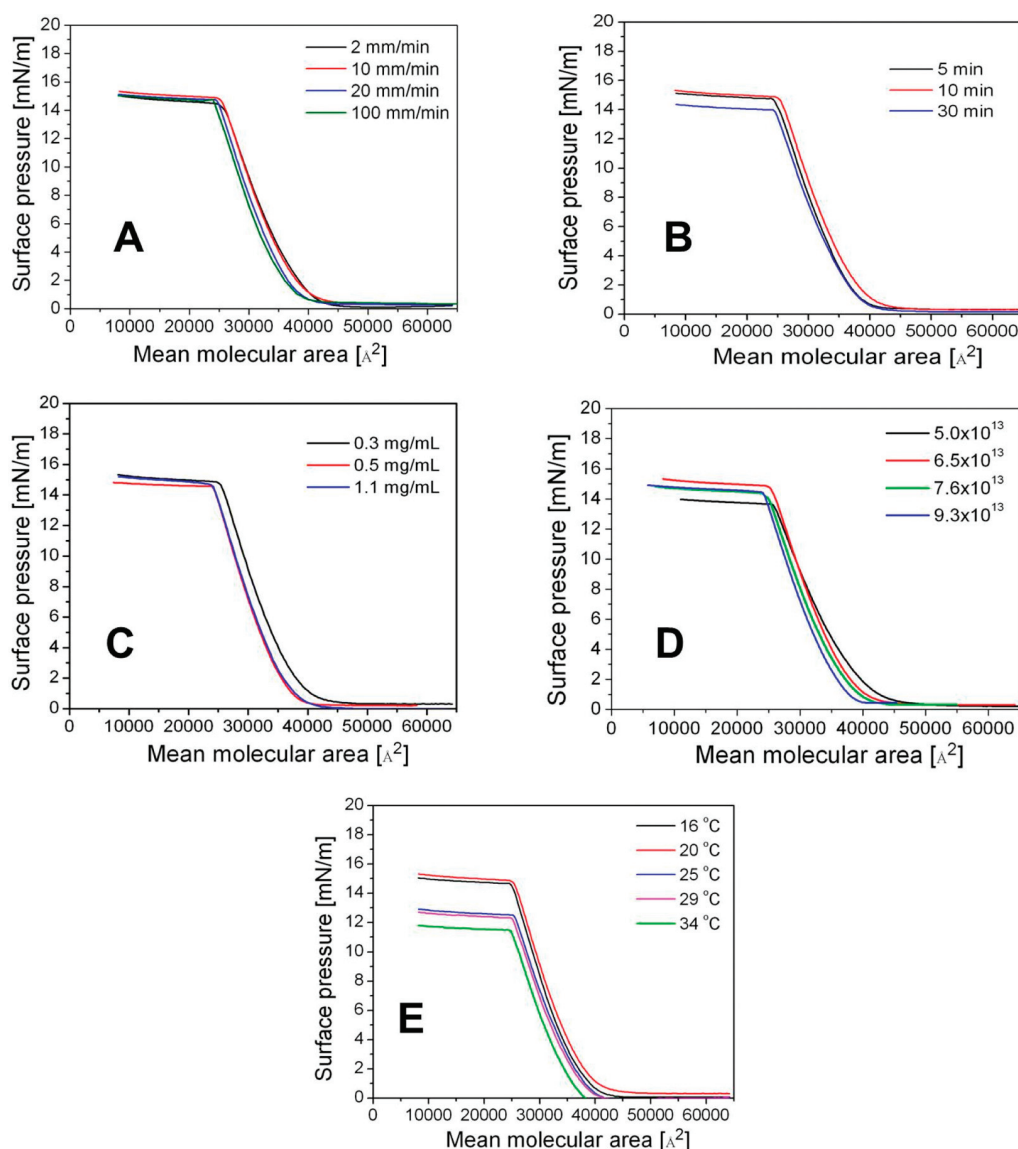


Figure 2. Surface pressure–area (π – A) isotherms of PHUE monolayers when changing experimental conditions: (A) compression speed, (B) solvent evaporation time, (C) spreading solution concentration, (D) number of molecules at the interface, and (E) subphase temperature.

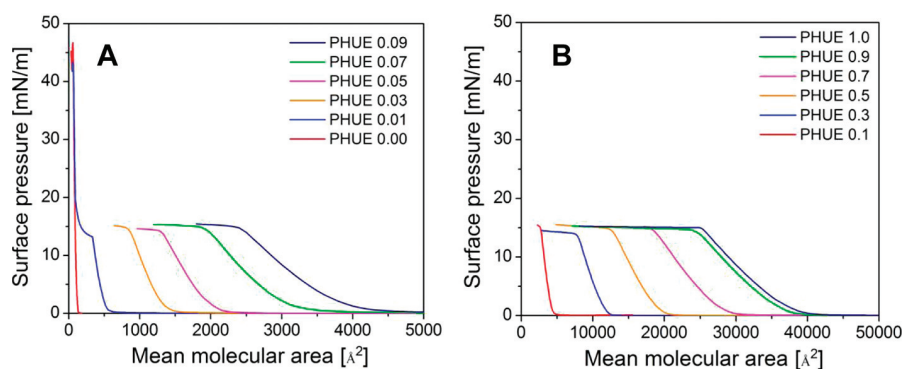


Figure 3. Surface pressure–area (π – A) isotherms from PHUE–DOPC mixed monolayers.

two-component monolayers, where two collapse pressures are recorded.⁴⁰ This was, however, impossible to detect here for

most of the mixed isotherms, due to the relatively small size of our Langmuir trough. We were able to record the second collapse

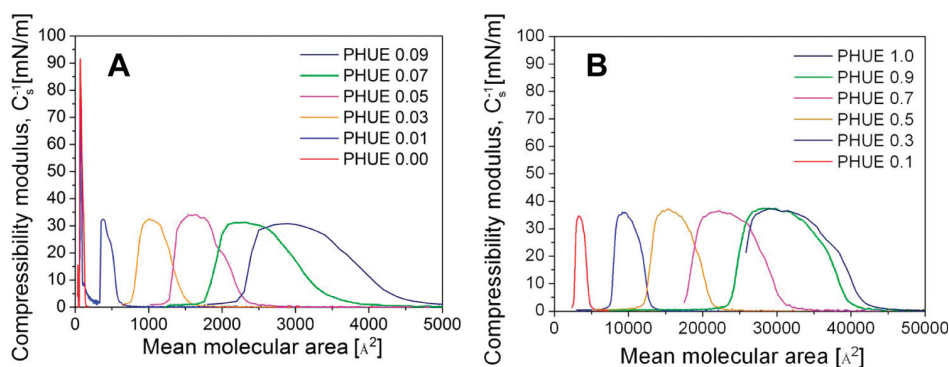


Figure 4. Compressibility modulus for PHUE–DOPC mixed films.

pressure only for the mixture with the lowest amount of the polymer ($X_{\text{PHUE}} = 0.01$). The second collapse pressure value corresponded to the value of the collapse pressure for the pure lipid (45 mN/m, at $56 \text{ \AA}^2/\text{molecule}$).

The compressibility moduli for two-component monolayers (Figure 4) slowly increased from 32 mN/m for the system with a low molar ratio of the polymer ($X_{\text{PHUE}} = 0.01$) to 37 mN/m for the mixture containing a high amount of PHUE ($X_{\text{PHUE}} > 0.9$). This means that the addition of DOPC slightly fluidizes the film by disturbing the packing of polymer molecules, but the presence of DOPC is not strong enough to force a really regular, ordered film organization as observed for pure DOPC and reflected by its compressibility modulus of ca. 90 mN/m. Nevertheless, this difference was too small to interpret in terms of changes in monolayer elasticity and indicated that the addition of lipid to the polymer did not change the phase behavior of the polymer film. For the mixture with the lowest molar ratio of polymer ($X_{\text{PHUE}} = 0.01$), we observed two maxima for the compressibility modulus, one close to the one of the pure polymer (approximately 32 mN/m) and the second one corresponding to the DOPC compressibility modulus (78 mN/m). These values confirm that the two investigated components are not miscible.

It should be noted that PHUE interactions with DOPC (or any other amphiphile) will depend on the polymer molecular mass. A polymer with different mass may, and most likely will, show different mixing behavior with the lipid. This will primarily result from differences in film organization—it can be expected that smaller but still different molecules will show denser packing and therefore stronger tendency to mix/demix.

In the case of the investigated polymer and lipid, there is a large size asymmetry between the film components; the mass of one polymer molecule is ca. 200 times larger than that of the lipid. This implies that, at the PHUE molar ratio of 0.1, the film still contains 22 times more polymer than lipid (mass ratio). In this situation, the addition of lipid does not change the global phase behavior of the polymer, and the very slight decrease in maximum C_s^{-1} for mixed films can be explained by the slight perturbation in polymer packing by the addition of lipid.

The isotherm data shown in Figure 3 were used to calculate the excess free energy of mixing (ΔG^{exc}) in the investigated systems from the following equation: $\Delta G^{\text{exc}} = N_A \int_0^\pi A^{\text{exc}} d\tau$, where A^{exc} is the excess area of mixing, π is surface pressure, and N_A is the Avogadro number.

The excess free energy of mixing gives quantitative information about miscibility and interactions between the two components. In short, a negative ΔG^{exc} suggests that miscibility is favored and

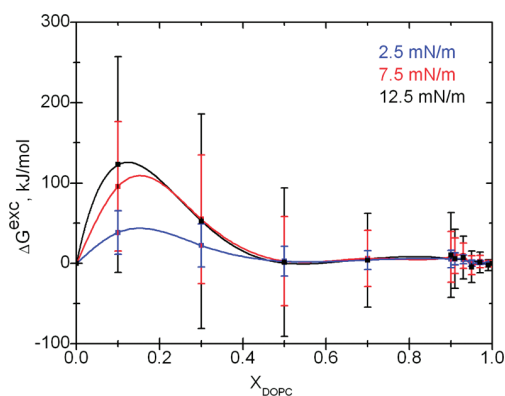


Figure 5. Excess free energy of mixing (ΔG^{exc}) versus composition for PHUE–DOPC mixed films.

the system becomes stabilized by attractive interactions. A positive ΔG^{exc} , on the contrary, generally indicates the tendency in the monolayer to partly or fully phase-separate (usually the case for compounds with very different chemical structures and/or dimensions). The excess free energies of mixing between the polymer and the lipid were calculated for monolayers at 2.5, 7.5, and 12.5 mN/m, following the approach described by Goodrich.⁴¹

As shown in Figure 5, the excess free energy of mixing for all mixtures was positive, which means that interactions between PHUE and DOPC are repulsive. Even though the errors calculated for ΔG^{exc} appear large (resulting from the large dimensions of the polymer and thus the error for the mean molecular area), a trend can be clearly observed, i.e., the surface pressure and molar ratio dependence.

The repulsion was stronger for more organized films (higher surface pressures), and one can notice two immiscibility regions. One is for the mixtures with the excess of polymer ($X_{\text{PHUE}} \geq 0.7$), for which the repulsion was much stronger, and the second for the mixtures with the excess of lipid ($X_{\text{PHUE}} \leq 0.5$), for which we observed weaker repulsion. This result showed that at high polymer molar ratios (where the amount of lipid is minimal), there was a stronger tendency to exclude lipid molecules from the well-organized polymer monolayer. With the higher lipid content, the packing of the polymer film was not so regular anymore, and further addition of the lipid did not change this situation much. Therefore, no changes in ΔG^{exc} are observed.

The values of the free energy of mixing for the investigated system were in a range of tenths of kJ/mol and appear reasonable

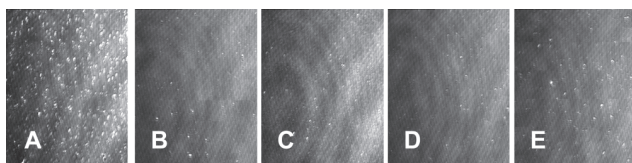


Figure 6. BAM images ($220 \times 250 \mu\text{m}^2$) of PHUE–DOPC monolayers at 12 mN/m. The polymer molar ratio is (A) 0.1, (B) 0.3, (C) 0.5, (D) 0.7, and (E) 0.9.

considering the structure and the molar mass of the polymer (165 500 g/mol), much higher than that of the lipid (786 g/mol). For example, mixed monolayers from DOPC with phytosterols (β -sitosterol and stigmasterol),⁴² which are small molecules (ca. 400 g/mol), give the ΔG^{exc} values smaller than 1 kJ/mol. When considering the amphiphilic block copolymers, e.g., poly(2-methyloxazoline)-*block*-poly(dimethylsiloxane)-*block*-poly(2-methyloxazoline) [PMOXA-PDMS-PMOXA, 23 200 g/mol], for mixed films with this lipid an increase of ΔG^{exc} to about a few kJ/mol was observed.²¹

Figure 6 presents BAM images of the mixed polymer–DOPC films (with different polymer–lipid molar ratios) at 12 mN/m. We observed a gray background and small white circular domains. Since BAM is sensitive to the film thickness, gray regions should correspond to the polymer monolayer (thinner due to less carbon atoms in side chains—C8), while white regions, to lipid domains (thicker, containing 18 carbon atoms), especially that we observed more domains for the PHUE–DOPC mixture at the molar ratio $X_{\text{PHUE}} = 0.1$. This means that the two materials tended to phase-separate in mixed monolayers, due to their size mismatch and very different chemical structures. The apparent inconsistency of BAM results with the calculated ΔG^{exc} (larger values at high polymer molar ratio; Figure 5) resulted from the fact that the excess free energy of mixing takes into account interactions at the level of individual molecules, while BAM is only able to visualize structures larger than $1-2 \mu\text{m}$ (the circular fringes in BAM images are due to the microscope geometry and optics). Quantitative analysis of the molecular distribution of the lipid between the mixed and pure phases with available techniques (e.g., ToF-SIMS) is impossible, due to the artifacts related to large differences in the ability of the two components to be desorbed from the film by heavy ions. Moreover, this method's resolution is not good enough to provide information at the molecular level.

4. CONCLUSIONS

This paper presents for the first time a thorough monolayer study of PHUE, a polymer from the medium-chain-length PHA family. PHUE formed stable monolayers at the air–water interface that were fairly insensitive to changes of experimental conditions. Their reversible behavior and high stability are advantageous for further thin film experiments using this polymer. Additionally, we investigated monolayer interactions between PHUE and DOPC. For all mixtures, interactions between polymer and lipid were repulsive and were stronger for the mixtures with the excess of the polymer. This effect is explained by the changes in polymer monolayer organization with the small addition of lipid. When more lipid is present in the polymer film, the energetic effect is not that strong anymore. However, the excess free energy of mixing remains positive, which indicates a tendency for the two

materials to phase-separate at the air–water interface. This notion was further confirmed by Brewster angle microscopy.

In summary, we have shown that PHUE is a good candidate for monolayer studies. This experimental approach is promising for further work, especially in the context of biomaterials development using PHAs, where the details of molecular organization and interactions with biologically relevant compounds may play an important role. We are currently optimizing PHUE and PHUE–lipid films to make them suitable for such applications.

■ ASSOCIATED CONTENT

S Supporting Information. Figure S1 showing the reversibility of the PHUE isotherm upon compression–expansion cycles and Figure S2 showing PHUE monolayer stability. This information is available free of charge via the Internet at <http://pubs.acs.org>.

■ AUTHOR INFORMATION

Corresponding Author

*E-mail: k.kita@unibas.ch.

Present Addresses

⁵Unilever R&D Port Sunlight, Quarry Road East, Bebington, Wirral CH63 3JW, U.K.

■ ACKNOWLEDGMENT

We thank the Swiss National Science Foundation and NCCR Nanoscience for financial support and Dr. Linda Thöny-Meyer for reading the manuscript.

■ REFERENCES

- (1) Chen, G.-Q.; Wu, Q. *Biomaterials* **2005**, *26* (33), 6565–6578.
- (2) Hartmann, R.; Hany, R.; Pletscher, E.; Ritter, A.; Witholt, B.; Zinn, M. *Biotechnol. Bioeng.* **2006**, *93* (4), 737–746.
- (3) Sodian, R.; Hoerstrup, S. P.; Sperling, J. S.; Daebritz, S.; Martin, D. P.; Moran, A. M.; Kim, B. S.; Schoen, F. J.; Vacanti, J. P.; Mayer, J. E. *Circulation* **2000**, *102* (19), 22–29.
- (4) Rezwani, K.; Chen, Q. Z.; Blaker, J. J.; Boccaccini, A. R. *Biomaterials* **2006**, *27* (18), 3413–3431.
- (5) Zinn, M.; Witholt, B.; Egli, T. *Adv. Drug Delivery Rev.* **2001**, *53* (1), 5–21.
- (6) Rai, R.; Keshavarz, T.; Roether, J. A.; Boccaccini, A. R.; Roy, I. *Mater. Sci. Eng., R-Rep.* **2011**, *72* (3), 29–47.
- (7) Rathbone, S.; Furrer, P.; Luebben, J.; Zinn, M.; Cartmell, S. *J. Biomed. Mater. Res., Part A* **2010**, *93A* (4), 1391–1403.
- (8) Kose, G. T.; Korkusuz, F.; Korkusuz, P.; Purali, N.; Ozkul, A.; Hasirci, V. *Biomaterials* **2003**, *24* (27), 4999–5007.
- (9) Sokolsky-Papkov, M.; Agashi, K.; Olaye, A.; Shakesheff, K.; Domb, A. J. *Adv. Drug Delivery Rev.* **2007**, *59* (4–5), 187–206.
- (10) Yun, S.; Gadd, G.; Latella, B.; Lo, V.; Russell, R.; Holden, P. *Polym. Bull.* **2008**, *61* (2), 267–275.
- (11) Foster, L. J. R.; Knott, R.; Sanguanchaipaiwong, V.; Holden, P. J. *Physica B* **2006**, *385*, 770–772.
- (12) Hazer, B.; Steinbuechel, A. *Appl. Microbiol. Biotechnol.* **2007**, *74* (1), 1–12.
- (13) Hany, R.; Bohlen, C.; Geiger, T.; Schmid, M.; Zinn, M. *Biomacromolecules* **2004**, *5* (4), 1452–1456.
- (14) Hany, R.; Boehlen, C.; Geiger, T.; Hartmann, R.; Kawada, J.; Schmid, M.; Zinn, M.; Marchessault, R. H. *Macromolecules* **2004**, *37*, 385–389.

- (15) Hany, R.; Hartmann, R.; Bohlen, C.; Brandenberger, S.; Kawada, J.; Lowe, C.; Zinn, M.; Witholt, B.; Marchessault, R. H. *Polymer* **2005**, *46* (14), 5025–5031.
- (16) Foster, L. J. R.; Schwahn, D.; Pipich, V.; Holden, P. J.; Richter, D. *Biomacromolecules* **2008**, *9* (1), 314–320.
- (17) Rosetti, C. M.; Maggio, B.; Oliveira, R. G. *Biochim. Biophys. Acta, Biomembr.* **2008**, *1778* (7–8), 1665–1675.
- (18) Sanchez-Gonzalez, J.; Galvez-Ruiz, M. J. Trends in Colloid and Interface Science IX. *Prog. Colloid Polym. Sci.* **1995**, *98*, 248–254.
- (19) Moore, B.; Knobler, C. M.; Broseta, D.; Rondelez, F. *J. Chem. Soc., Faraday Trans. 2* **1986**, *82* (10), 1753–1761.
- (20) Hoenic, D.; Moebius, D. *J. Phys. Chem.* **1991**, *95*, 4590–4592.
- (21) Kita-Tokarczyk, K.; Iteł, F.; Grzelakowski, M.; Egli, S.; Rossbach, P.; Meier, W. *Langmuir* **2009**, *25*, 9847–9856.
- (22) Nobes, G. A. R.; Holden, D. A.; Marchessault, R. H. *Polymer* **1994**, *35* (2), 435–437.
- (23) Lambeek, G.; Vorenkamp, E. J.; Schouten, A. J. *Macromolecules* **1995**, *28*, 2023–2032.
- (24) Jo, N.-J.; Iwata, T.; Lim, K. T.; Jung, S.-H.; Lee, W.-K. *Polym. Degrad. Stabil.* **2007**, *92* (7), 1199–1203.
- (25) Frey, S. L.; Zhang, D.; Carignano, M. A.; Szeleifer, I.; Lee, K. Y. C. *J. Chem. Phys.* **2007**, *127* (11), 114904.
- (26) Lygre, H.; Moe, G.; Skålevik, R.; Holmsen, H. *Eur. J. Oral Sci.* **2003**, *111* (3), 216–222.
- (27) Amado, E.; Blume, A.; Kressler, J. *React. Funct. Polym.* **2009**, *69* (7), 450–456.
- (28) Zinn, M.; Hany, R. *Adv. Eng. Mater.* **2005**, *7* (5), 408–411.
- (29) Furrer, P.; Hany, R.; Rentsch, D.; Grubelnik, A.; Ruth, K.; Panke, S.; Zinn, M. *J. Chromatogr. A* **2007**, *1143* (1–2), 199–206.
- (30) Terada, M.; Marchessault, R. H. *Int. J. Biol. Macromol.* **1999**, *25* (1–3), 207–215.
- (31) Bassas, M.; Marques, A. M.; Manresa, A. *Biochem. Eng. J.* **2008**, *40* (2), 275–283.
- (32) Funasaki, N.; Nakagaki, M. *Bull. Chem. Soc. Jpn.* **1975**, *48* (10), 2727–2731.
- (33) Lamer, V. K.; Aylmore, L. A. G.; Healy, T. W. *J. Phys. Chem.* **1963**, *67*, 2793–2795.
- (34) Salz, E.; Hummel, J. P.; Flory, P. J.; Plavsic, M. *J. Phys. Chem.* **1981**, *85*, 3211–3215.
- (35) Harkins, W. D., *Physical Chemistry of Surface Films*; Reinhold: New York, 1952.
- (36) Cheyne, R. B.; Moffitt, M. G. *Langmuir* **2006**, *22*, 8387–8396.
- (37) Barton, S. W.; Thomas, B. N.; Flom, E. B.; Rice, S. A.; Lin, B.; Peng, J. B.; Ketterson, J. B.; Dutta, P. *J. Chem. Phys.* **1988**, *89* (4), 2257–2270.
- (38) Stine, K. J.; Stratmann, D. T. *Langmuir* **1992**, *8*, 2509–2514.
- (39) Buzin, A. I.; Sautter, E.; Godovsky, Y. K.; Makarova, N. N.; Pechhold, W. *Colloid Polym. Sci.* **1998**, *276* (12), 1078–1087.
- (40) Dynarowicz-Łątka, P.; Kita, K. *Adv. Colloid Interface Sci.* **1999**, *79* (1), 1–17.
- (41) Goodrich, F. C. *Proceedings of the International Congress of Surface Activity* **1957**, *1*, 85–91.
- (42) Hąc-Wydro, K.; Wydro, P.; Jagoda, A.; Kapusta, J. *Chem. Phys. Lipids* **2007**, *150* (1), 22–34.

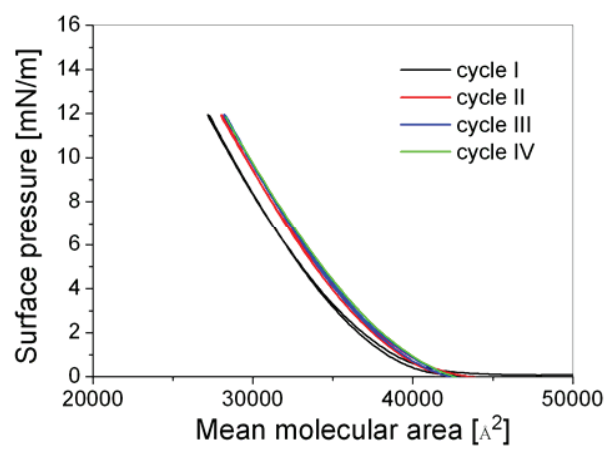


Figure S1. Compression-expansion cycles of PHUE monolayer.

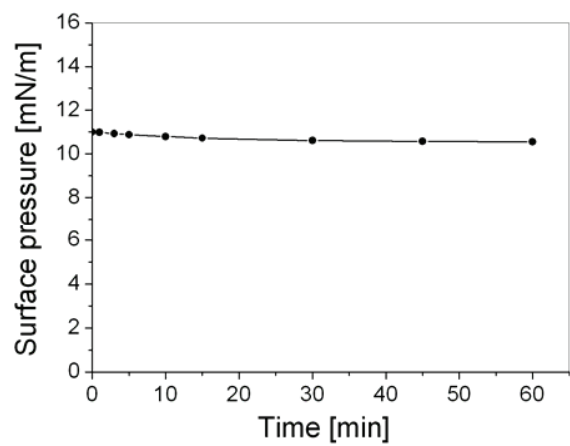


Figure S2. PHUE monolayer stability (constant-area experiment at 28 400 Å²/molecule).

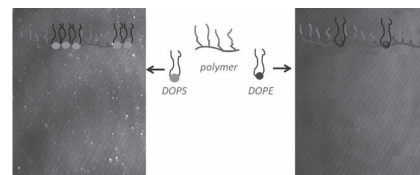
3.2. PHUE-lipid mixed films

Results were published in: “Head group influence on lipid interactions with a polyhydroxyalkanoate biopolymer”, *Macromolecular Chemistry and Physics*, **2012**, 213 (18), 1922-1932, A. Jagoda, M. Zinn, W. Meier, K. Kita-Tokarczyk.

Head Group Influence on Lipid Interactions With a Polyhydroxyalkanoate Biopolymer

Agnieszka Jagoda, Manfred Zinn, Wolfgang Meier,
Katarzyna Kita-Tokarczyk*

Poly([R]-3-hydroxy-10-undecenoate) (PHUE) is a biodegradable/biocompatible polyester from polyhydroxyalkanoates (PHAs) family, used in biomedical applications. PHA's introduction to the body may have implications on cell membrane stability—this motivates studies of interactions between PHAs and phospholipids, main membrane constituents. Interaction analysis in PHUE monolayers with two phospholipids (different hydrophilic groups), phosphatidylserine (DOPS), and phosphatidylethanolamine (DOPE), shows that repulsive interactions between PHUE and DOPS and attractive between PHUE and DOPE resulted from different lipid headgroup size and orientation at the air–water interface (PE, parallel to the interface, attracted PHUE via hydrogen bonds, ion–dipole, and dipole–dipole interactions).



1. Introduction

Polyhydroxyalkanoates (PHAs) are polyesters synthesized by living microorganisms.^[1] Depending on the substrate and the bacterial strain used for synthesis, one can tune the monomer composition and thus change polymer properties.^[2] A number of features, for example, the possibility to control the polymer crystallinity (by monomer composition), easiness of staining,^[3] or processing into fibers,^[4] and most importantly biodegradability and biocompatibility,^[5,6] make PHAs very interesting candidates for various applications. In the biomedical field, they can be used as drug delivery carriers,^[7] in wound management (sutures, skin substitutes) or as implants, for example in the cardiovascular system (stents, vascular grafts, or heart valves).^[3,8]

In biomedical applications, any foreign material introduced to the body will interact not only with the serum but also with cellular membrane components. Understanding these interactions should be a fundamental step in the development of new materials for biomedical applications. For PHAs, however, there have been no reports so far on how PHA polymers interact with physiologically relevant molecules, apart from our previous paper,^[9] which focused more on one model system, method development, and optimization. We have shown that the Langmuir monolayer systems are useful to investigate interactions between the polymer and phospholipids.

Langmuir (insoluble) monolayers form when amphiphilic or hydrophobic molecules spread on the air–water interface and self-organize in two dimensions. Such thin films are valid models to study material behavior at the molecular level in asymmetric (interfacial) environments. Analysis of mixed films provides quantitative information about interactions in the monolayer, defining mixing/demixing of the components. Mixed monolayers have been studied to understand interactions between, for example, cell membrane components themselves,^[10–15] in combination with drugs^[16,17] or substances provided to the human body with a daily diet.^[18]

Few reports exist on PHA monolayers, focusing rather on short-chain-length PHAs.^[19–21] Regarding medium-chain-length (mcl) PHAs, we reported the

A. Jagoda, Prof. W. Meier, Dr. K. Kita-Tokarczyk^[+]
Department of Chemistry, University of Basel,
4056 Basel, Switzerland
E-mail: katarzyna.kita@mail.com
Prof. M. Zinn
Bioprocesses and Biomaterials, Institute of Life Technologies,
University of Applied Sciences Western Switzerland
(HES-SO Valais), 1950 Sion, Switzerland
Present address: Unilever R&D Port Sunlight, Bebington,
Wirral, CH63 3JW, UK

behavior of poly([R]-3-hydroxy-10-undecenoate) (PHUE) at the air–water interface,^[9] showing that PHUE forms stable and elastic monolayers. A simple PHA–lipid (1,2-dioleoyl-*sn*-glycero-3-phosphocholine; DOPC) system allowed us to validate the monolayer approach to study the interactions. We found that PHUE and DOPC phase-separate, with repulsive interactions indicated by positive excess free energy of mixing. Motivated by those results, we found it important to provide a more comprehensive picture of the PHA–lipid interaction dependence on the properties of lipid head group.

2. Experimental Section

2.1. Polymer Synthesis and Characterization

The synthesis, purification, and analysis of PHUE were reported before.^[9,22] Briefly, PHUE is a statistical copolymer of 3-hydroxy- ω -alkenoate monomers containing 7, 9, and 11 carbon atoms (Figure S1, Supporting Information), with the molecular weight of $\bar{M}_w = 294\,600\text{ g mol}^{-1}$, $\bar{M}_n = 165\,600\text{ g mol}^{-1}$, and polydispersity index (PDI) of 1.8. It has to be noted that the biosynthesis route, from which PHUE originates, is an excellent means to control the polymer properties, yet it renders random polymers that contain a certain amount of shorter chains attached to the polyester backbone. This is, however, intrinsic to the synthesis due to β -oxidation and cannot be avoided.^[23] As a result, the investigated polymer is a random terpolymer. This should not, however, influence the interactions with lipids (compared with pure homopolymers' interactions with lipids). In particular, considering mixed monolayers from small insoluble amphiphiles with chains of the same chemistry and small length difference, their mixing properties show ideal or almost ideal mixing behavior.^[24,25] If the interactions in the film do not change with the addition of slightly shorter/longer chains, the monolayer morphology should not change, either.

2.2. Lipids

DOPS [(1,2-dioleoyl-*sn*-glycero-3-phospho-L-serine-sodium salt), mass 810 g mol^{-1}] and DOPE [(1,2-dioleoyl-*sn*-glycero-3-phosphoethanolamine), mass 744 g mol^{-1}] were purchased from Avanti Polar Lipids, Inc. (Alabama, USA) as chloroform solutions (10 mg mL^{-1}). Both lipids were in *cis* configuration and had a double bond at the ninth carbon atom. To avoid oxidation, stock solutions were stored in a freezer under argon. Diluted solutions (1 mg mL^{-1} in chloroform) were used for experiments.

2.3. Langmuir Monolayers

Monolayer experiments were performed as described before,^[9] using a KSV Inc. (Finland) Langmuir Teflon® trough (area 420 cm^2) together with the Brewster angle microscopy (BAM) setup (EP³SW system, Accurion, Göttingen, Germany). Bi-distilled water (pH 5.5) was used as subphase.

Polymer–lipid mixtures ($500\text{ }\mu\text{L}$, 1 mg mL^{-1}) at different molar ratios (from 0.1 to 0.9 in steps of 0.2) were prepared freshly by mixing appropriate volumes of PHUE and lipid solutions in chloroform. It should be noted that the polymer molar mass is about 200 times larger than those of the investigated lipids. Therefore, even for the lowest molar ratio of polymer ($X_{\text{PHUE}} = 0.1$) in the mixed film, the polymer will be in a great (ca. 20 times) mass excess. Mixed monolayers were prepared by spreading dropwise an adequate number of molecules (usually 10^{13} – 10^{15}). After the solvent has evaporated, the monolayers were compressed at 10 mm min^{-1} and simultaneously imaged with BAM.

3. Results and Discussion

Properties of Langmuir monolayers from the pure components used for this study were published before.^[9,26–28] For reference, surface pressure–area (π – A) isotherm of PHUE ($X_{\text{PHUE}} = 1$) is shown together with the isotherms of mixed films (Figure 1A and 4A). Starting from about $40\,000\text{ }\text{\AA}^2$ per

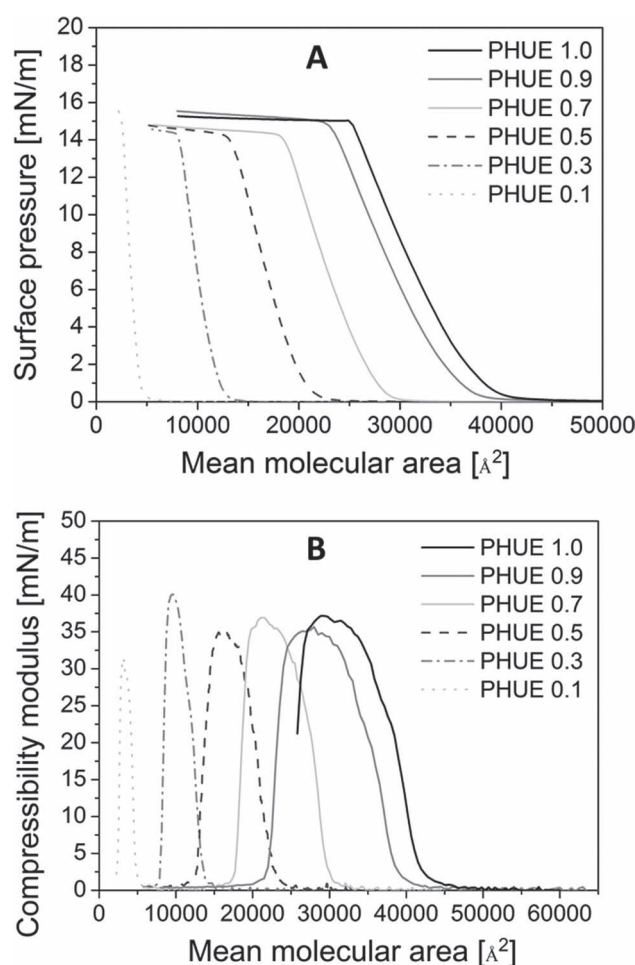


Figure 1. PHUE-DOPS films: (A) π – A isotherms, (B) compressibility moduli.

molecule, a smooth monolayer was observed with BAM (cf. also Figure 3F and 6F), which collapsed at about 15 mN m^{-1} ($25\,000 \text{ \AA}^2$ per molecule). The compressibility modulus $C_s^{-1} \approx 36 \text{ mN m}^{-1}$ suggested the liquid-expanded phase of the film.

DOPS and DOPE have identical hydrophobic tails (18:1(9Z)/18:1(9Z)), and different hydrophilic groups (Figure S2 and S3, Supporting Information). Briefly, for both lipids, the surface pressure started to increase at about 110 \AA^2 per molecule, and the monolayers collapsed at 52 and 47 \AA^2 per molecule for DOPS and DOPE, respectively. The difference in mean molecular areas is due to the differences in size and orientation of the head groups at the air–water interface (see “Comparison of mixed monolayers from PHUE with DOPS, DOPE, and DOPC” for discussion). The maximum compressibility modulus values were similar (108 and 104 mN m^{-1} for DOPS and DOPE, respectively), corresponding to liquid-condensed films.

3.1. Two-Component Monolayers

Data from π -A isotherms were used to calculate the compressibility modulus (phase behavior), excess area per molecule (type of interactions), and excess free energy of mixing (interaction strength) at different surface pressures. The mixed films were also imaged with BAM to analyze monolayer homogeneity/phase separation.

The excess area of mixing (A^{exc}) provides qualitative information about the miscibility of the components in the mixed monolayer (see Supporting Information for details). Additional information about miscibility and molecular interactions in the film can be obtained from the excess free energy of mixing, ΔG^{exc} , calculated as:

$$\Delta G^{\text{exc}} = N_A \int_0^\pi A^{\text{exc}} d\pi \quad (1)$$

where N_A is the Avogadro number, π -surface pressure, and A^{exc} -excess area of mixing. Systems in which components tend to mix well (attractive interactions are favored), have negative ΔG^{exc} , while a positive ΔG^{exc} indicates phase separation and repulsive interactions. For PHUE-lipid systems, both A_{id} (molecular area in a mixed monolayer for non-interacting components) and ΔG^{exc} were calculated at 2.5 , 7.5 , and 12.5 mN m^{-1} .

3.2. PHUE and DOPS Mixed Monolayers

π -A isotherms from PHUE and DOPS mixed films are shown in Figure 1A. Similarly to PHUE-DOPC films,^[9] the addition of lipid (DOPS) to the polymer film caused a decrease of a mean molecular area of the corresponding binary films. The collapse pressure values were the same

for all the mixed films (15 mN m^{-1}), matching the collapse pressure of the pure polymer film, and indicating that PHUE and DOPS did not mix at the molecular level. For films from immiscible components, one could in fact observe two collapse pressures, corresponding to the individual component each.^[29] In all our systems, masswise, there was much less lipid than polymer. Therefore, it was unlikely that we would be able to force the lipid molecules to collapse and record their collapse pressure. We were able to detect the second collapse pressure (corresponding to the π_{coll} of the lipid) only for the mixture with a very asymmetric molar ratio ($X_{\text{PHUE}} = 0.01$, $X_{\text{DOPS}} = 0.99$), and the smallest mass ratio of 2 to 1 (polymer:lipid) (Figure S4A, Supporting Information).

Figure 1B shows the compressibility moduli, $C_s^{-1} = A \cdot \left(\frac{\partial \pi}{\partial A}\right)_T$ for PHUE-DOPS films, the values below 50 mN m^{-1} indicate a liquid-expanded state of a monolayer. There was no visible trend relating the polymer-lipid molar ratio and compressibility moduli values. Even in the film with high molar excess of lipid ($X_{\text{PHUE}} = 0.1$), the lipid did not force a more regular packing of the film, and the increase of the compressibility modulus. Further addition of the lipid up to $X_{\text{DOPS}} = 0.99$, leading to a less asymmetric polymer to lipid mass ratio, also did not influence the compressibility moduli (Figure S4B, Supporting Information). In summary, the introduction of DOPS to the polymer film does not change its phase behavior.

A comparison of the experimental (solid lines) and theoretical (dotted lines) mean molecular areas from PHUE-DOPS mixed monolayers is shown in Figure 2A. For all the investigated mixtures, the experimental values were slightly positive, which could be assigned to repulsion between molecules. These values did not show large deviations from linearity as a function of the polymer molar ratio, suggesting that PHUE and DOPS either mix well or are immiscible.

The excess free energy of mixing for PHUE and DOPS (Figure 2B) was positive (repulsive interactions were favored) for all molar ratios, which confirmed immiscibility of the polymer and the lipid. An increase of ΔG^{exc} with surface pressure is due to denser molecular packing, where the interactions are more pronounced. The errors of the excess free energy of mixing are high (see Error Analysis, Supporting Information), and even though they do not allow for quantitative analysis of interaction strength, nonetheless valuable trends can be inferred from the calculations.

The values of the excess free energy of mixing PHUE and DOPS were, not surprisingly, in the same range (tens of kJ mol^{-1}) as the values for the PHUE-DOPC system.^[9] Compared with the polymeric films obtained from, for example, poly(2-methyloxazoline)-*block*-poly(dimethylsiloxane)-*block*-poly(2-methyloxazoline) [PMOXA-PDMS-PMOXA] (mass $23\,000 \text{ g mol}^{-1}$), mixed

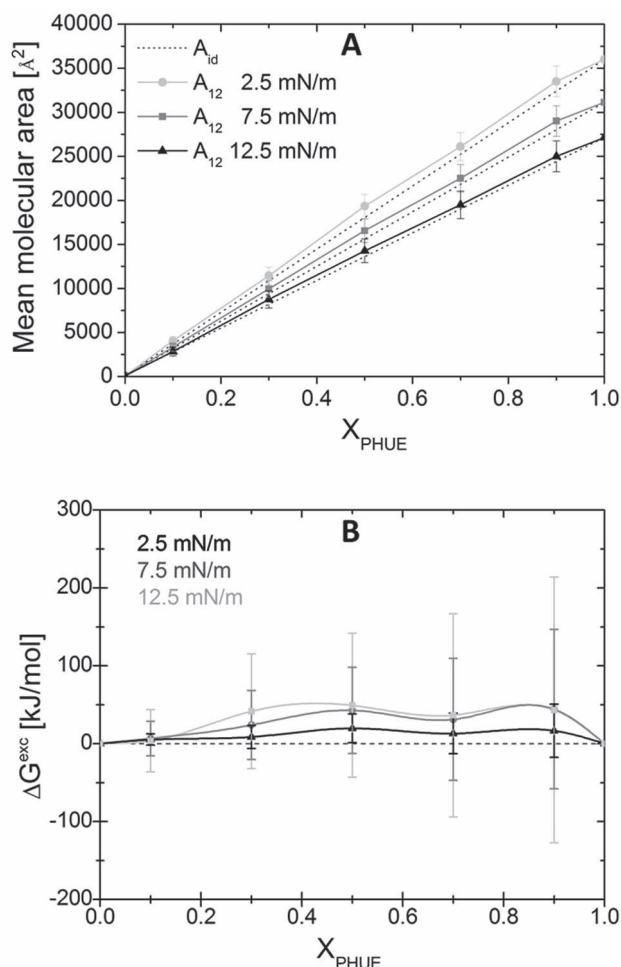


Figure 2. PHUE–DOPS films: (A) the comparison of experimental (solid lines) and theoretical (dotted lines) mean molecular areas and (B) excess free energy of mixing, versus molar ratio of PHUE.

with DOPC^[30] or alamethicin (an antimicrobial peptide),^[31] an increase by approximately one order of magnitude (from a few kJ mol^{-1}) was observed for the present system. Larger ΔG^{exc} can be attributed to the larger size of the polymer used here and therefore larger contribution of weak interactions.

It has to be noted that despite the interactions between these two components are repulsive, it does not disqualify them from using in material science. The interactions between the components, for example, when considering polymer-based materials interacting with cell membranes, should be neither strongly repulsive nor strongly attractive. In the first case, too strong repulsion would inhibit cell adhesion, an important step in integration of biomaterials. On the contrary, too strong attraction between the polymer and cell membrane phospholipids would lead to membrane destruction.^[32]

PHUE–DOPS monolayers were visualized with BAM, the images recorded at 12 mN m^{-1} are shown in Figure 3.

For all molar ratios, gray background with white domains appeared. As BAM is sensitive to the film thickness (thicker objects appear brighter), we identified the white domains as lipid domains.^[9] These results provide strong evidence that PHUE and DOPS phase separate at the micrometer scale at all the investigated polymer–lipid molar ratios. The domain formation implies that interactions between pure components are stronger than the possible interactions between the polymer and the lipid, as discussed further (“Comparison of mixed monolayers from PHUE with DOPS, DOPE, and DOPC”).

In summary, the π – A isotherms, collapse pressure behavior, the excess area of mixing, and BAM imaging revealed the immiscibility of PHUE and DOPS (Table 1); all of the investigated mixed films were in liquid expanded state; and the excess free energy of mixing indicated the repulsive interactions between the polymer and the lipid. We conclude that PHUE and DOPS phase separate at the molecular level. Detailed analysis of PS head group charge influence on the interactions with PHUE in binary films is discussed in “Comparison of mixed monolayers from PHUE with DOPS, DOPE, and DOPC”.

3.3. PHUE and DOPE Mixed Monolayers

Figure 4A shows the π – A isotherms from PHUE–DOPE films. Similarly to other lipids (DOPC,^[9] DOPS) mixed with PHUE, the mean molecular area decreased linearly (Figure 5A) with increasing DOPE molar ratio. The collapse pressure of the mixed films remained at 15 mN m^{-1} , corresponding to the polymer film collapse pressure and again suggested immiscibility of the two components.

Regarding the compressibility moduli in mixed PHUE–DOPE systems (Figure 4B), they remain in the similar range as for other PHUE–lipid systems (below 50 mN m^{-1} , liquid expanded phase), yet with DOPE a clear trend was observed: the compressibility modulus decreased with the lipid molar ratio, from 37 mN m^{-1} (pure polymer), to 31 mN m^{-1} (mixed film with the lowest polymer molar ratio- $X_{\text{PHUE}} = 0.1$). That suggested that DOPE molecules disturbed the regular packing of the polymer film, making it more liquid, and at the same time became homogeneously distributed across the film. As a consequence, with DOPE, one can control the fluidity of the mixed film by varying the polymer-to-lipid molar ratio.

The experimental mean molecular areas were slightly smaller than the calculated ones (Figure 5A), meaning that the excess area of mixing was negative, which could suggest condensation of the monolayer caused by attractive interactions between the polymer and the lipid molecules. However, the linear trend does not indicate large deviations from ideal mixing behavior. Furthermore, the excess free energy of mixing (Figure 5B) with its negative values for all polymer–lipid ratios (indicating attractive

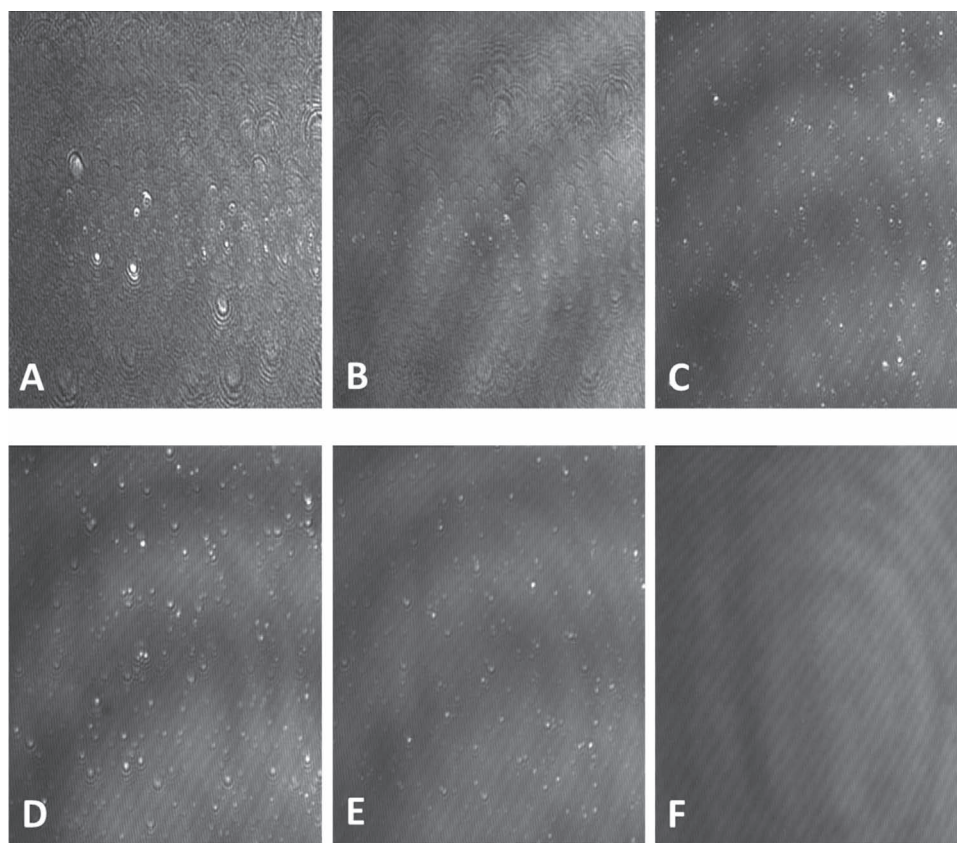


Figure 3. BAM images ($220 \times 250 \mu\text{m}$) from PHUE–DOPS films at 12 mN m^{-1} . The polymer molar ratio is: (A) 0.1, (B) 0.3, (C) 0.5, (D) 0.7, (E) 0.9, (F) 1.0.

interactions) also confirmed better miscibility of PHUE and DOPE compared with PHUE–DOPC and –DOPS. The absolute values of ΔG^{exc} were in the range of tens of kJ mol^{-1} , similarly to PHUE mixed films with DOPS and DOPC.^[9]

BAM images of the PHUE–DOPE films are shown in Figure 6. We could again observe gray background with white domains (lipid aggregates), however, these only started to be clearly visible for the higher proportion of lipid ($X_{\text{PHUE}} \leq 0.3$), whereas for mixtures with DOPC and DOPS domains were visible already at very low lipid molar ratio ($X_{\text{PHUE}} = 0.9$). The BAM images suggest that to some extent the polymer and DOPE were miscible (meaning the interactions between the polymer and the lipid were favored).

To summarize (Table 2), for PHUE–DOPE films, we have observed that: (i) the π –A isotherms, collapse pressure, and the experimental mean molecular areas behavior were similar to PHUE–DOPS and PHUE–DOPC mixed films, suggesting immiscibility between the two components; (ii) the compressibility modulus values indicated the liquid-expanded state of mixed monolayers, with C_s^{-1} decreasing upon lipid addition; (iii) interestingly, the excess free energy of mixing were negative, suggesting the attractive nature of interactions between PHUE and DOPE; (iv) BAM images showed phase separation only for high excess of lipid ($X_{\text{DOPE}} \geq 0.7$). It appears plausible that the isotherm measurements are insufficient to conclude about miscibility/immiscibility in these systems, as the isotherm behavior is similar.

Table 1. A summary of the results for PHUE–DOPS films.

| Parameter | Result | Miscibility |
|-------------------------|--|----------------------------------|
| π_{coll} | $\pi_{\text{coll mix}} = \pi_{\text{coll PHUE}}$ | Immiscibility |
| A_{12} | linearly decreases; $A_{12} > A_{\text{id}}$ | Immiscibility; repulsion |
| ΔG^{exc} | Positive | Repulsion |
| BAM images | Domains | Immiscibility (phase separation) |

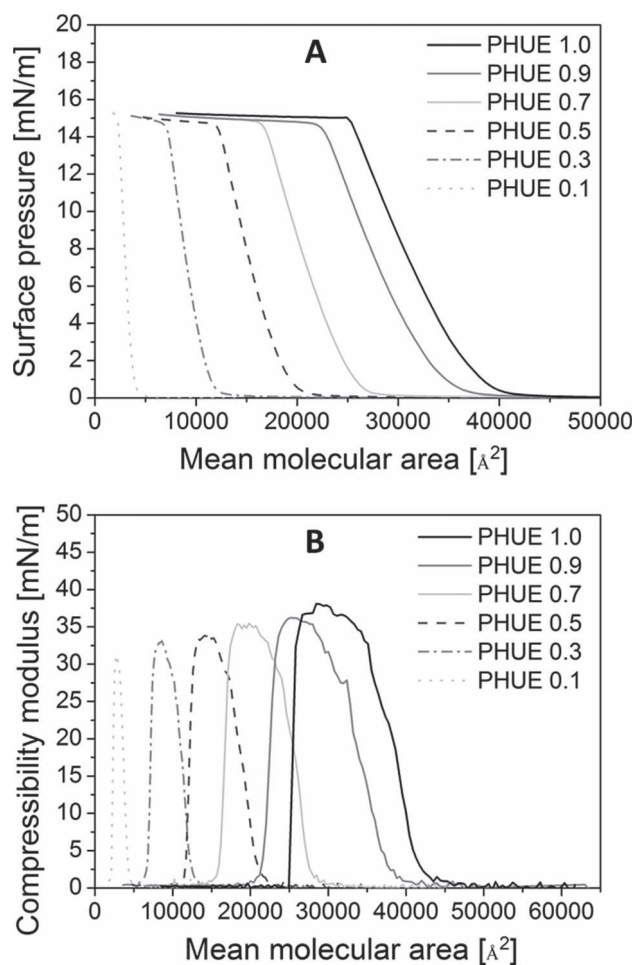


Figure 4. PHUE-DOPE films: (A) π -A isotherms, (B) compressibility moduli.

Considering, however, molecular structures of the lipids and a detailed analysis of the mixing behavior (A_{12} , ΔG^{exc}), different interactions become apparent between the polymer and respective lipids, caused by difference in the lipid size and its orientation at the interface, as discussed further.

3.4. Comparison of Mixed Monolayers From PHUE with DOPS, DOPE, and DOPC

The lipids studied here and previously (DOPC)^[9] have identical hydrophobic parts, but different hydrophilic heads (phosphatidylserine-PS, phosphatidylethanolamine-PE, phosphatidylcholine-PC, Figure S2, Supporting Information), and thus different size, polar group thickness, ionization constants, and dipole moments (Table 3). We aim to explain here the effect of these parameters on the interactions between the polymer and lipid, and the resulting organization and properties of mixed films.

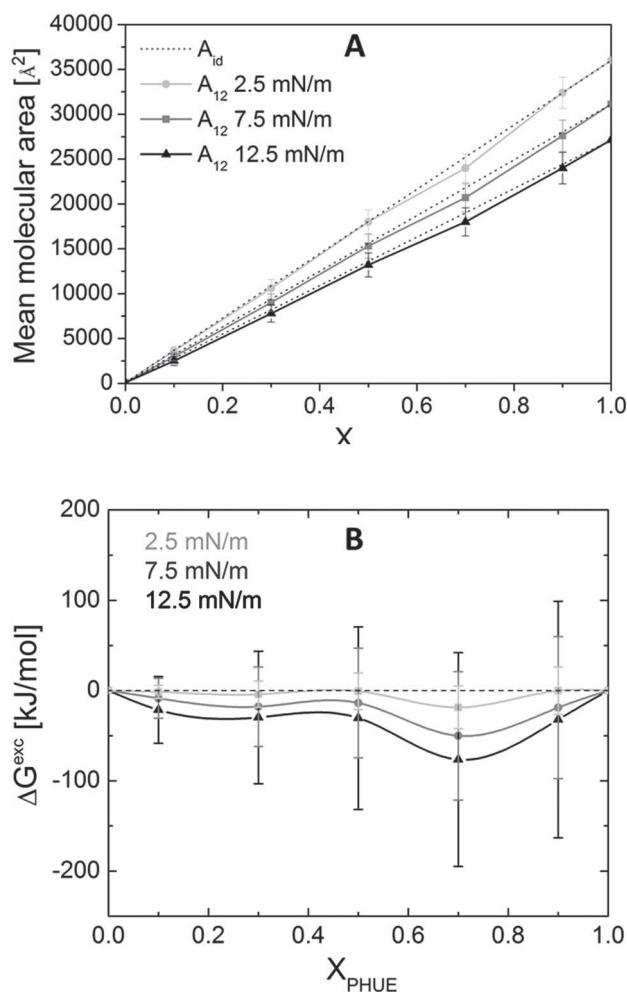


Figure 5. PHUE-DOPE films: (A) the comparison of experimental (solid lines) and theoretical (dotted lines) mean molecular areas and (B) excess free energy of mixing, versus molar ratio of PHUE.

3.5. Size of the Head Group

PS is a charged group, and for that reason, here we only compare the results for PHUE-DOPE with PHUE-DOPC mixed films.^[9] As seen in Figure S2 (Supporting Information), the only structural difference between these two lipids are the substituents in the amine group; PC contains three methyl groups, while PE contains three hydrogen atoms. Since PC is much larger than PE, the parameters to be taken into account when discussing the size of the lipid head group are its orientation with respect to the interface, hydration shell, presence of hydrogen bonds, etc. PC groups were reported to orient perpendicular to the air-water interface in lipid monolayers, whereas PE groups are arranged parallel.^[33–35] That difference was explained as a result of increased size of the PC head group, causing steric repulsion, and also due to the inability of spatially

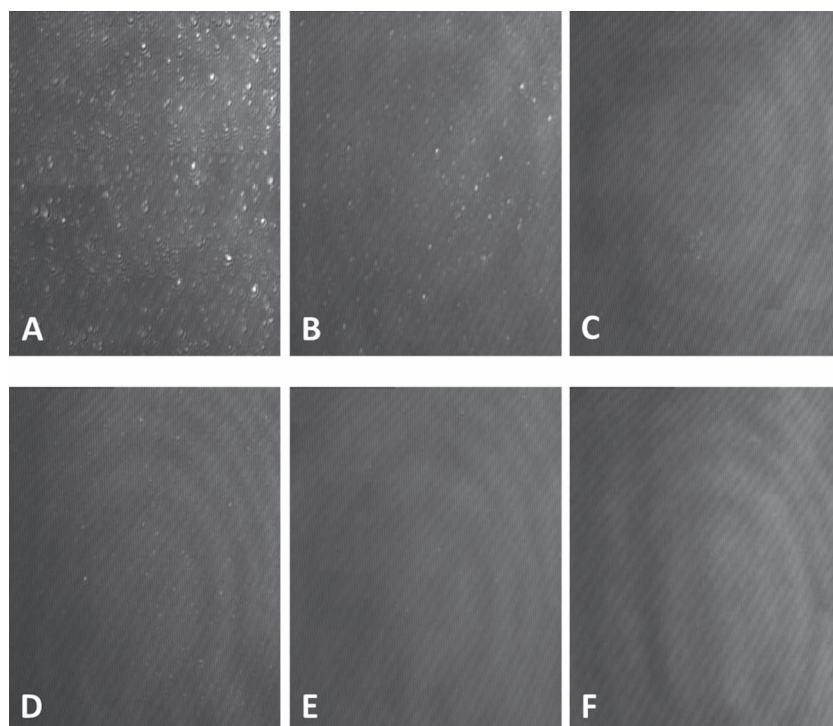


Figure 6. BAM images ($220 \times 250 \mu\text{m}$) from PHUE–DOPE films at 12 mN m^{-1} . The polymer molar ratio is: (A) 0.1, (B) 0.3, (C) 0.5, (D) 0.7, (E) 0.9, (F) 1.0.

extensive PC group to form hydrogen bonds.^[22] The parallel orientation of the PE head groups leads to the alternating positions of phosphate (negatively charged) and amine (positively charged), and as a result electrostatic attraction between the neighboring molecules.^[22] Among PC groups, if aligned perpendicular to the air–water interface, electrostatic repulsion occurs. Incorporation of hydrogen-bonded water molecules among phosphate oxygens decreases the repulsion strength and leads to stronger hydration of PC groups in comparison to PE.^[36] Consequently, the energy of compression was found higher for DOPC ($21.87 \text{ kJ mol}^{-1}$) than for DOPE ($17.32 \text{ kJ mol}^{-1}$).^[26,34] Moreover, it is known that PE monolayers are stabilized by hydrogen bonds (see Figure 7A) between the ammonium hydrogens and phosphate oxygens.^[34,37] All these factors influence the thickness of the polar group, which is larger for PC than for PE (Hauser et al.^[34] reported the thickness of the 1,2-dilauroyl-sn-glycero-3-phosphatidylethanolamine polar part at

7.9 \AA and for 1,2-dimyristoyl-sn-glycero-3-phosphatidylcholine 10.4 \AA ^[34]; similar values, 8 \AA for PE and 11 \AA for PC, were obtained from X-ray experiments in bulk.^[33])

Altogether, the absence of methyl groups, intermolecular hydrogen bonds, smaller hydration shell, and parallel orientation of the head group results in PE group occupying a smaller area at the air–water interface compared to PC (good agreement with mean molecular areas for DOPC- 55 \AA^2 , and DOPE- 47 \AA^2 ; Figure S3, Supporting Information, and Table 3).

The difference in size and thickness of the PC and PE groups is likely to affect lipid interactions with the PHUE polymer. It is worth to note that, even though PHUE is a statistical copolymer with certain amount of the shorter chains, the polymer interactions with lipids head groups take place mostly in the hydrophilic part of the monolayer (polyester backbone), which is not affected by side chain lengths. The excess free energy of mixing for PHUE–

DOPE monolayers was negative, which indicated attractive interactions. To the contrary, ΔG^{exc} for the PHUE–DOPC mixed films, was positive, and suggested repulsion between the two components.^[9] As the PC head group is much bigger than PE, it will constitute steric hindrance, inhibiting the tight packing of the monolayer components. In fact, the polymer tended to exclude DOPC from the film even at very low molar ratio of the lipid (lipid domain formation).

An opposite situation was observed with DOPE. Smaller lipid molecules, arranged parallel to the air–water interface, separate the polymer molecules, and participate in attractive interactions. It means that the strength of the hydrogen bonds between the lipid molecules is overcome by polymer–lipid interactions. These may be also hydrogen bonds, as PHUE contains many oxygen atoms (which could serve as hydrogen-bond acceptors) and terminal hydroxyl groups (donors of hydrogen bond).

Table 2. A summary of the results for PHUE – DOPE films.

| Parameter | Result | Miscibility |
|-------------------------|--|---|
| π_{coll} | $\pi_{\text{coll mix}} = \pi_{\text{coll PHUE}}$ | Immiscibility |
| A_{12} | linearly decreases; $A_{12} < A_{\text{id}}$ | Immiscibility; attraction |
| ΔG^{exc} | Negative | Attraction |
| BAM images | Domains $X_{\text{PHUE}} \leq 0.3$ | Immiscibility $X_{\text{PHUE}} \leq 0.3$ Miscibility $X_{\text{PHUE}} \geq 0.5$ |

Table 3. Molecular and monolayer parameters for DOPS, DOPE, DOPC, and PHUE.

| Parameter | DOPS | DOPE | DOPC ^[9] | PHUE |
|--|---|---|--|---|
| Molar mass [g mol ⁻¹] | 810 | 744 | 786 | 165 600 |
| Monolayer thickness [Å] ^{[48]a)} | 16 ± 1 | 15 ± 2 | 16 ± 2 | N/D |
| Head group thickness [Å] | N/D | 7.90 ^[34] , 9.04 ^[49] | 10.40 | N/D |
| Total dipole moment μ [C m] ^{[46]a)} | +0.79 × 10 ⁻³⁰ | N/D | +2.04 × 10 ⁻³⁰ | N/D |
| Head group dipole moment μ [C m] ^{[46]b)} | -1.10 × 10 ⁻³⁰ | -0.17 × 10 ⁻³⁰ | +0.23 × 10 ⁻³⁰ | +6.00 × 10 ^{-30c)} |
| Hydrogen bonds | Yes | Yes | No | Possible |
| π _{coll} [mN m ⁻¹] | 47.8 (52 Å ² /molecule) | 48.5 (47 Å ² /molecule) | 46.7 (55 Å ² /molecule) | 15 (25 000 Å ² /molecule) |
| Maximum C _s ⁻¹ [mN m ⁻¹] | 108 | 104 | 92 | 36 |
| Monolayer state | LC at 33 mN m ⁻¹ ; 64 Å ² molecule ⁻¹ | LC at 41 mN m ⁻¹ ; 56 Å ² molecule ⁻¹ | L at 32 mN m ⁻¹ ; 70 Å ² molecule ⁻¹ | LE at 10 mN m ⁻¹ ; 29 000 Å ² molecule ⁻¹ |
| Head group pK _a | 2.4 (-COOH), 9.6 (-NH ₃ ⁺) ^[40] | 10.7 | 9.8 | N/A |

^{a)}Values at the air-water interface at 30 mN m⁻¹; ^{b)}Values at the buffer; ^{c)}Dipole moment of an ester group, according to ref. [39]. N/D—no data. N/A—not applicable. LE - liquid expanded; L - liquid; LC - liquid condensed.

Even though bonding via hydroxyl groups (Figure 7C) is stronger,^[38] they are less likely to prevail as there are only two hydroxyl groups per polymer chain. Bonding of carbonyl oxygens is thus more probable (Figure 7B). Furthermore, since DOPE molecules are smaller than DOPC, they probably fit much better within a PHUE film, and as a consequence did not drastically disturb its packing. It appears that DOPE molecules were embedded within the mixed films with the lipid molar ratio below 0.7, as no lipid domains were observed with BAM (Figure 6). The lipid domains were visible only at high molar excess of the lipid in the film ($X_{\text{DOPE}} \geq 0.7$).

3.6. Head Group Charge

Our experiments were performed using bi-distilled water with pH of 5.5, at which we essentially investigated two zwitterionic lipids (DOPE and DOPC) and an anionic lipid—DOPS. PHUE is a neutral polyester that, due to the ester group, has a dipole moment oriented nearly antiparallel to the C=O bond.^[39]

All lipid head groups contained the phosphate group with pK_a in the range between 1 and 2,^[40] which was deprotonated and in anionic form. DOPS additionally contains a serine group (Figure S2, Supporting Information), with negatively charged carboxylic group (pK_a = 2.4) and positively charged amine (pK_a = 9.6),^[40] and negative total charge. Both zwitterionic lipids, apart

from the anionic phosphate, contain also positively charged amine groups (ethanolamine and choline- trimethyletanolamine, for DOPE and DOPC, respectively). The reported values of amine pK_a are in the range of 9 to 11,^[41] and both lipids (DOPE and DOPC) were reported neutral at pH 5.5.^[42,43] Even though both have a similar charge distribution and are zwitterionic, there is a tremendous difference in the organization of their head groups at the air-water interface, as discussed above. Consequently, in a pure DOPE monolayer, charges are neutralized because of molecular attraction (Figure 7A).^[33,44] This is not observed for DOPC molecules and has implications on the interactions between these lipids with the polymer. In particular, the parallel orientation of PE molecules would result in ion-dipole interactions with the polymer (Figure 8A).

Regarding DOPS (Figure S2, Supporting Information), the PS head group is spatially extensive and may serve as a steric hindrance. This notion is supported by the mean molecular area of DOPS (52 Å² molecule⁻¹), which is close to the one of DOPC. It was also reported that since DOPS has an amine group, it is likely to be involved in hydrogen bonding (Figure 8C).^[45]

When discussing PHUE-DOPS repulsive interactions (as indicated by the excess free energy of mixing for these two components), we assume that DOPS molecules are (i) stabilized by hydrogen bonds (this results in domains formation) and (ii) oriented perpendicular

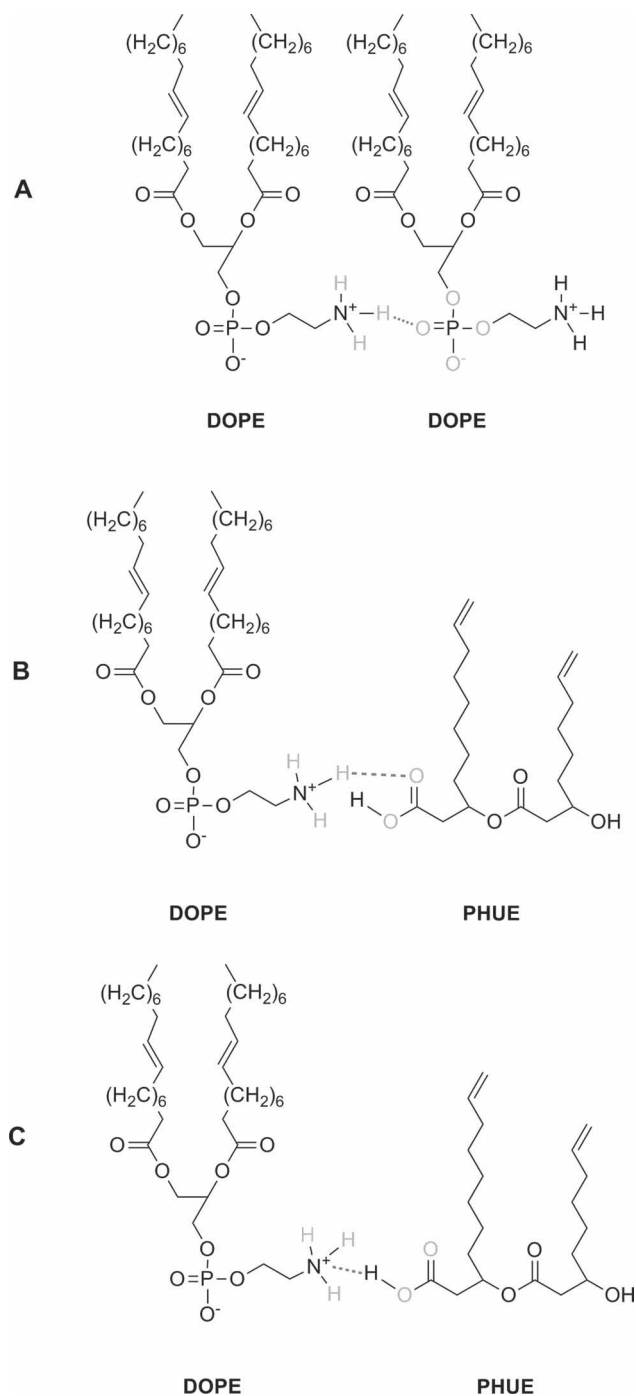


Figure 7. Probable hydrogen bonds between (A) DOPE molecules, (B) DOPE (hydrogen donor) and PHUE (hydrogen acceptor), and (C) DOPE (hydrogen acceptor) and PHUE (hydrogen donor). Such bonds cannot be formed between DOPC and DOPC–PHUE molecules.

(or at an angle) to the air–water interface. This organization would result in repulsive interactions between negatively charged phosphate group and PHUE dipoles (Figure 8B), the hydrogen bonds between DOPS and

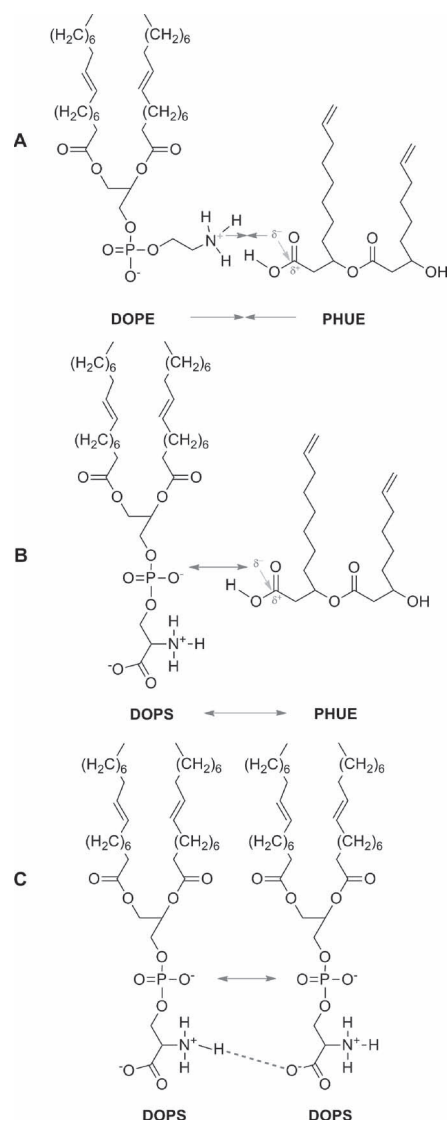


Figure 8. A schematic representation of ion–dipole interactions in (A) DOPE–PHUE attraction and (B) DOPS–PHUE repulsion; and (C) DOPS–DOPS interactions.

PHUE are unlikely to be formed in that configuration of molecules.

The excess free energy of mixing for PHUE with both DOPC (zwitterionic) and DOPS (anionic) were positive, meaning that the repulsive interactions were favored and the components phase separated. In the case of the PHUE–DOPE (zwitterionic) mixed films, the excess free energy of mixing was negative, suggesting attractive interactions between these two components. As can be seen, there is no straightforward relationship between the charge of the lipid and type of the interactions between the polymer and lipid. This means that not the head group charge alone but rather the orientation of the lipid molecules is the main driving force influencing the interactions, as it

is responsible for the presence of hydrogen bonds, ion-dipole and dipole-dipole interactions.

3.7. Dipole Moments

The lipids investigated here have the same hydrophobic part (18:1(9Z)), bringing equal contribution to the total dipole moment. For many lipids (including PE and PC), the dipole moment of the terminal methyl group in packed (ca. 20 mN m⁻¹) hydrocarbon chains at the monolayer-air interface was reported as $+1.17 \times 10^{-30}$ C m.^[46] It was also shown that the number of methylene groups in a hydrocarbon chain, in closed-packed monolayers, separating the water-lipid and lipid-air interfaces, does not contribute to the total dipole moment.^[46] Thus, the main contribution to the total dipole moment comes from the effective local dipole moment of the hydrated head group (see Table 3 for example values of total and head group dipole moments for the investigated phospholipids). Dipole moment values depend not only on the type of molecules and their organization at the air-water interface (surface pressure, domain formation), but also charge density, subphase pH, etc. For that reason, a quantitative analysis requires more specific experiments. Nevertheless, we suppose that dipole-dipole interactions (ca. 2 kJ mol⁻¹ ^[47]), being weaker than hydrogen or ion-dipole interactions, will have a minor effect on the lipid's interaction with the polymer. It is likely that PE and PHUE dipoles attract, as they are organized at the air-water interface in a favored configuration (Figure 9). The interactions between PC and PS dipoles with PHUE will be rather unfavorable due to their perpendicular orientation in respect to the air-water interface.

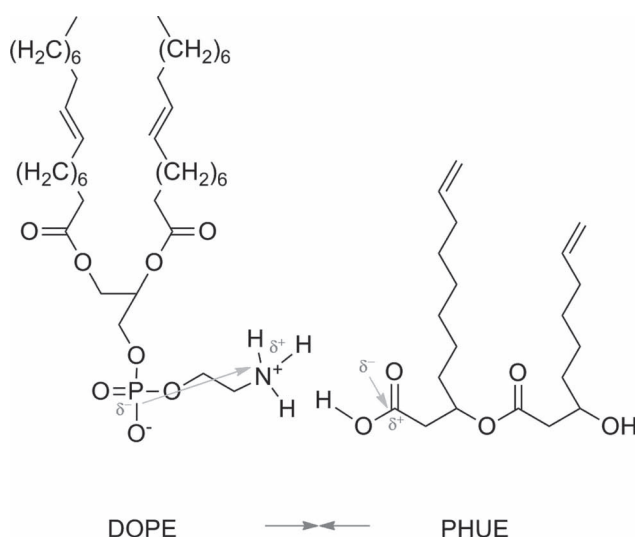


Figure 9. A schematic representation of dipole-dipole interactions between PE and PHUE.

4. Conclusions

The Langmuir monolayer technique was used to study the interactions between PHUE, naturally synthesized polyester, and various phospholipids, chosen on the basis of different head group size and charge (DOPS and DOPE). These results are compared with previously reported data for PHUE-DOPC monolayers.

We showed that the interactions between PHUE and negatively charged DOPS as well as with zwitterionic DOPC^[9] are repulsive, indicated by positive excess free energy of mixing; phase-separation of these two components was confirmed by Brewster angle microscopy. To the contrary, the excess free energy of mixing for PHUE-DOPE systems was negative, meaning that attractive interactions between the polymer and the lipid were favored. The main driving forces influencing these interactions are the size of the phospholipid head group and its orientation at the air-water interface. Due to the small size and parallel to the interface orientation of DOPE molecules, attractive interactions were possible: not only hydrogen bonds but also ion-dipole and dipole-dipole interactions. These interactions were not considered plausible between PHUE and either DOPC or DOPS, which both have much bigger head groups, aligned perpendicular to the interface.

We believe these results will contribute to the understanding of interactions between different classes of materials. The monolayer model may be also applied for other systems relevant for biology and materials science, where asymmetric environments are present and interfacial compatibility is important for materials properties.

Supporting Information

Supporting Information is available from the Wiley Online Library or from the author.

Acknowledgements: We thank the Swiss National Science Foundation, NCCR Nanoscience and Swiss Nanoscience Institute for financial support.

Received: April 26, 2012; Revised: June 18, 2012; Published online: August 7, 2012; DOI: 10.1002/macp.201200232

Keywords: monolayers; phospholipids; polyhydroxyalkanoates (PHA); poly([R]-3-hydroxy-10-undecenoate) (PHUE); Brewster angle microscopy

- [1] K. Sudesh, H. Abe, Y. Doi, *Prog. Polym. Sci.* **2000**, *25*, 1503.
- [2] R. Hartmann, R. Hany, T. Geiger, T. Egli, B. Witholt, M. Zinn, *Macromolecules* **2004**, *37*, 6780.
- [3] G. Q. Chen, *Chem. Soc. Rev.* **2009**, *38*, 2434.
- [4] R. Hufenus, F. A. Reifler, K. Maniura-Weber, A. Spierings, M. Zinn, *Macromol. Mater. Eng.* **2012**, *297*, 75.

- [5] S. Y. Lee, *Biotechnol. Bioeng.* **1996**, *49*, 1.
- [6] W. Amass, A. Amass, B. Tighe, *Polym. Int.* **1998**, *47*, 89.
- [7] C. W. Pouton, S. Akhtar, *Adv. Drug Delivery Rev.* **1996**, *18*, 133.
- [8] M. Zinn, B. Witholt, T. Egli, *Adv. Drug Delivery Rev.* **2001**, *53*, 5.
- [9] A. Jagoda, P. Ketikidis, M. Zinn, W. Meier, K. Kita-Tokarczyk, *Langmuir* **2011**, *27*, 10878.
- [10] K. Hac-Wydro, K. Jedrzejek, P. Dynarowicz-Latka, *Colloid Surf. B* **2009**, *72*, 101.
- [11] K. Hac-Wydro, P. Dynarowicz-Latka, *J. Phys. Chem. B* **2008**, *112*, 11324.
- [12] J. Minones, S. Pais, J. Minones, O. Conde, P. Dynarowicz-Latka, *Biophys. Chem.* **2009**, *140*, 69.
- [13] P. Wydro, K. Hac-Wydro, *J. Phys. Chem. B* **2007**, *111*, 2495.
- [14] K. Hac-Wydro, P. Wydro, *Chem. Phys. Lipids* **2007**, *150* (1), 66.
- [15] H. Jing, H. Kim, D. Choi, D. R. Lee, J. S. Lee, C. J. Yu, K. Shin, *Biointerphases* **2011**, *6*, 73.
- [16] K. Hac-Wydro, P. Dynarowicz-Latka, J. Grzybowski, E. Borowski, *Thin Solid Films* **2008**, *516*, 1197.
- [17] K. Hac-Wydro, J. Kapusta, A. Jagoda, P. Wydro, P. Dynarowicz-Latka, *Chem. Phys. Lipids* **2007**, *150*, 125.
- [18] K. Hac-Wydro, P. Wydro, A. Jagoda, J. Kapusta, *Chem. Phys. Lipids* **2007**, *150*, 22.
- [19] G. A. R. Nobes, R. H. Marchessault, D. A. Holden, *Polymer* **1994**, *35*, 435.
- [20] G. Lambeek, E. J. Vorenkamp, A. J. Schouten, *Macromolecules* **1995**, *28*, 2023.
- [21] N. J. Jo, T. Iwata, K. T. Lim, S. H. Jung, W. K. Lee, *Polym. Degrad. Stabil.* **2007**, *92*, 1199.
- [22] R. Hartmann, R. Hany, E. Pletscher, A. Ritter, B. Witholt, M. Zinn, *Biotechnol. Bioeng.* **2006**, *93*, 737.
- [23] M. Zinn, R. Hany, *Adv. Eng. Mater.* **2005**, *7*, 408.
- [24] N. Funasaki, M. Nakagaki, *B. Chem. Soc. Jpn.* **1975**, *48*, 2727.
- [25] V. K. Lamer, L. A. G. Aylmore, T. W. Healy, *J. Phys. Chem.* **1963**, *67*, 2793.
- [26] W. Stoffel, H. D. Pruss, *H.-S. Z. Physiol. Chem.* **1969**, *350*, 1385.
- [27] Y. F. Dufrene, W. R. Barger, J.-B. D. Green, G. U. Lee, *Langmuir* **1997**, *13*, 4779.
- [28] A. P. Dabkowska, G. Fragneto, A. V. Hughes, P. J. Quinn, M. J. Lawrence, *Langmuir* **2009**, *25*, 4203.
- [29] P. Dynarowicz-Latka, K. Kita, *Adv. Colloid Interfac* **1999**, *79*, 1.
- [30] K. Kita-Tokarczyk, F. Itel, M. Grzelakowski, S. Egli, P. Rossbach, W. Meier, *Langmuir* **2009**, *25*, 9847.
- [31] T. Haefele, K. Kita-Tokarczyk, W. Meier, *Langmuir* **2006**, *22*, 1164.
- [32] C. Tribet, *Biochimie* **1998**, *80*, 461.
- [33] M. C. Phillips, E. G. Finer, H. Hauser, *Biochim. Biophys. Acta* **1972**, *290*, 397.
- [34] H. Hauser, I. Pascher, R. H. Pearson, S. Sundell, *Biochim. Biophys. Acta* **1981**, *650*, 21.
- [35] M. M. Standish, B. A. Pethica, *Trans. Faraday Soc.* **1968**, *64*, 1113.
- [36] D. A. Cadenhead, R. J. Demchak, M. C. Phillips, *Kolloid Z. Z. Polym.* **1967**, *220*, 59.
- [37] K. A. Dill, D. Stigter, *Biochemistry* **1988**, *27*, 3446.
- [38] B. Lesyng, G. A. Jeffrey, H. Maluszynska, *Acta Crystallogr. B* **1988**, *44*, 193.
- [39] E. Salz, J. P. Hummel, P. J. Flory, M. Plavsic, *J. Phys. Chem.* **1981**, *85*, 3211.
- [40] K. Dolowy, *Prog. Surf. Sci.* **1984**, *15*, 245.
- [41] A. Watts, T. W. Poile, *Biochim. Biophys. Acta* **1986**, *861*, 368.
- [42] M. C. Phillips, D. Chapman, *Biochim. Biophys. Acta* **1968**, *163*, 301.
- [43] H. Hauser, R. M. C. Dawson, *Eur. J. Biochem.* **1967**, *1*, 61.
- [44] D. J. Vaughan, K. M. Keough, *FEBS Lett.* **1974**, *47*, 158.
- [45] A. A. Polyansky, P. E. Volynsky, D. E. Nolde, A. S. Arseniev, R. G. Efremov, *J. Phys. Chem. B* **2005**, *109*, 15052.
- [46] V. Vogel, D. Mobius, *J. Colloid Interface Sci.* **1988**, *126*, 408.
- [47] P. W. Atkins, *Physical Chemistry*, Oxford University press, OxfordUK **1998**.
- [48] H. P. Ta, K. Berthelot, B. Couлары-Salin, B. Desbat, J. Gean, L. Servant, C. Cullin, S. Lecomte, *Langmuir* **2011**, *27*, 4797.
- [49] T. L. Kuhl, J. Majewski, P. B. Howes, K. Kjaer, A. von Nahmen, K. Y. C. Lee, B. Ocko, J. N. Israelachvili, G. S. Smith, *J. Am. Chem. Soc.* **1999**, *121*, 7682.

Supporting Information

for *Macromol. Chem. Phys.*, DOI = 10.1002/macp.201200232

Head group influence on lipid interactions with a polyhydroxyalkanoate biopolymer

Agnieszka Jagoda, Manfred Zinn, Wolfgang Meier, Katarzyna Kita-Tokarczyk

Supporting Information: Polymer synthesis, extraction, and purification. Polymer characterization. Figure S1 – Structure of PHUE. Figure S2 – Chemical structures of phospholipids. Figure S3 - Surface pressure - area (π -A) isotherms from phospholipid films. Excess area of mixing. Figure S4 - π -A isotherms from PHUE-DOPS mixed films with low molar ratio of polymer. Error analysis.

Polymer synthesis, extraction, and purification. To obtain poly([R]-3-hydroxy-10-undecenoate) [PHUE], the bacterial strain *Pseudomonas putida* GPo1 was grown in a chemostat at a dilution rate of 0.1 1/h using 10-undecenoic acid as a single carbon source [1]. Collected cells were centrifuged and the pellets lyophilized (12°C, 0.5 mbar, 72 h). Dry cell biomass was suspended in ethyl acetate (60 g L⁻¹), the suspension was stirred for at least 2 h, filtered and concentrated by solvent distillation in a vacuum dryer until it became viscous (40°C, 240 mbar). The polymer was then precipitated in cold methanol (4°C), vacuum-dried for 2 days (40°C, 30 mbar), and stored at -20°C.

Polymer characterization. The molecular weight of PHUE was determined by gel permeation chromatography (GPC, ViscotekTriSEC Model 302). For analysis, typically 50 mg of purified polymer was dissolved in 10 mL of tetrahydrofuran (THF, Fisher Scientific, analytical

grade) and filtered with a nylon filter (Titan2, 0.45 μm). The monomer composition was determined by gas chromatography (GC) using a method developed by Furrer et al., [2] and confirmed by NMR. ^1H and ^{13}C NMR experiments in solution were performed on a Bruker AV-400 spectrometer at 297 K using a 5 mm broad-band probe. [2, 3]

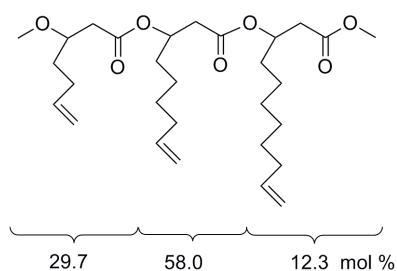


Figure S1. Structure of PHUE.

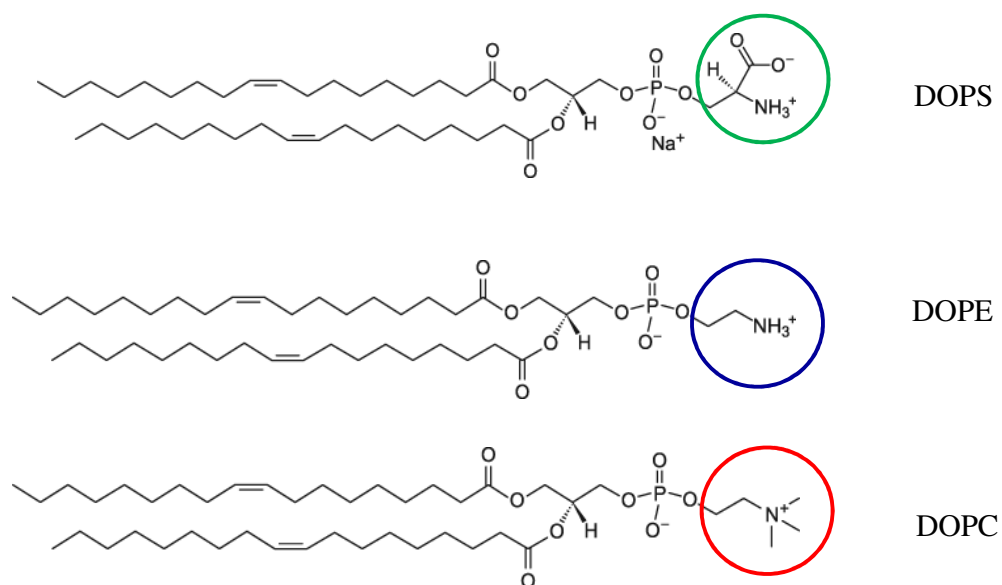


Figure S2. Structures of DOPS, DOPE, and DOPC.

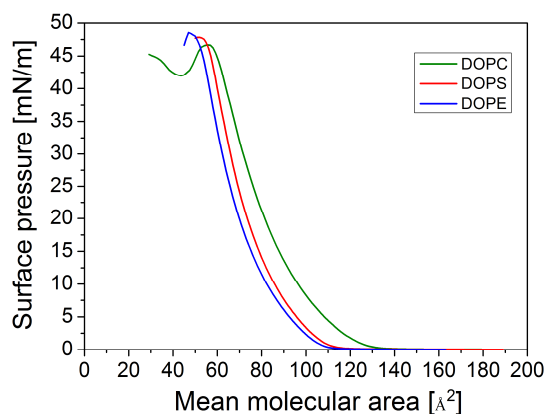


Figure S3. π -A isotherms from DOPC, DOPS and DOPE films.

Excess area of mixing: A^{exc} is a difference between the experimental area per molecule (A_{12}) and the theoretical one (A_{id}), resulting from the additivity rule ($A_{\text{id}} = A_1X_1 + A_2X_2$, where, at constant surface pressure, A_1 and A_2 are the molecular areas of components 1 and 2, respectively, and X_1 and X_2 are their molar ratios). A^{exc} is zero when two components mix ideally or are immiscible, and deviations indicate miscibility of components: negative A^{exc} suggests attractive interactions leading to monolayer contraction, while positive A^{exc} is a result of repulsive interactions (monolayer expansion).

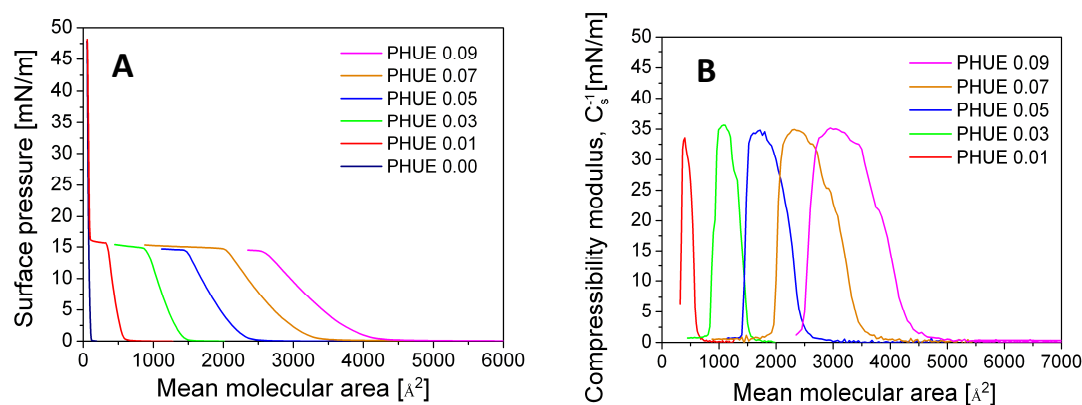


Figure S4. π -A isotherms (A) and compressibility moduli (B) from PHUE-DOPS mixed films with low molar ratio of polymer.

Error analysis. The following errors were considered for the error calculation: volume error (syringe, 10^{-9} m^3), concentration ($0.01 \text{ kg (m}^3)^{-1}$), molar mass (0.1 kg mol^{-1}), dimensions of the Langmuir trough (10^{-6} m^2), and surface pressure (0.1 mN m^{-1}). Errors of the number of molecules, mean molecular area, and excess free energy of mixing were calculated using Gaussian error propagation. Error of the compressibility modulus is equal to surface pressure measurement error (0.1 mN m^{-1}). The large error of ΔG^{exc} is a consequence of the large error of the mean molecular area (due to large polymer size), and decreases with a decrease of the polymer molar ratio.

- [1] R. Hartmann; R. Hany; E. Pletscher; A. Ritter; B. Witholt; M. Zinn, *Biotechnol Bioeng* **2006**, *93* (4), 737.
- [2] P. Furrer; R. Hany; D. Rentsch; A. Grubelnik; K. Ruth; S. Panke; M. Zinn, *J. Chromatogr. A* **2007**, *1143* (1-2), 199.
- [3] R. Hany; C. Boehlen; T. Geiger; R. Hartmann; J. Kawada; M. Schmid; M. Zinn; R. H. Marchessault, *Macromolecules* **2004**, *37*, 385.

3.3. PHUE and PHUE-lipid film mineralization

Results were published in: “Biodegradable polymer-lipid monolayers as templates for calcium phosphate mineralization”, *Journal of Materials Chemistry B*, **2013**, *1* (3), 368-378, A. Jagoda, M. Zinn, E. Bieler, W. Meier, K. Kita-Tokarczyk.

Biodegradable polymer–lipid monolayers as templates for calcium phosphate mineralization†

Cite this: *J. Mater. Chem. B*, 2013, **1**, 368

Agnieszka Jagoda,^a Manfred Zinn,^b Eva Bieler,^c Wolfgang Meier^a and Katarzyna Kita-Tokarczyk^{‡*a}

A combination of poly([R]-3-hydroxy-10-undecenoate) (PHUE), a biodegradable polymer from the group of polyhydroxyalkanoates (PHAs), and lipids of different head groups was used to support the growth of calcium phosphate, the main component of mammalian bones. Crystallization took place under two-dimensional films (Langmuir monolayers). The addition of a negatively charged lipid, 1,2-dioleoyl-*sn*-glycero-3-phospho-L-serine, to a PHUE film led to the formation of lipid domains (rich in negative charge), and resulted in excellent mineralization control: crystals with uniform size and morphology were formed. The results show that carefully optimized combinations of materials can lead to better control of calcium phosphate crystallization compared to one-component organic scaffolds.

Received 5th September 2012
Accepted 31st October 2012

DOI: 10.1039/c2tb00083k

www.rsc.org/MaterialsB

Introduction

There were over 2 million surgeries on the skeletal system in the United States in 2009 (latest data according to Centers for Disease Control and Prevention), including total hip or knee replacements, partial excision of bone, and reduction of fracture. This trend is increasing: *e.g.*, in OECD countries an increase by 27% and 87% was observed in hip and knee replacements, respectively, over the past decade.¹ The main reasons are ageing societies, changing lifestyle, or drawbacks of current bone implants, especially regarding cell attachment and growth and inflammatory reactions. Consequently, the demand for novel bone implant materials increases. Apart from biological requirements such as stimulation of cell differentiation,

support of the bone growth, and formation of structural and functional linkage at the contact point with bone,^{2,3} materials for bone implants must exhibit tissue-specific mechanical properties.⁴

Polyhydroxyalkanoates (PHAs) are interesting biomaterial candidates.^{5,6} These biocompatible polyesters are synthesized naturally by various microorganisms, which store the polymer intracellularly in granules, serving as an energy and carbon source.⁵ PHAs have already been used in medical applications, for example in stents, vascular grafts, heart valves, *etc.*^{5–7} A few reports describe their potential use in orthopedic applications; however, these focused on bulk short-chain-length (scl)-PHAs: poly(3-hydroxybutyrate) (P(3HB))^{8–10} and its copolymers with poly(3-hydroxyvalerate) (P(3HV))^{11,12} or poly(3-hydroxyhexanoate) (P(3HH)).^{8–10,13} These polymers have been reported to favor cell attachment and proliferation, and, when blended with hydroxyapatite (a calcium phosphate phase found in bone and teeth), bone growth-enhancing scaffolds could be produced.⁹ We focus on a medium-chain-length (mcl)-PHA, poly([R]-3-hydroxy-10-undecenoate) (PHUE), and investigate its crystal templating properties alone and in combination with two lipids, phosphatidylserine (PS) and phosphatidylethanolamine (PE).

Phosphatidylserines (PS) are phospholipids naturally present in cell membranes and especially, in high content, in the membrane of ‘matrix vesicles’ (MVs), pre-nucleation clusters for calcium phosphate formation in cells. Negatively charged PSs bind with calcium, supplied to the phosphate-rich interior of MVs *via* a calcium-selective channel (Annexin V), which leads to precipitation of amorphous calcium phosphate (ACP, a hydroxyapatite precursor) inside MVs.^{14,15} The growing ACP crystals disrupt the vesicles, and finally merge with other nucleation clusters.^{16,17} PSs were already used, for example, as

^aDepartment of Chemistry, University of Basel, Klingelbergstrasse 80, 4056 Basel, Switzerland. E-mail: katarzyna.kita@mail.com

^bBioprocesses and Biomaterials, Institute of Life Technologies, University of Applied Sciences Western Switzerland (HES-SO Valais), Route Rawyl 47, 1950 Sion, Switzerland

^cThe Center for Microscopy (ZMB), Biozentrum/Pharmazentrum, University of Basel, Klingelbergstrasse 50-70, 4056 Basel, Switzerland

† Electronic supplementary information (ESI) available: Surface pressure–area isotherms from PHUE–DOPE and PHUE–DOPS mixed films, PHUE–DOPS mixed films recorded on water and HEPES with Ca²⁺ ions, and from PHUE on water and buffer (HEPES with Ca²⁺, 2 mM, pH ≈ 7.5); TEM images of calcium phosphate crystallization without the PHUE film and of calcium phosphate grown beneath PHUE–DOPS (0.9 : 0.1) films; the EDX spectrum of crystals grown under standard conditions (2 mM, 1 h) beneath PHUE–DOPE (0.9 : 0.1) films and PHUE–DOPS (0.1 : 0.9) films; schematic representation of DOPE and DOPS organization at the air–water interface; Table S1: the interaction parameter (α) and interaction energy (Δh) for PHUE–lipid mixed films. See DOI: 10.1039/c2tb00083k

‡ Present address: Unilever R&D Port Sunlight, Quarry Road East, Bebington, Wirral, CH63 3JW, UK; phone: +44 (0)7564010250; email: katarzyna.kita@mail.com

coatings for titanium implants to induce rapid mineralization,¹⁸ they significantly reduced the inflammatory response¹⁹ and showed good osseointegrative potential.^{18,20,21} Moreover, PS-coated implants facilitated osteoblast differentiation and calcium deposition.^{22,23} PS as an additive to calcium phosphate cement enhanced the material strength and improved osteoblast proliferation and differentiation.²⁴

Hartgerink *et al.*²⁵ designed a peptide amphiphile, which contained, among others, phosphorylated serine to interact with calcium ions and to direct mineralization of hydroxyapatite. Such peptides were self-assembled to form 3D fibrous networks to template calcium phosphate mineralization. It was already shown that after 30 minutes the peptide nanofibers' surface was covered with hydroxyapatite, preferentially aligned with the long fiber axis. A similar approach was used by Spoerke *et al.*,²⁶ who enriched amphiphilic peptide nanofibers with acidic and phosphorylated residues, known to accelerate mineral formation. The fibers formed scaffolding frameworks, and were then subjected to enzymatic mineralization. It was shown that the combination of the designed nanofiber surface with enzyme-controlled release of phosphate ions led to a spatially selective and biomimetic hydroxyapatite formation in a 3D environment.

In this study, we were interested in how 2D molecular organization in surface films from PHA and PHA-lipid mixtures influences the growth of calcium phosphate. Organic surface films on which crystallization may start by heterogeneous nucleation were prepared by the Langmuir monolayer technique (to control the molecular organization in thin films). Depending on film-forming molecules, the well-controlled surface density and intermolecular distances may be required for good structural matching between inorganic crystals and the templating film. Langmuir monolayers were used previously as templates to grow inorganic materials, mainly CaCO₃,^{27–29} and BaSO₄.^{30–32} Calcium phosphate was only grown using (one-component) monolayers from fatty acids and their derivatives,^{33–37} a phospholipid (dipalmitoylphosphatidylcholine, DPPC),³⁷ and acrylate-based block copolymers.^{38–40}

These earlier studies used amphiphilic but non-biodegradable and non-biocompatible synthetic materials, with limited use in biomedical applications. Here we used PHUE, a naturally synthesized polymer, neutral, and largely hydrophobic but nevertheless forming stable monolayers on the free water surface.⁴¹ PHUE-PS mixed films phase separate forming lipid domains,⁴² which may act as nucleation centers, presumably due to the accumulation of negative charge. The aim of this work was to study calcium phosphate crystallization templating properties of these mixed films. DOPS was chosen because of its importance in natural precipitation of calcium phosphate, while DOPE served as a control: even though its structure is similar to DOPS, the interactions with PHUE are different.⁴² Furthermore, the addition of lipids to the polymer film improves the film's amphiphilic character, which can further influence cell adhesion as well. This work also presents, for the first time, calcium phosphate mineralization using pure DOPS and DOPE monolayers. To better understand the mineralization process, parameters such as mineralization time, ion concentrations and polymer-lipid molar ratios were investigated.

Materials and methods

Materials

POLY([R]-3-HYDROXY-10-UNDECENOATE) [PHUE]. The synthesis, purification and characterization of poly([R]-3-hydroxy-10-undecenoate) [PHUE] were described before.^{41,43} Briefly, PHUE is a statistical copolymer of 3-hydroxy- ω -alkenoate monomers containing 7, 9, and 11 carbon atoms (Fig. 1A), with $M_w = 294\,600\text{ g mol}^{-1}$, $M_n = 165\,600\text{ g mol}^{-1}$, and a polydispersity index (PDI) of 1.8.

LIPIDS. DOPS [(1,2-dioleoyl-*sn*-glycero-3-phospho-L-serine sodium salt), mass 810 g mol^{-1}] and DOPE [(1,2-dioleoyl-*sn*-glycero-3-phosphoethanolamine), mass 744 g mol^{-1}] were purchased from Avanti Polar Lipids, Inc. (Alabama, USA) as chloroform solutions (10 mg mL^{-1}). Both lipids had a double bond (*cis* configuration) at the 9th carbon atom, Fig. 1B and C.

SALTS AND BUFFERS. Sodium phosphate monobasic monohydrate, 4-(2-hydroxyethyl)piperazine-1-ethanesulfonic acid (HEPES), and calcium chloride dihydrate (Sigma Aldrich) were used as received. All buffers and salt solutions were prepared using bi-distilled water. Experiments were performed at physiological pH ≈ 7.5 , when necessary the pH was adjusted with 5 M NaOH. Experiments with DOPS films were performed using HEPES buffer containing CaCl₂ (2 or 0.5 mM), and an appropriate volume (2 or 0.5 mL) of sodium phosphate (0.25 M) was injected into the subphase (below the monolayer) to obtain a 2 mM (unless otherwise specified) concentration of phosphate ions. For mineralization experiments with DOPE monolayers, sodium phosphate buffer (2 mM) served as a subphase, into which CaCl₂ (0.25 M) was injected to obtain a 2 mM concentration of calcium ions.

Langmuir monolayers and mineralization

Langmuir monolayers were prepared as described before^{41,42} using a KSV Inc. (Finland) Langmuir-Blodgett Teflon® trough (area 242 cm^2). PHUE and lipids were spread from chloroform solutions. Polymer-lipid mixtures ($500\ \mu\text{L}$, 1 mg mL^{-1}) at

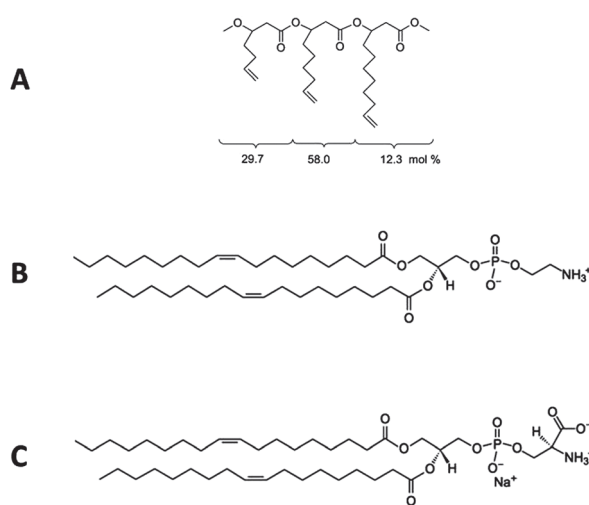


Fig. 1 Structures of (A) PHUE, (B) DOPE, and (C) DOPS.

different molar ratios (0.1 : 0.9 and 0.9 : 0.1) were prepared freshly every day by mixing appropriate volumes of PHUE and lipid solutions.

Before compression (10 mm min^{-1} , target surface pressure 12 mN m^{-1}), 10 minutes were allowed for chloroform evaporation. After 5 minutes of equilibration at 12 mN m^{-1} , salt solution was injected below the monolayer with a Hamilton syringe. During mineralization, a constant surface pressure was held at 12 mN m^{-1} , and the subphase was continuously stirred with a small stirring rod, placed in a dipping well of the Langmuir-Blodgett trough. After a mineralization time of 1 or 4 hours, films were transferred to TEM grids for further analysis.

Electron microscopy (TEM, SEM) and energy dispersive X-ray (EDX) spectroscopy

TEM carbon-coated copper grids were cleaned in a plasma cleaner right before the transfer of mineralized films. TEM images were taken with a Philips CM100 operating at 80 kV. Before SEM imaging, samples were mounted on carbon tabs and sputter-coated with 10 nm of silver in a High Vacuum Coating System, MED 020 (Bal-tec, Liechtenstein – present Leica). The samples obtained from PHUE mineralization on sodium phosphate buffer were sputter-coated with platinum. SEM images were recorded using a Nova Nano SEM (FEI, Netherlands) operated at 10 kV. EDX analysis was done with a SDD detector Apollo XV, Software Genesis by EDAX. In some EM images, contrast and/or brightness were adjusted to allow better visibility and easier interpretation.

Image analysis was done with ImageJ⁴⁴ using at least 3 images. We assumed the spherical shape of crystals and compared their diameters and the average area fractions (area of the image covered by crystals) \pm standard deviation.

Results

Firstly, mineralization was performed with one-component monolayers (Fig. 1; see ESI, Fig. S1† for surface pressure–area isotherms) as controls before experiments with mixed monolayers. Depending on the compound, we analyzed the influence of mineralization time (PHUE, DOPE, DOPS and their mixed films), ion concentrations (PHUE–DOPS), and subphase buffer (PHUE). Following Casse *et al.*³⁸ we used 1 hour mineralization time and 2 mM ion concentration (the same as calcium and phosphate concentrations in human blood and saliva,⁴⁵ to at least partially mimic the natural conditions for bone and tooth formation and regeneration) as ‘standard conditions’ for mineralization.

pH is one of the key parameters in the crystallization process, however it is known that pH in the monolayer may differ from subphase pH,⁴⁶ the difference depends on the subphase ion strength and the properties of film-forming materials (polyions show a particularly strong effect^{38–40}). In this work, the subphase pH was kept constant (at 7.5) and is assumed not to change in the monolayer region since the polymer is neutral, and its monolayer behaviour is pH- and buffer-insensitive (Fig. S2, ESI†).

Mineralization of PHUE monolayers

The following control experiments were performed: (i) PHUE isotherms recorded on sodium phosphate and HEPES (with Ca^{2+} ions) buffers were identical to those on bi-distilled water;⁴¹ (ii) mineralization without the polymer film (crystals growing in bulk solution), to understand the PHUE monolayer templating influence on the morphology of calcium phosphate crystals; and (iii) mineralization in the presence of a PHUE film, but without subphase stirring, to assess the influence of ion diffusion. In (ii), only a few small crystals (diameter below 45 nm; Fig. S3, ESI†) were obtained, while in (iii) the results were similar to those with subphase stirring. Next, we analyzed the influence of subphase buffer (HEPES with calcium ions or sodium phosphate) and mineralization time on the crystal formation.

TEM images, EDX spectra and image analysis for mineralization experiments with PHUE monolayers are shown in Fig. 2. Regardless of the experimental conditions, calcium phosphate crystals were formed beneath the polymer films, as confirmed by EDX. Usually, we observed two populations of crystals, the first one were small, in the range of tens of nm, and the second one consisted of almost spherical crystals with a diameter up to a few μm . The crystals were randomly distributed and most likely grew uncontrolled, independent of the subphase buffer and mineralization time. In EDX spectra, besides peaks from Ca and P, we observed peaks from carbon (polymer and/or lipid, and SEM sample holders), oxygen (polymer and calcium phosphate), aluminum (SEM sample holder), copper (TEM grid), sulfur (HEPES buffer), sodium and chlorine (subphase, salt solutions). Peaks from silver and platinum originated from the sputtering, while traces of silicon may have resulted from solutions stored in glass bottles/vials.

Mineralization of DOPE monolayers

Crystal templating properties of DOPE and PHUE–DOPE monolayers were investigated to discriminate whether the

| | Standard conditions (2 mM, 1 h) | | 2 mM, 4 h | | | | |
|-------------------|---------------------------------|-----------------------------------|------------------|-----------------------------------|----------------------------------|----------------|------|
| | Sodium phosphate | HEPES with Ca^{2+} ions | Sodium phosphate | | HEPES with Ca^{2+} ions | | |
| TEM | | | | | | | |
| EDX | | | | | | | |
| Results | Group of crystals | I | II | I | II | I | II |
| | Diameter [nm] | mostly 240–1200, a few up to 2600 | < 80 | mostly 360–1600, a few up to 3160 | < 50 | 360–3000 | < 80 |
| Area fraction [%] | 4.7 \pm 1.1 | 21.9 \pm 8.9 | 7.5 \pm 0.3 | 10.2 \pm 3.8 | 4.0 \pm 1.7 | 13.9 \pm 3.3 | |

Fig. 2 Mineralization results for PHUE monolayers. Regardless of the crystal growth conditions (buffer and time; see top of the figure), two groups of randomly distributed crystals were observed.

| | | Standard conditions (2 mM, 1 h) | 2 mM, 4 h |
|---------|-------------------|---------------------------------|------------|
| | | Sodium phosphate buffer | |
| Results | Diameter [nm] | ≤ 260 | ≤ 260 |
| | Area fraction [%] | 0.9 ± 0.4 | 20.4 ± 2.9 |

Fig. 3 Mineralization results for DOPE monolayers. Crystals with diameters below 260 nm were obtained, regardless of growth conditions. The area occupied by crystals increased with longer mineralization time.

observed calcium phosphate crystallization under PHUE films was either a consequence of the polymer's surface organization or the mere presence of a non-ionic organic monolayer. DOPE is zwitterionic at physiological pH, and therefore, in a pure DOPE film, its head groups' orientation parallel to the interface results in charge neutralization between the molecules. Mineralization was carried out under 'standard conditions' (1 hour, 2 mM), and also for 4 hours, keeping calcium and phosphate concentrations at 2 mM.

The results from mineralization of DOPE films are shown in Fig. 3. Crystals grown for 1 and 4 hours had the same size (diameter below 260 nm), however, the former (1 h) were statistically distributed on the grid, while the latter (4 h) were organized in the form of chains. With the longer mineralization time their area fraction in the film increased from 0.9% (1 h) to 20% (4 h). The EDX analysis was not feasible in this case, because of the small (nm range) size of the crystals: the penetration depth and the excitation volume of the specimen by primary electrons are usually up to a few micrometers.

Mineralization beneath PHUE-DOPE mixed films

PHUE-DOPE mixed films at two extreme molar ratios ($X_{\text{PHUE}} = 0.9$ and 0.1) were investigated to assess the influence of the lipid amount on the crystal formation. Apart from standard conditions (1 h), mineralization was conducted for a longer mineralization time (4 hours).

PHUE-DOPE (0.9 : 0.1) mixed films

In both cases (1 and 4 h), the crystals were randomly distributed on the grid and were smaller (diameter below 500 nm) for the longer mineralization time than for 1 hour (diameters up to 800 nm), Fig. 4. Additionally, with the increased mineralization time the crystals covered a larger area (14% for 1 h and 22% for 4 h). The EDX spectrum confirmed the formation of calcium phosphate after one hour mineralization (Fig. S4, ESI[†]).

PHUE-DOPE (0.1 : 0.9) mixed films

Compared to mineralization using PHUE-DOPE films with $X_{\text{PHUE}} = 0.9$, the results for $X_{\text{PHUE}} = 0.1$ (Fig. 5) looked dramatically different. Regardless of the mineralization time,

| | | Standard conditions (2 mM, 1 h) | 2 mM, 4 h |
|---------|-------------------|-----------------------------------|-----------------------------------|
| | | Sodium phosphate buffer | |
| Results | Diameter [nm] | mostly 12 – 800, a few up to 1600 | mostly 12 – 500, a few up to 1100 |
| | Area fraction [%] | 13.5 ± 2.2 | 21.5 ± 3.3 |

Fig. 4 The results from mineralization of PHUE-DOPE (0.9 : 0.1) films. The crystals were randomly distributed, and smaller (below 500 nm) for the longer (4 h) mineralization time than for 1 hour (up to 800 nm).

two populations of crystals were observed, differing in size, distribution, and morphology. The crystals formed under standard conditions (1 h, 2 mM) consisted of randomly distributed, large 'spherical' crystals, group I (diameter up to 500 nm, with a few larger ones – up to 1600 nm), and group II – 'patches' of smaller crystals (below 80 nm and a few crystals with larger diameters – up to 360 nm), organized in the form of chains. An increase of mineralization time to 4 hours caused: (i) the growth of group I crystals to 800 nm (some even up to 3400 nm); (ii) the decrease in the size of the crystals from group II (to below 40 nm); and (iii) the change of the morphology and distribution of crystals from group II: from randomly distributed patches to a uniformly distributed network. The area

| | | Standard conditions (2mM, 1h) | 2 mM, 4 h |
|---------|-------------------|-----------------------------------|------------|
| | | Sodium phosphate buffer | |
| Results | Group of crystals | I | II |
| | Diameter [nm] | mostly 80 – 500, a few up to 1600 | ≤ 80 |
| Results | Group of crystals | I | II |
| | Diameter [nm] | mostly 40 – 800, a few up to 3400 | ≤ 40 |
| Results | Area fraction [%] | 9.7 ± 4.5 | 19.7 ± 3.1 |
| | Area fraction [%] | 10.7 ± 5.6 | 22.5 ± 5.7 |

Fig. 5 The results from mineralization of PHUE-DOPE (0.1 : 0.9) films. Two groups of crystals were formed; large (less controlled) crystals grew beneath the polymer-rich film, smaller crystals were controlled by the lipid-rich mixed film.

fraction occupied by crystals in TEM images did not seem to change with mineralization time (group I – *ca.* 10% and group II – *ca.* 20%). In both cases, EDX confirmed the formation of calcium phosphate crystals.

Mineralization of DOPS monolayers

The second investigated lipid was DOPS, which is negative at physiological pH. Anionic hydrophilic groups are helpful in triggering calcium phosphate crystallization since they can be complexed by calcium, and thus increase its local concentration, which leads to nucleation primarily at the monolayer. Similarly to DOPE, we first studied the templating properties of pure DOPS films, and then its mixtures with PHUE at two molar ratios ($X_{\text{PHUE}} = 0.9$ and 0.1).

A surface pressure–area isotherm from DOPS on the HEPES subphase with Ca^{2+} ions (2 mM) was identical to that recorded on water (Fig. S5, ESI†). Good time-dependent stability of a DOPS film on the buffer subphase at 12 mN m⁻¹ was also confirmed. Mineralization of the DOPS films was performed for 1 h and 4 h, keeping calcium and phosphate concentrations constant (2 mM).

The mineralization results are shown in Fig. 6. The crystals obtained after 1 hour had a spherical shape (with a maximal diameter of 260 nm) and were organized in chains, which covered 24% of the image area. These crystals were too small for both quantitative and qualitative EDX analyses. The presented EDX spectrum was recorded from a random spot on the grid, for an overview of what materials were present. Not surprisingly, the signals from Ca and P are very weak compared to carbon (lipid film). The increased time of mineralization led to the

| | | Standard conditions (2mM, 1h) | 2 mM, 4 h | | |
|---------|-------------------|----------------------------------|------------|------------|--|
| | | HEPES with Ca^{2+} ions | | | |
| Results | Group of crystals | I | I | II | |
| | Diameter [nm] | ≤ 260 | 500 - 1600 | ≤ 140 | |
| | Area fraction [%] | 23.9 ± 4.4 | 2.5 ± 0.6 | 28.8 ± 2.3 | |

Fig. 6 The results of mineralization of DOPS monolayers. Crystals had very uniform size (below 260 nm) and distribution, while with longer mineralization time two groups of crystals were observed.

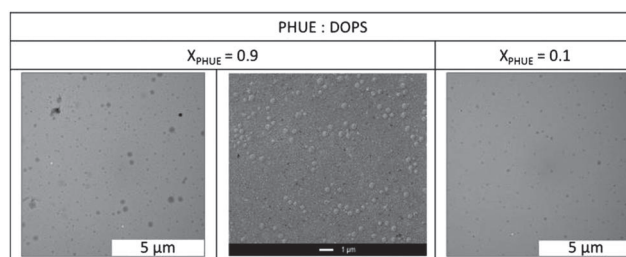


Fig. 7 EM images of non-mineralized PHUE–DOPS monolayers. The lipid domains were larger (average diameter 12–120 nm) for the mixed films with $X_{\text{PHUE}} = 0.9$, than for the mixed films with $X_{\text{PHUE}} = 0.1$ (average diameter 12–36 nm).

formation of completely different (in morphology and size) crystals. A few were large (between 500 and 1600 nm) and randomly distributed (area fraction of 2.5%) – group I. Group II contained ‘patches’ of crystals with diameters below 140 nm (area fraction of 29%). They were connected by thin ‘arms’ (with diameters difficult to measure at this image resolution). EDX proved that these were calcium phosphate crystals.

Mineralization beneath PHUE–DOPS mixed films

PHUE and DOPS were mixed at two extreme molar ratios, $X_{\text{PHUE}} = 0.9$ and 0.1, to analyze the influence of DOPS on the crystallization process. We have previously observed that lipid domains were formed in these mixed films, and we suppose that they could have a profound influence on the nucleation control. The mixed, non-mineralized films at both $X_{\text{PHUE}} = 0.9$ and 0.1 indeed show small domains under EM (Fig. 7). We observed circular domains, larger for $X_{\text{PHUE}} = 0.9$: diameters between *ca.* 12 and 120 nm, and a few with diameters up to 360 nm. The diameter of domains for $X_{\text{PHUE}} = 0.1$ was between 12 and 36 nm, again with a few larger ones (diameters up to 260 nm). The area fraction for both mixtures was similar (3.4 ± 0.4 for $X_{\text{PHUE}} = 0.9$ and 3.3 ± 1.3 for $X_{\text{PHUE}} = 0.1$). Both mixed films were used to study mineralization at different times (1 and 4 hours) and ion concentrations (0.5 and 2 mM).

PHUE–DOPS (0.9 : 0.1) mixed films

The results from mineralization of PHUE–DOPS (0.9 : 0.1) films are summarized in Fig. 8. After mineralization of the mixed film under ‘standard conditions’ (1 h, 2 mM) two groups of crystals were observed. The first group (area fraction 5%) contained crystals randomly distributed with diameters below 500 nm and a few larger ones, up to 1600 nm. There were also patches of small crystals that covered the grid almost completely. Their size was, however, difficult to measure due to their irregular shapes. After increasing the mineralization time to 4 h, the crystals revealed the same morphology as after 1 hour, but their size increased. The largest crystals (diameter 1600–3200 nm) covered 5% of the image. The smaller crystals had diameters up to 700 nm and covered 6% of the area. The EDX spectra contain peaks for calcium and phosphate. Mineralization was also performed using a lower concentration of calcium and phosphate ions (0.5 mM, for 4 hours). Here we observed structures

| | | 2 mM, 1 h | 2 mM, 4 h | 0.5 mM, 4 h |
|----------------------------------|-------------------|---------------------------------|-----------|-------------|
| HEPES with Ca ²⁺ ions | | | | |
| TEM | | | | |
| | | | | |
| Results | Group of crystals | I | I | II |
| | Diameter [nm] | mostly 12-500, a few up to 1600 | 1600-3200 | < 700 |
| | Area fraction [%] | 4.9 ± 1.2 | 4.7 ± 2.1 | 5.8 ± 0.2 |

Fig. 8 Mineralization of PHUE–DOPS (0.9 : 0.1) films. Two groups of crystals were observed regardless of the mineralization time, consistent with the DOPS domain size in mixed films. Crystallization strongly depended on the ion concentration.

that had uniform size (up to 360 nm) and distribution, and covered 6% of the area. They were, however, too small for EDX analysis.

PHUE–DOPS (0.1 : 0.9) mixed films

The results from mineralization of PHUE–DOPS (0.1 : 0.9) films are shown in Fig. 9. Under ‘standard conditions’ (1 h, 2 mM), the crystals were homogeneously distributed on the grid and had diameters between 12 and 270 nm (area fraction 19%). The EDX spectrum (Fig. S6, ESI[†]) confirmed the presence of calcium phosphate. After 4 h of mineralization the crystal size and distribution changed drastically. They grew much larger (diameter 1600 to 2600 nm) but covered only 1.3% of the analyzed grid area. The structures observed after 4 hours of mineralization from the lower ion concentration (0.5 mM) had a smaller size (maximal diameter 18 nm) than the crystals grown from 2 mM solutions. Consistently, they occupied a larger area (area fraction 16%, compared to 1.3% from 2 mM).

| | | 2 mM, 1 h | 2 mM, 4 h | 0.5 mM, 4 h |
|----------------------------------|-------------------|------------|-----------|-------------|
| HEPES with Ca ²⁺ ions | | | | |
| TEM | | | | |
| SEM | | | | |
| Results | Diameter [nm] | < 270 | 1600-2600 | < 40 |
| | Area fraction [%] | 18.8 ± 1.2 | 1.3 ± 0.2 | 15.6 ± 1.4 |

Fig. 9 The results from mineralization of PHUE–DOPS (0.1 : 0.9) films. A dense network of crystals (diameters below 270 nm) formed beneath PHUE–DOPS (0.1 : 0.9) films under standard conditions, and disappeared with longer mineralization time forming a few large crystals.

Discussion

PHUE monolayer mineralization

PHUE is a hydrophobic, neutral polymer, which forms stable (at least for the duration of the experiment – up to 4 hours) monolayers and therefore it is not assumed to degrade and release monomer/oligomer units to the subphase. Regarding the subphase buffer, it did not play any role in the organization of the polymer at the air–water interface (isotherms recorded on the buffers and bi-distilled water were identical), and thus the film morphology should not influence the mineralization experiments.

Usually, two populations of crystals were formed underneath PHUE films, which may suggest two (simultaneous or subsequent) processes controlling the crystal growth. A schematic representation of the proposed nucleation process is shown in Fig. 10A. The possibility of the formation of mechanically embedded crystals in between the polymer molecules was not confirmed by a control experiment (mineralization in the presence of the PHUE film, without subphase stirring): the results were identical. We cannot, however, exclude specific interactions to drive crystallization under the polymer film due to the ability of carbonyl groups to coordinate calcium ions^{47,48} and high dipole moment ($+6.00 \times 10^{-30}$ C m)⁴⁹ of the polymer's ester groups. Mineralization could also be induced by the polymer's terminal hydroxyl and carboxyl groups, which are known to influence nucleation and crystal growth.^{34,37,50} On the other hand, the approximated distances (calculated using the PHUE mean molecular area at 12 mN m⁻¹ and assuming a molecule occupies an area of a square) between PHUE terminal groups were large (*ca.* 130 Å), which makes it unlikely for the two terminal groups to be in such a close proximity to allow for the matching of the crystal lattice. Since the polymer is soft and polydisperse, it cannot be completely excluded that at some point the terminal groups were close enough to be complexed by calcium and thus initiate crystal growth. Calcium phosphate formation beneath PHUE films could also result from heterogeneous nucleation on the surface of a template (*e.g.* dust, scratch, or a monolayer) present in the system. This way the crystals' surface energy would be minimized, leading also to the lowering of activation energy for nucleation, and as a result faster nucleation would occur. It is worth noting that the morphology of crystals formed underneath PHUE films was different from crystals formed in the subphase. It is not clear, however, whether the influence of PHUE on the crystal size and morphology is unique or if the same nucleation effect could be induced by any other organic interface present in the system (mineralization of DOPE films was performed to discriminate between these possibilities). Formation of two populations of crystals may also suggest that there was a second nucleation process at a later time or the growth of large crystals could be caused by Ostwald ripening, where larger crystals grow at the expense of smaller and more soluble ones.⁵¹ This was clearly the case for the experiments with longer mineralization time. The total area occupied by crystals remained constant (*ca.* 17%, for both 1 and 4 h), but the size distribution was different: the crystals were larger and had more uniform size, while the small ones either disappeared or grew only slightly (Fig. 2).

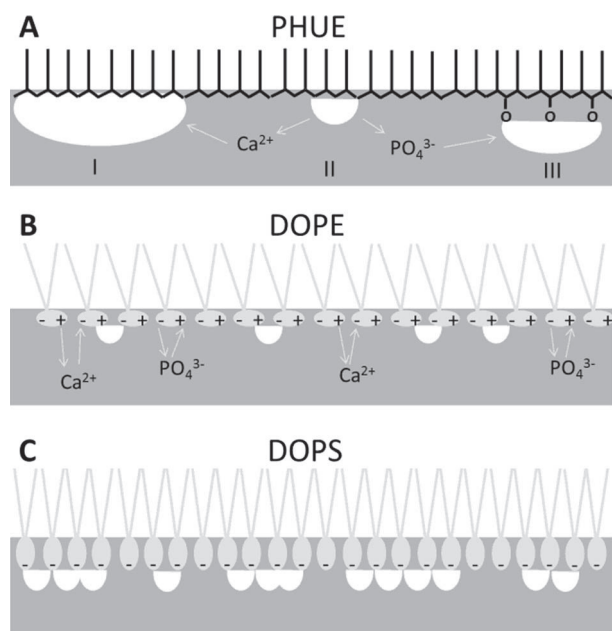


Fig. 10 Schematic representation (not to scale) of crystal (white) formation under standard conditions beneath monolayers of: (A) PHUE (I) heterogeneous nucleation, (II) Ostwald ripening, and (III) nucleation *via* complexation of polyester groups; (B) DOPE (arrows indicate electrostatic attraction and repulsion) and (C) DOPS.

Regarding the influence of the subphase on PHUE film mineralization, larger crystals were formed from Ca^{2+} -containing HEPES buffer than from sodium phosphate buffer. It is known that Ca^{2+} adsorption is a crucial step for calcium phosphate mineralization.⁵² Considering our experimental procedure, Ca^{2+} ions could complex the polymer's ester groups immediately after film spreading and during the monolayer formation. Since the polymer contains no groups that could be complexed by phosphate ions, mineralization from Ca^{2+} containing buffer appears to be better controlled.

At this point, the kinetic details of the formation of the two groups of crystals still need to be investigated to better understand whether they originate from different nucleation processes occurring simultaneously or in a time-dependent sequence. It is clear, however, that PHUE facilitates calcium phosphate formation, but the crystallization control it provides is still relatively poor. These results indicate that for orthopedic applications PHUE is a promising candidate only when mixed with crystal growth inducing materials to improve mineralization control while providing biodegradability and -compatibility to the composites. At the same time, it should not be considered for applications where it may induce pathological crystallization (*e.g.* calcification of blood vessels, formation of urinary stones or dental calculus).

DOPE monolayer mineralization

Experiments with DOPE served as a 'control', because its structure is very similar to that of DOPS, and it has zero net charge, similar to neutral PHUE. The two lipids have a different organization at the air–water interface (Fig. S7, ESI[†]): PE's head

groups lie parallel to the air–water interface,^{53–55} while PSs perpendicular or at an angle to the interface.⁴² Due to parallel orientation of PE head groups, the phosphate and amine groups are alternating, and thus charge neutralization occurs, which attenuates mineralization.

In contrast to PHUE monolayers, DOPE films induced growth of only a few small, randomly distributed crystals (Fig. 10B); the area fraction was also very small. These results confirmed that there was no complexation of PE groups. Since the experiments were performed on phosphate buffer, the amine groups could be nucleated first, however they are known to have very low nucleating ability.^{56–58} While Ca^{2+} rather than PO_4^{3-} adsorption is a crucial step in the formation of calcium phosphate,⁵² Ca^{2+} binding to DOPE monolayers is inhibited by internal salt bridges formed between phosphate and amine groups.⁵⁹ Furthermore, the literature $\text{p}K_a$ values of the amine group at the air–water interface vary from 7.5 to 9.7,⁶⁰ thus it is plausible that at typical physiological pH (body fluid) it was only slightly charged. With the increased mineralization time, the crystals formed beneath DOPE monolayers had generally the same size as after 1 hour of crystallization but were organized in chains, thus also covering a larger area. The results suggested that the small crystals obtained after 1 hour evoked changes in charge neutralization equilibrium, which caused the subsequent crystals to preferentially grow nearby, resulting in chain morphologies. These results also confirmed that specific interactions rather than the heterogeneous nucleation are responsible for calcium phosphate growth beneath PHUE monolayers (if heterogeneous nucleation was a dominant factor, crystals would also grow on DOPE films).

PHUE–DOPE monolayer mineralization

The negative excess free energy of mixing for PHUE–DOPE indicates attraction between these molecules,⁴² and the interaction energy (Δh)^{61,62} was larger for the mixed film with $X_{\text{PHUE}} = 0.9$ (Table S1, ESI[†]). Moreover, the mixed monolayer at $X_{\text{PHUE}} = 0.9$ showed good miscibility, while in the film with $X_{\text{PHUE}} = 0.1$, the DOPE phase separated forming domains.⁴²

The difference in miscibility of PHUE and DOPE at different compositions influenced the results of mineralization as shown in Fig. 11A. The crystals grown beneath the mixed monolayer with $X_{\text{PHUE}} = 0.9$ were *ca.* two times smaller than those grown under the PHUE monolayer. This was caused by the lipid molecules stabilized in between PHUE, which blocked the access to the nucleation-inducing PHUE's polyester groups, further inhibiting the crystal growth. Calcium phosphate crystals grown beneath the film at higher lipid molar excess ($X_{\text{PHUE}} = 0.1$) showed two populations. The first one contained randomly distributed spherical crystals, slightly smaller than those grown on the PHUE–DOPE (0.9 : 0.1) film, because more lipid molecules were available to inhibit crystal growth. The second group contained patches of smaller crystals forming chains, similar to those observed for 4 hours mineralization of DOPE films. In phosphatidylcholine (PC)–PE mixed films already a low amount of PC ($X_{\text{PC}} = 0.3$) drastically modifies the ionic properties of PE films, since PC does not possess a

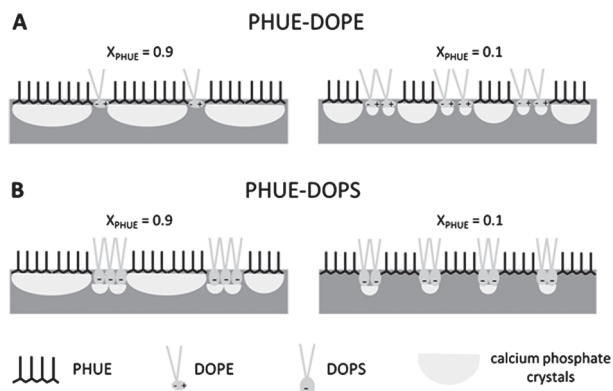


Fig. 11 Schematic representation (not to scale) of crystal formation under standard conditions beneath mixed monolayers of: (A) PHUE–DOPE and (B) PHUE–DOPS.

dissociable proton, which could be involved in hydrogen bonding between phosphate and amine groups.⁶³ Thus, it seems reasonable that charge neutralization was disturbed also by the polymer molecules and crystals had been first nucleated on the areas where polymer and lipid molecules were mixed.

The longer mineralization time of the PHUE–DOPE mixed film with $X_{\text{PHUE}} = 0.9$ did not follow the Ostwald ripening observed for PHUE and PHUE–DOPS films. The crystals were slightly smaller than after 1 hour mineralization, however covered *ca.* 2.5 times larger area. Plausibly, crystals also grew in the *z*-direction (not detected by TEM), however it appears that a small addition of a zwitterionic lipid to a PHUE film did not improve the crystal templating properties, but rather disturbed the nucleation process. In the case of PHUE–DOPE monolayers with a low polymer molar ratio ($X_{\text{PHUE}} = 0.1$), the growth of larger crystals with increased time of mineralization was observed, suggesting the Ostwald ripening mechanism again.

DOPS monolayer mineralization

In contrast to PHUE and DOPE, DOPS is ionic and apart from phosphate ($\text{p}K_{\text{a}} \approx 3.7$) and amine groups ($\text{p}K_{\text{a}} \approx 7.5$) it contains also a carboxylic group ($\text{p}K_{\text{a}} \approx 4.0$) responsible for Ca^{2+} adsorption.⁶³ The mineralization experiments were conducted at pH 7.5, where DOPS films were negatively charged. Identical isotherms recorded on HEPES buffer with Ca^{2+} ions and on bi-distilled water suggested that 2 mM Ca^{2+} concentration was not sufficient to change the film behavior of DOPS, even though complexation of anionic groups by Ca^{2+} is still expected.⁶⁴ Assuming that PS groups are perpendicular (or at the angle) to the air–water interface, the repulsion between lipid molecules would be reduced when calcium is present in the subphase. A tremendous difference in crystal formation was observed for DOPS monolayer mineralization compared to PHUE and DOPE. The crystals had more uniform size and shape, and formed chains. Mineralization of DOPS monolayers was much better controlled than that of PHUE films, due to the negative charge, a driving force to concentrate calcium, which then attracted phosphate ions, and initiated the nucleation of calcium phosphate crystals, Fig. 10C.

With four times longer mineralization time, the small spherical crystals forming chains were digested and as a result a network of small patches with thin arms remained, the dissolved ions supported the formation of larger crystals by Ostwald ripening. The SEM image of these large crystals (Fig. 6; 2 mM, 4 h) showed that crystals are covered with “the polymer blanket”, similar to those observed previously.³⁸ This is because calcium phosphate particles were large and stiff, and due to our transfer procedure to an EM grid (from the subphase side) the soft and flexible polymer film was on top and followed the contours of the crystals. The morphology of these large crystals resembled the ones observed by Wuthier and Eanes, attributed to hydroxyapatite (HAP).⁶⁵ It is worth noting that HAP formation requires regularly distributed nucleation centers, with the distances around 4, 6.3, 7.9, 9.0, and 9.6 Å (corresponding to the distances between Ca^{2+} ions in HAP).⁶⁶ The mean area of a DOPS molecule in the film at 12 mN m^{−1} was 95 Å², resulting in an average intermolecular distance of about 9.7 Å, in good agreement with the distance between Ca^{2+} ions in HAP. Quantitative EDX analysis (Ca/P ratio) of the crystals was not possible due to the small crystal size and the presence of phosphorus also in the lipid film. The low amount of material was also not sufficient to perform X-ray or electron diffraction experiments.

PHUE–DOPS monolayer mineralization

Mixed PHUE–DOPS films phase separate at the nano- and micrometer scale.⁴² For both molar ratios studied ($X_{\text{PHUE}} = 0.9$ and 0.1), circular domains were observed, larger for the higher polymer molar ratio. This difference could be explained by the comparison of interaction energies (Δh) in these two mixed films^{61,62} (Table S1, ESI[†]). The repulsion was *ca.* 12 times stronger for the mixed film with higher polymer molar ratio, resulting in larger domains.

In the mineralization experiments, both mixed films induced growth of densely packed patches of crystals, which were smaller and more uniform (in size and spatial distribution) for the mixed film with a lower polymer molar ratio ($X_{\text{PHUE}} = 0.1$). It suggested that formation of these crystallized patches was controlled by the lipid domains, rich in negative charge. Additionally, a few large crystals were formed underneath the mixed monolayer with higher polymer molar ratio. It appears plausible that these large crystals grew below the polymer, as they were randomly localized and had a large size distribution, Fig. 11B.

Similar to pure PHUE and DOPS films, longer mineralization of PHUE–DOPS monolayers led to the dissolution of the previously (1 h) observed patches of mineralized films, to support the growth of larger crystals. This was much more visible for the PHUE–DOPS (0.1 : 0.9) film, where the area fraction decreased from *ca.* 19% to 1%, and could be a result of crystal growth in 3D (not detectable by TEM), slow diffusion of dissolved ions or the differences in the rate of dissolution (fast) of small crystals and growth (slow) of larger crystals. The morphology of the large crystals was identical to that of the ones formed after 4 h beneath DOPS films and could be attributed to HAP (see Fig. S8, ESI[†] for the high resolution TEM image). These results

suggested that as long as DOPS is present in the film, HAP was formed, regardless of the polymer molar ratio. Even though the ability to control the calcium phosphate crystallization by PHUE–DOPS (0.1 : 0.9) and pure DOPS films is similar, the advantage of using mixed films is the higher stability against degradation, due to the presence of the high molar mass polymer.

Calcium phosphate crystallization under PHUE–DOPS monolayers was further analyzed for its dependence on the initial ion concentration (0.5 mM and 2 mM). At low concentration, the crystal growth would be limited by the ion diffusion. For both mixed films the TEM image revealed the structures to be uniformly distributed on the grids, with sizes corresponding to the size of lipid domains. This could suggest that the crystal size was identical to that of lipid domains, or that crystals were not formed at all and the observed structures were lipid domains. The latter would be the case if diffusion was very slow, and although the experiments were performed for 4 hours and the subphase was continuously stirred, this could have been insufficient to start the nucleation process. However, from the comparison of the area fraction of non-mineralized and mineralized mixed films, it can be observed that the area fraction increased (*ca.* 2 times for $X_{\text{PHUE}} = 0.9$ and *ca.* 5 times for $X_{\text{PHUE}} = 0.1$) after the mineralization, which indicates facilitated crystal formation. Additionally, the qualitative difference in SEM images (Fig. 7 vs. Fig. 8 and 9) points to crystal formation: before mineralization, the lipid domains had regular circular shape, while after mineralization from the lower ion concentration they became more ‘fuzzy’. These structures were however too small for EDX analysis.

In summary, we observed growth of calcium phosphate crystals under all investigated films. The average size of the crystals obtained under standard conditions (1 h, 2 mM) increases in the following order (polymer molar ratio in brackets):

DOPS; DOPE < PHUE–DOPS (0.1) < PHUE–DOPE (0.1);
PHUE–DOPS (0.9) < PHUE–DOPE (0.9) < PHUE.

With a longer mineralization time (4 h), the average size of crystals changes leading to the order:

DOPE < PHUE–DOPE (0.9) < PHUE–DOPE (0.1) < DOPS <
PHUE–DOPS (0.1) < PHUE \approx PHUE–DOPS (0.9).

In both cases, the smallest crystals were grown on DOPE films. As discussed above, nucleation of calcium phosphate is not possible using DOPE monolayers, due to the charge neutralization between the neighbouring molecules, internal salt bridges and poor nucleating ability of amine groups. Within the first hour of crystallization, the size of the crystals is limited by the neutral polymer, which weakly interacts with calcium phosphate. For that reason, with more polymer in the film larger crystals were grown. DOPS as a negatively charged lipid strongly interacts with calcium, resulting in a small size of

Table 1 Summary of the templating properties of the investigated materials; where – indicates poor control of crystallization, + good control of crystallization, and +++ very good control of crystallization

| One-component films | | |
|---------------------|---------------------------------|---------------------------------|
| PHUE | DOPE | DOPS |
| – | – | +++ |
| Two-component films | | |
| | PHUE($X_{\text{PHUE}} = 0.9$) | PHUE($X_{\text{PHUE}} = 0.1$) |
| DOPE | – | + |
| DOPS | + | +++ |

calcium phosphate crystals. After 4 hours of crystallization, the size of the crystals strongly reflects the properties of a templating material. The smallest crystals grew on pure and mixed DOPE films, followed by the negatively charged lipid and its mixtures with PHUE. The largest crystals were again formed beneath PHUE, as a result of its neutral charge and thus poor control over the crystal growth.

Conclusions

The aim of this study was to use PHUE–lipid monolayers to evaluate their applicability as biocompatible templates to grow calcium phosphate. Even though the polymer was neutral, we obtained amorphous calcium phosphate crystals beneath its monolayers. There was, however, a tremendous difference in mineralization using pure lipid monolayers, which we reported here for the first time – DOPS facilitated calcium phosphate growth, mineralization was very well controlled, while with DOPE only a few small crystals were formed. This difference was due to negative DOPS head groups, low nucleation ability of DOPE amine groups, and different orientation of these lipids at the air–buffer interface that leads to charge neutralization in DOPE films and maintains the DOPS charge. At higher molar ratios of DOPS in the mixed film, crystals with more uniform size and morphology were formed, as a result of a regular distribution of phase-separated lipid domains (rich in negative charge). In contrast, DOPE inhibited the growth of crystals under the mixed PHUE–DOPE film. For all the investigated films, the longer time of mineralization induced formation of larger crystals at the expense of smaller ones, following the Ostwald ripening process. The polymer–lipid molar ratio plays the dominant role in crystal size control in the first hour, while after 4 hours crystal size depends strongly on the material templating properties.

An interesting outcome of this study is that while PHUE alone somewhat facilitated calcium phosphate growth to obtain a good control of the process it appears necessary that PHUE was combined with other crystallization-inducing materials such as PS, which, even at very small molar ratios, provides a homogeneous size and shape distribution of the resulting crystals (Table 1). Another possibility to induce such mineralization is to functionalize the polymer with similar functional groups which is under investigation at the moment. This is the first report on mineralization using two-component thin films and clearly shows how crystals with desirable size and

morphology may be obtained by choosing appropriate additives and experimental conditions.

Acknowledgements

We thank the Swiss National Science Foundation, NCCR Nanoscience and Swiss Nanoscience Institute for financial support, and Gianni Morson (ZMB, Uni Basel) for help with TEM. A.J. is grateful to A. Spielhofer and B. Banusch (Nanoscience students, Uni Basel) for help with the experiments.

Notes and references

- 1 Health at a Glance 2011: OECD Indicators, 2011.
- 2 M. M. Stevens, *Mater. Today*, 2008, **11**, 18–25.
- 3 T. Albrektsson and C. Johansson, *Eur. Spine J.*, 2001, **10**, S96–S101.
- 4 E. S. Place, J. H. George, C. K. Williams and M. M. Stevens, *Chem. Soc. Rev.*, 2009, **38**, 1139–1151.
- 5 G. Q. Chen, *Chem. Soc. Rev.*, 2009, **38**, 2434–2446.
- 6 M. Zinn, B. Witholt and T. Egli, *Adv. Drug Delivery Rev.*, 2001, **53**, 5–21.
- 7 D. B. Hazer, E. Kilicay and B. Hazer, *Mater. Sci. Eng., C: Biomimetic Supramol. Syst.*, 2012, **32**, 637–647.
- 8 Y. W. Wang, Q. Wu and G. Q. Chen, *Biomaterials*, 2004, **25**, 669–675.
- 9 Y. W. Wang, Q. Wu, J. Chen and G. Q. Chen, *Biomaterials*, 2005, **26**, 899–904.
- 10 Y. W. Wang, F. Yang, Q. Wu, Y. C. Cheng, P. H. Yu, J. Chen and G. Q. Chen, *Biomaterials*, 2005, **26**, 755–761.
- 11 G. T. Kose, H. Kenar, N. Hasirci and V. Hasirci, *Biomaterials*, 2003, **24**, 1949–1958.
- 12 J. Y. Sun, J. Wu, H. Y. Li and J. Chang, *Eur. Polym. J.*, 2005, **41**, 2443–2449.
- 13 Y. Wang, Y. Z. Bian, Q. Wu and G. Q. Chen, *Biomaterials*, 2008, **29**, 2858–2868.
- 14 A. Merolli and M. Santin, *Molecules*, 2009, **14**, 5367–5381.
- 15 R. E. Wuthier, G. S. Rice, J. E. Wallace, Jr, R. L. Weaver, R. Z. LeGeros and E. D. Eanes, *Calcif. Tissue Int.*, 1985, **37**, 401–410.
- 16 E. D. Eanes, A. W. Hailer, R. J. Midura and V. C. Hascall, *Glycobiology*, 1992, **2**, 571–578.
- 17 C. L. Raggio, B. D. Boyan and A. L. Boskey, *J. Bone Miner. Res.*, 1986, **1**, 409–415.
- 18 M. Bosetti, M. Santin, A. W. Lloyd, S. P. Denyer, M. Sabbatini and M. Cannas, *J. Mater. Sci.: Mater. Med.*, 2007, **18**, 611–617.
- 19 M. Bosetti, A. W. Lloyd, M. Santin, S. P. Denyer and M. Cannas, *Biomaterials*, 2005, **26**, 7572–7578.
- 20 A. Merolli, M. Bosetti, L. Giannotta, A. W. Lloyd, S. P. Denyer, W. Rhys-Williams, W. G. Love, C. Gabbi, A. Cacchioli, P. T. Leali, M. Cannas and M. Santin, *J. Mater. Sci.: Mater. Med.*, 2006, **17**, 789–794.
- 21 M. Santin, W. Rhys-Williams, J. O'Reilly, M. C. Davies, K. Shakesheff, W. G. Love, A. W. Lloyd and S. P. Denyer, *J. R. Soc., Interface*, 2006, **3**, 277–281.
- 22 N. Satsangi, A. Satsangi, R. Glover, J. L. Ong and R. K. Satsangi, *J. Mater. Sci.: Mater. Med.*, 2004, **15**, 693–697.
- 23 A. Satsangi, N. Satsangi, R. Glover, R. K. Satsangi and J. L. Ong, *Biomaterials*, 2003, **24**, 4585–4589.
- 24 A. Reinstorf, M. Ruhnnow, M. Gelinsky, W. Pompe, U. Hempel, K. W. Wenzel and P. Simon, *J. Mater. Sci.: Mater. Med.*, 2004, **15**, 451–455.
- 25 J. D. Hartgerink, E. Beniash and S. I. Stupp, *Science*, 2001, **294**, 1684–1688.
- 26 E. D. Spoerke, S. G. Anthony and S. I. Stupp, *Adv. Mater.*, 2009, **21**, 425–430.
- 27 E. DiMasi, V. M. Patel, M. Sivakumar, M. J. Olszta, Y. P. Yang and L. B. Gower, *Langmuir*, 2002, **18**, 8902–8909.
- 28 B. Stripe, A. Uysal, B. H. Lin, M. Meron and P. Dutta, *Langmuir*, 2012, **28**, 572–578.
- 29 Y. Chen, J. Xiao, Z. Wang and S. Yang, *Langmuir*, 2009, **25**, 1054–1059.
- 30 B. R. Heywood and S. Mann, *J. Am. Chem. Soc.*, 1992, **114**, 4681–4686.
- 31 B. R. Heywood and S. Mann, *Langmuir*, 1992, **8**, 1492–1498.
- 32 B. R. Heywood and S. Mann, *Adv. Mater.*, 1992, **4**, 278–282.
- 33 G. Xu, I. A. Aksay and J. T. Groves, *J. Am. Chem. Soc.*, 2001, **123**, 2196–2203.
- 34 C. L. Ma, H. B. Lu, R. Z. Wang, L. F. Zhou, F. Z. Cui and F. Qian, *J. Cryst. Growth*, 1997, **173**, 141–149.
- 35 H. B. Lu, C. L. Ma, H. Cui, L. F. Zhou, R. Z. Wang and F. Z. Cui, *J. Cryst. Growth*, 1995, **155**, 120–125.
- 36 A. Dey, P. H. Bomans, F. A. Muller, J. Will, P. M. Frederik, G. de With and N. A. Sommerdijk, *Nat. Mater.*, 2010, **9**, 1010–1014.
- 37 L. J. Zhang, H. G. Liu, X. S. Feng, R. J. Zhang, L. Zhang, Y. D. Mu, J. C. Hao, D. J. Qian and Y. F. Lou, *Langmuir*, 2004, **20**, 2243–2249.
- 38 O. Casse, O. Colombani, K. Kita-Tokarczyk, A. H. E. Mueller, W. Meier and A. Taubert, *Faraday Discuss.*, 2008, **139**, 179–197.
- 39 M. Junginger, K. Kita-Tokarczyk, T. Schuster, J. Reiche, F. Schacher, A. H. E. Muller, H. Colfen and A. Taubert, *Macromol. Biosci.*, 2010, **10**, 1084–1092.
- 40 M. Junginger, K. Bleek, K. Kita-Tokarczyk, J. Reiche, A. Shkilnyy, F. Schacher, A. H. E. Muller and A. Taubert, *Nanoscale*, 2010, **2**, 2440–2446.
- 41 A. Jagoda, P. Ketikidis, M. Zinn, W. Meier and K. Kita-Tokarczyk, *Langmuir*, 2011, **27**, 10878–10885.
- 42 A. Jagoda, M. Zinn, W. Meier and K. Kita-Tokarczyk, *Macromol. Chem. Phys.*, 2012, **213**, 1922–1932.
- 43 R. Hartmann, R. Hany, T. Geiger, T. Egli, B. Witholt and M. Zinn, *Macromolecules*, 2004, **37**, 6780–6785.
- 44 Image J, <http://rsbweb.nih.gov/ij/>, accessed 08.05.2012.
- 45 H. K. Walker, W. D. Hall and J. W. Hurst, *Clinical Methods: The History, Physical, and Laboratory Examinations*, Butterworths, Boston, 1990.
- 46 P. Dynarowicz-Latka, A. Cavalli and O. N. Oliveira, *Thin Solid Films*, 2000, **360**, 261–267.
- 47 N. Marcotte, S. Fery-Forgues, D. Lavabre, S. Marguet and V. G. Pivovarenko, *J. Phys. Chem. A*, 1999, **103**, 3163–3170.
- 48 J. Maynadié, B. Delavaux-Nicot, D. Lavabre, B. Donnadiou, J.-C. Daran and A. Sournia-Saquet, *Inorg. Chem.*, 2004, **43**, 2064–2077.

- 49 E. Salz, J. P. Hummel, P. J. Flory and M. Plavsic, *J. Phys. Chem.*, 1981, **85**, 3211–3215.
- 50 G. K. Toworfe, R. J. Composto, C. S. Adams, I. M. Shapiro and P. Ducheyne, *Bioceramics 18, Pts 1 and 2*, 2006, vol. 309–311, pp. 275–278.
- 51 S. Mann, *Biomaterialization Principles and Concepts in Bioinorganic Materials Chemistry*, Oxford university Press, Oxford, 2005.
- 52 B. C. Yang, J. Weng, X. D. Li and X. D. Zhang, *J. Biomed. Mater. Res.*, 1999, **47**, 213–219.
- 53 H. Hauser, I. Pascher, R. H. Pearson and S. Sundell, *Biochim. Biophys. Acta*, 1981, **650**, 21–51.
- 54 M. C. Phillips, E. G. Finer and H. Hauser, *Biochim. Biophys. Acta*, 1972, **290**, 397–402.
- 55 M. M. Standish and B. A. Pethica, *Trans. Faraday Soc.*, 1968, **64**, 1113.
- 56 K. Sato, Y. Kumagai and J. Tanaka, *J. Biomed. Mater. Res.*, 2000, **50**, 16–20.
- 57 M. Tanahashi and T. Matsuda, *J. Biomed. Mater. Res.*, 1997, **34**, 305–315.
- 58 G. K. Toworfe, R. J. Composto, I. M. Shapiro and P. Ducheyne, *Biomaterials*, 2006, **27**, 631–642.
- 59 D. O. Shah and J. H. Schulman, *J. Lipid Res.*, 1967, **8**, 227–233.
- 60 T. Seimiya and S. Ohki, *Biochim. Biophys. Acta*, 1973, **298**, 546–561.
- 61 P. Joos and R. A. Demel, *Biochim. Biophys. Acta*, 1969, **183**, 447.
- 62 C. Mestres, M. A. Alsina, M. Espina, L. Rodriguez and F. Reig, *Langmuir*, 1992, **8**, 1388–1391.
- 63 T. Seimiya, H. Miyasaka, T. Kato, T. Shirakawa, K. Ohbu and M. Iwahashi, *Chem. Phys. Lipids*, 1987, **43**, 161–177.
- 64 H. Hauser, A. Darke and M. C. Phillips, *Eur. J. Biochem.*, 1976, **62**, 335–344.
- 65 R. E. Wuthier and E. D. Eanes, *Calcif. Tissue Res.*, 1975, **19**, 197–210.
- 66 L. W. Schroeder, R. L. Bowen and J. S. Ferris, *J. Biomed. Mater. Res.*, 1980, **14**, 83–90.

Biodegradable polymer-lipid monolayers as templates for calcium phosphate mineralization

Supporting Information

A. Jagoda, M. Zinn, E. Bieler, W. Meier and K. Kita-Tokarczyk

Received (in XXX, XXX) Xth XXXXXXXXXX 20XX, Accepted Xth XXXXXXXXXX 20XX

DOI: 10.1039/b000000x

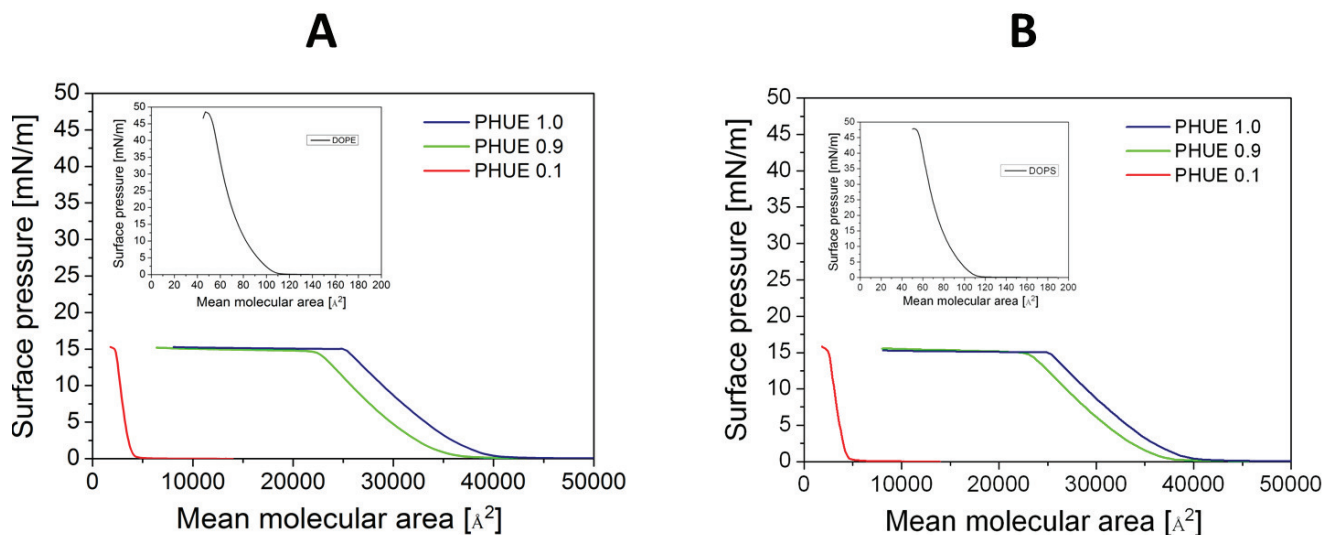


Fig. S1 π -A isotherms from PHUE-DOPE (A) and PHUE-DOPS (B) mixed films

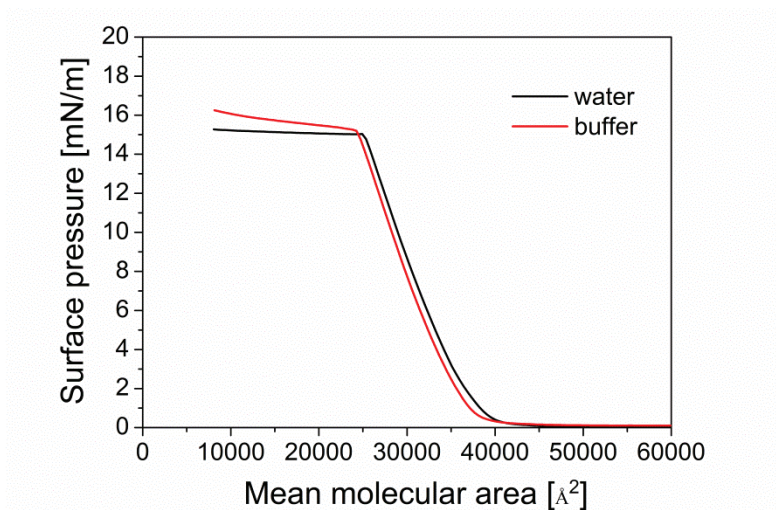


Fig. S2 π -A isotherms from PHUE on water and buffer (HEPES with Ca^{2+} , 2 mM, pH=7.5)

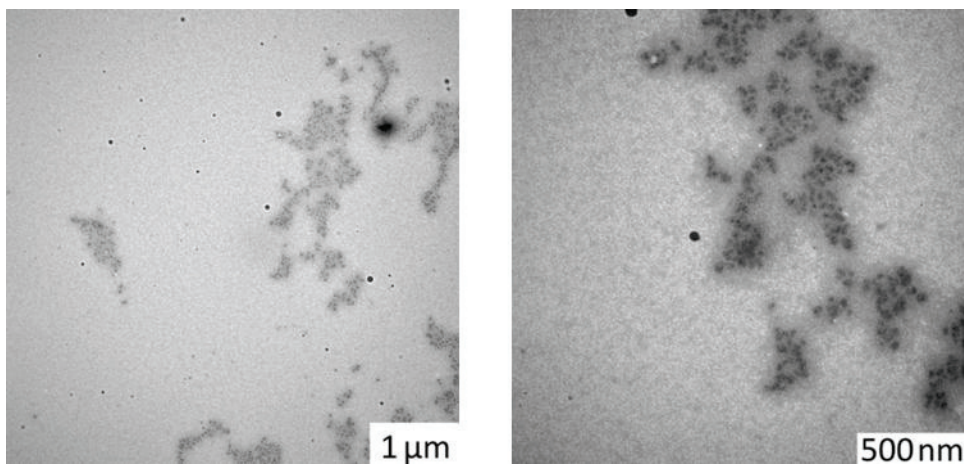


Fig. S3 TEM images of calcium phosphate grown without a PHUE film

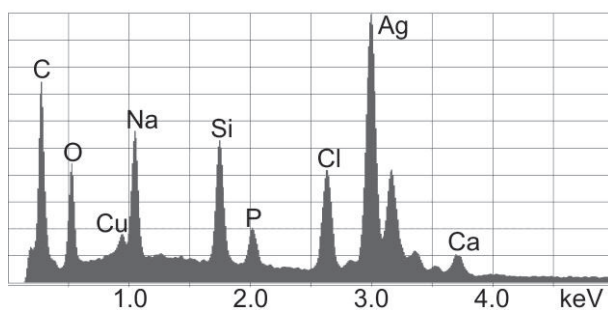


Fig. S4 EDX spectrum of crystals grown in standard conditions (2 mM, 1 h) beneath PHUE-DOPE (0.9 : 0.1) films

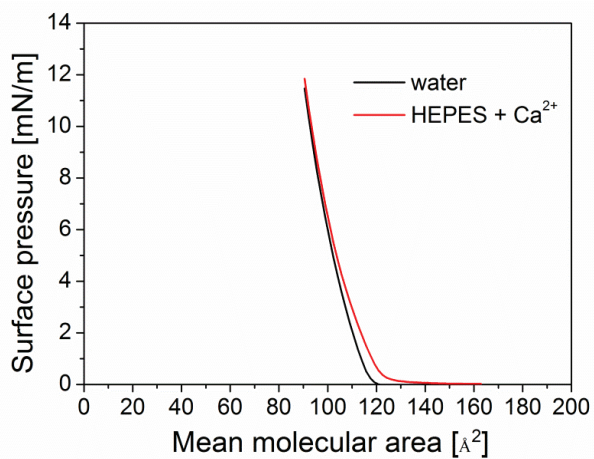


Fig. S5 π -A isotherms from DOPS mixed films recorded on water and HEPES with Ca^{2+} ions

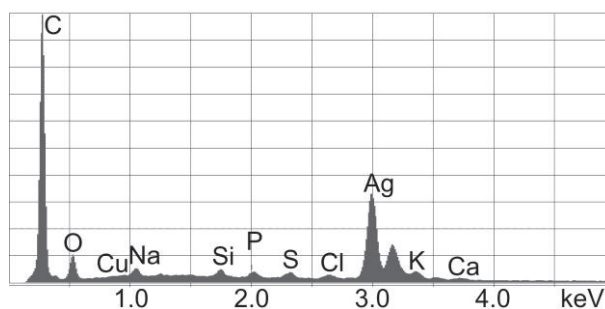


Fig. S6 EDX spectrum of crystals grown in standard conditions (2 mM, 1 h) beneath PHUE-DOPS (0.1 : 0.9) films

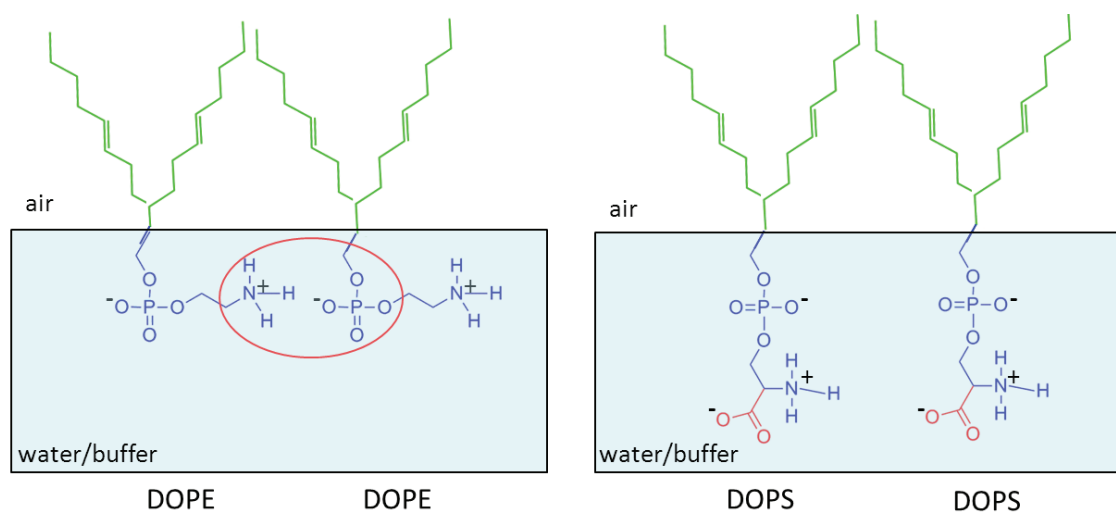


Fig. S7 Schematic representation of DOPE and DOPS organization at the air-water interface. Red contour indicates groups involved in charge neutralization between DOPE molecules

Table 1 The ΔG^{exc} , interaction parameter (α) and interaction energy (Δh) for PHUE-lipid mixed films

| X_{PHUE} | ΔG^{exc} [kJ/mol] | α | Δh [kJ/mol] |
|--------------------|-------------------------------------|----------|------------------------|
| PHUE : DOPE | | | |
| 0.9 | -32.10 | -146.50 | -59.45 |
| 0.1 | -21.39 | -97.62 | -39.61 |
| PHUE : DOPS | | | |
| 0.9 | 43.18 | 197.04 | 79.96 |
| 0.1 | 3.59 | 16.39 | 6.65 |

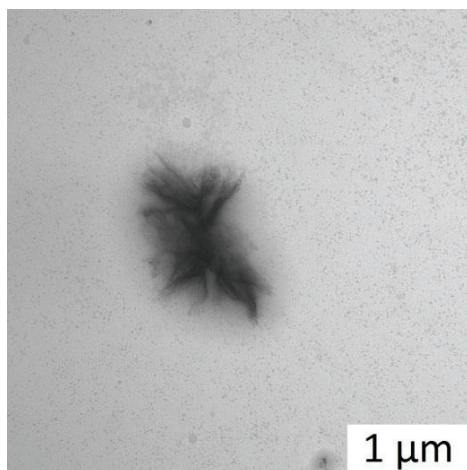


Fig. S8 TEM image of calcium phosphate grown beneath PHUE-DOPS (0.9 : 0.1) films

4. Conclusions and outlook

In this thesis, polyhydroxyalkanoate-based thin films are described in terms of their interfacial properties and optimization for templated growth of calcium phosphate, as potential materials for future orthopedic applications. Poly([R]-3-hydroxy-10-undecenoate) (PHUE) was selected as a representative of mcl-PHAs and Langmuir monolayer technique as an experimental approach.

PHUE properties on the free water surface were studied, including influence of various experimental conditions on the polymer monolayer behavior. Despite the fact that PHUE has a more hydrophobic than amphiphilic character, it formed stable monolayers insensitive to change of the film compression rate, solvent evaporation time and the spreading solution concentration. PHUE monolayers were only slightly influenced by the subphase temperature (since the solubility of shorter polymer chains increases at higher temperatures) and by the number of molecules spread at the interface (more molecules at the interface limit the spreading ability and lead to clustering). Furthermore, the polymer monolayer behavior was elastic, as shown by reversible isotherm behavior upon several compression-expansion cycles.

In the next step, PHUE interactions with various phospholipids, containing the same hydrophobic tail and different hydrophilic head groups, were evaluated. The liquid expanded PHUE monolayer phase was not affected by the addition of DOPC and DOPS. It was, however, possible to control the monolayer fluidity by varying the PHUE-DOPE molar ratio (the more DOPE in the mixed film, the more liquid film). Regarding the polymer interactions with lipids, they were highly dependent on the lipid head group size and its orientation at the air-water interface. Repulsive interactions, manifested as film demixing, were observed with DOPC and DOPS whose head groups are large and perpendicular to the interface. Attractive interactions, due to hydrogen bonding, ion-

dipole, and dipole-dipole interactions, were observed with DOPE, possessing a small head group oriented parallel to the interface.

The final step was to analyze the templating properties of pure (PHUE, DOPS, DOPE) and mixed (PHUE-DOPS, PHUE-DOPE) monolayers for calcium phosphate crystallization. Experiments performed in various experimental conditions (mineralization time, ion concentration, polymer-lipid molar ratio), allowed to find the optimum crystal growth parameters. PHUE itself facilitated crystal formation, but did not offer a good crystallization control, due to its neutral charge. Different orientation of lipids at the air-water interface as well as lipid charge strongly influenced mineralization results. Briefly, with pure DOPS (negative, perpendicular to the interface), fine crystals were formed, whereas with DOPE (zwitterionic, parallel to the interface) only a few crystals appeared. Consequently, the addition of DOPS to the polymer film led to uniformity in crystals size and morphology, while DOPE addition inhibited the growth of large crystals. Additionally, longer mineralization time induced dissolution of smaller crystals and the growth of larger crystals according to the Ostwald ripening mechanism.

Summarizing, PHUE-based materials containing biologically active molecules (phospholipids) were studied and showed different behavior depending on the phospholipid ratio and head group properties. This work could be further extended to analyze the PHAs interactions with other biomembrane components (e.g. proteins, sugars) to obtain firstly, more comprehensive information about material-living cells interactions, and secondly, to obtain materials with novel properties.

Additionally, PHUE-based thin films, depending on the film composition and the growth conditions, were shown to induce calcium phosphate mineralization. To obtain a good control of crystallization using only pure PHA films, one would have to functionalize the polymer, with e.g. carboxylic or phosphate groups, in order to increase

its hydrophilicity, which also improves cell adhesion. The work using carboxyl-functionalized PHA polymer is in progress at the moment. Last, but not least, the obtained PHUE(-lipid)-calcium phosphate composite materials should be further studied in the context of their cell compatibility. The outcome of the present work may be applied not only to understand PHA-based materials, but also other materials, where interfacial compatibility with tissue cells plays an important role.

5. Appendix

5.1. Polymer molar mass optimization

Two PHUE polymers with lower molar mass (PHUE3k, PHUE6k) were investigated in order to find out whether the polymer packing properties will improve, leading also to the increase in the monolayer collapse surface pressure with a decrease of the polymer molar mass. Polymer characterization results are compiled in Table 2. Monolayer experiments were performed as described before [Jagoda *et al.*, *Langmuir* **2011**, 27 (17), 10878].

Table 2. Polymer characterization results.

| Polymer | M_w (g/mol) | M_n (g/mol) | PDI |
|---------|---------------|---------------|-----|
| PHUE3k | 7 705 | 3 132 | 2.5 |
| PHUE6k | 13 745 | 5 950 | 2.3 |

The monolayers results are compared with those previously published for PHUE ($M_n = 165\ 000$ g/mol; PHUE165k) [Jagoda *et al.*, *Langmuir*, **2011**, 27 (17), 10878].

5.1.1. One-component films

Surface pressure-area isotherms, together with compressibility moduli, from PHUE3k and PHUE6k are shown in Figure 7 A.

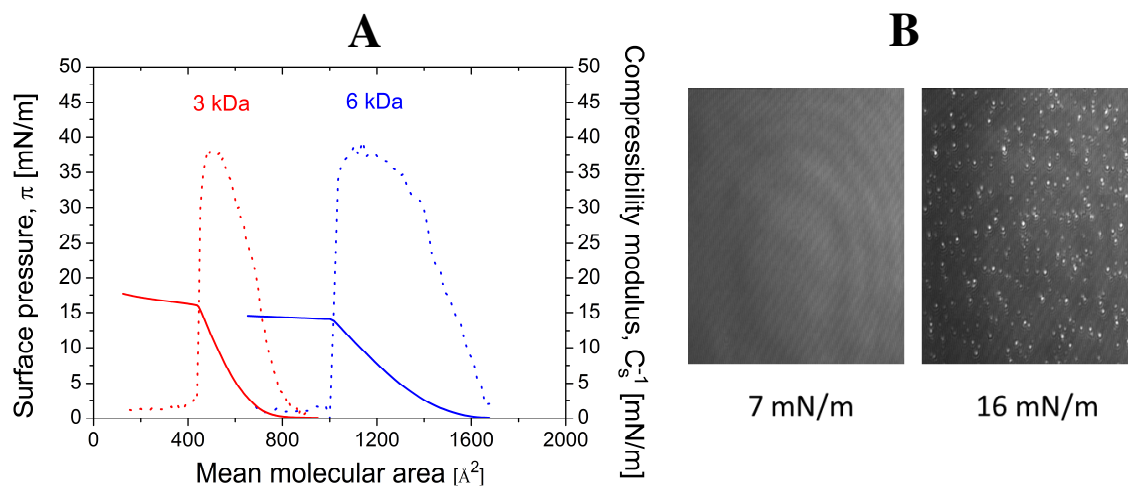


Figure 7. A) Surface pressure-area (π -A) isotherm (solid line) and compressibility modulus C_s^{-1} (dotted line) from PHUE3k (red) and PHUE6k (blue) monolayers. B) BAM images (220 x 250 μm) of the PHUE3k monolayer at 7 and 16 mN/m.

As expected, the surface pressure-area isotherms from smaller polymers (PHUE3k and PHUE6k) were shifted to the lower mean molecular areas (760 Å² for PHUE3k, and 1 600 Å² for PHUE6k, vs. 40 000 Å² for PHUE165k at isotherm lift-off). However, the collapse pressures remained the same (ca. 15 mN/m), which suggested that it is not possible to prepare more densely packed PHUE monolayers. The compressibility modulus values were similar (38 mN/m) as for PHUE165k (36 mN/m), indicating liquid expanded state of the monolayers. Also, the morphology of PHUE3k film (observed with BAM) did not change comparing to PHUE165k. During the film compression, from the lift-off (760 Å² per molecule, $\pi = 0$ mN/m) to the collapse, a smooth monolayer was observed, Figure 7 B. After the monolayer reached the collapse pressure very bright, crystalline domains were formed.

5.1.2. PHUE3k-DOPS mixed films

PHUE3k was mixed with DOPS at two extreme molar ratios ($X_{\text{PHUE}} = 0.9$ and 0.1) to investigate if the polymer molar mass influences the interactions with the lipid. Surface pressure-area isotherms (Figure 8) were recorded until the pressure reached 12 mN/m (the pressure at which the following mineralization experiments were conducted).

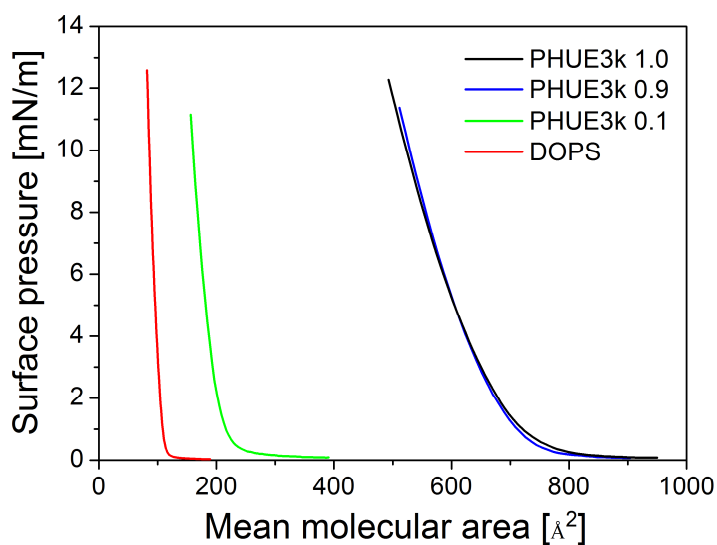


Figure 8. π -A isotherms from PHUE3k-DOPS films.

Similarly to previously studied PHUE165k-lipid systems [Jagoda *et al.*, *Langmuir*, **2011**, 27 (17), 10878; Jagoda, *et al.*, *Macromol. Chem. Phys.*, **2012**, 213 (18), 1922.], the addition of DOPS to the polymer film caused a decrease of a mean molecular area of the mixed films, in particular for the mixed film with $X_{\text{PHUE}} = 0.1$. There was, however no difference in mean molecular areas for the pure PHUE3k film and for the mixed film with $X_{\text{PHUE}} = 0.9$ - this effect is reproducible but its origin is not clear at the moment, and would need further investigations. The excess free energy of mixing (Table 3) was positive (similarly to the mixed films containing the larger polymer-PHUE165k) and indicated repulsive interactions between the two components, leading to their

immiscibility. However, the values of ΔG^{exc} of PHUE3k-DOPS films were smaller than the ones of PHUE165k-DOPS system, due to a smaller mass difference between the polymer and the lipid (about 4 times, while with PHUE165k it is about 200 times). The large errors result from the error of the mean molecular area, typical for polymers and large molecular mass materials. These results confirmed that interactions between PHUE and DOPS are specific, and depend on the materials chemistry rather than molecular size.

Table 3. Comparison of the excess free energy of mixing for PHUE3k-DOPS and PHUE165k-DOPS mixed films.

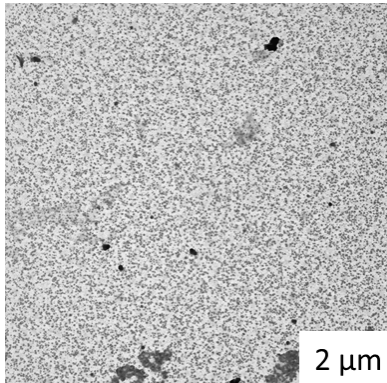
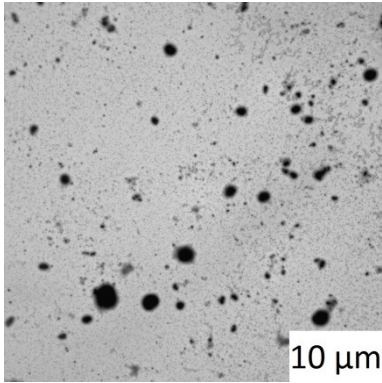
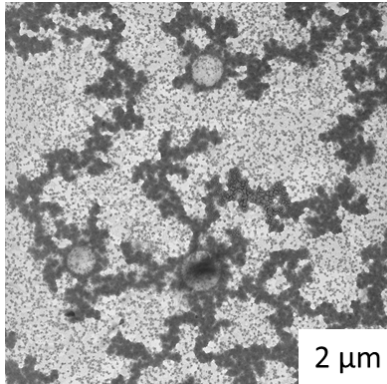
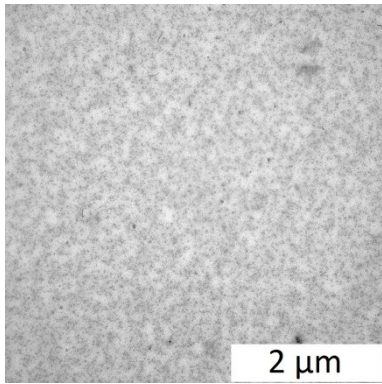
| X_{PHUE} | Surface Pressure [mN/m] | PHUE3k | PHUE165k |
|-------------------|----------------------------|----------------------------------|--------------------|
| | | ΔG^{exc} [kJ/mol] | |
| 0.9 | 2.5 | 0.81 ± 0.83 | 16.43 ± 34.10 |
| | 7.5 | 2.44 ± 2.48 | 44.26 ± 102.29 |
| | 12.5 | 3.12 ± 3.64 | 43.18 ± 170.48 |
| 0.1 | 2.5 | 0.57 ± 0.36 | 5.25 ± 7.39 |
| | 7.5 | 1.39 ± 1.07 | 6.51 ± 22.16 |
| | 12.5 | 1.97 ± 1.57 | 3.59 ± 39.94 |

5.1.3. Mineralization of PHUE3k-DOPS films

The PHUE3k-DOPS mixed films were used as templates to grow calcium phosphate. Mineralization experiments were carried out as described in [Jagoda *et al.*, *Journal of Materials Chemistry B*, **2013**, *1* (3), 368-378], on HEPES buffer containing Ca^{2+} ions at 2 mM, for 1 hour. As shown in Table 4, the polymer size had a tremendous effect on the crystals formation. First of all, the crystals were more homogeneously distributed than on PHUE165k-DOPS films. Secondly, they had more uniform size and morphology. Mineralization using the smaller polymer in the mixed films was much better controlled than with the larger PHUE. Furthermore, we could not observe large

crystals (diameters in μm range) that were found using PHUE165k-DOPS monolayers. It suggested that either a larger amount of DOPS (mass-wise, due to the smaller mass asymmetry) present in the film dominated the nucleation, or the smaller PHUE controlled mineralization better, leading to the smaller crystals. Despite better control of crystallization achieved with the low molar mass polymer than with PHUE165k, one could expect also faster degradation and lower stability of the PHUE3k films. For example, Jo et al. investigated PLLA and P(3HB) monolayers, with five-fold difference in polymer masses; the polymer with higher molar mass (P(3HB)) degraded much slower than the PLLA [Jo et al., *Polym. Degrad. Stabil.*, **2007**, 92 (7), 1199].

Table 4. TEM images of PHUE3k-DOPS and PHUE165k-DOPS films mineralized with calcium phosphate.

| X_{PHUE} | PHUE3k | PHUE165k |
|-------------------|---|--|
| 0.9 |  |  |
| 0.1 |  |  |

5.2. Langmuir-Blodgett transfers

PHUE monolayers were transferred to various substrates in order to evaluate feasibility for preparation of solid-supported PHUE films/membranes.

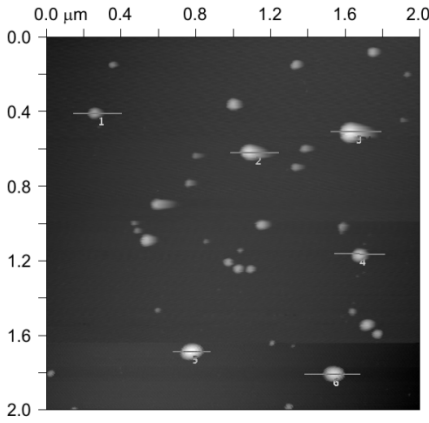
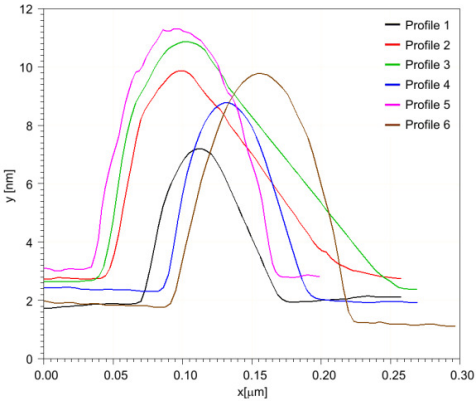
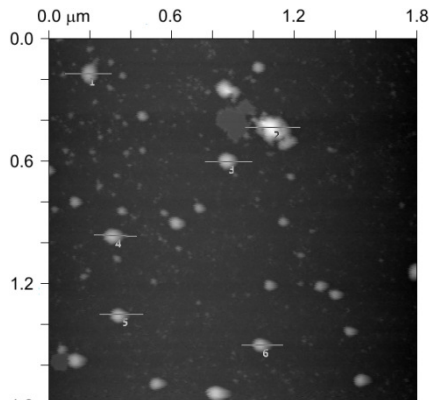
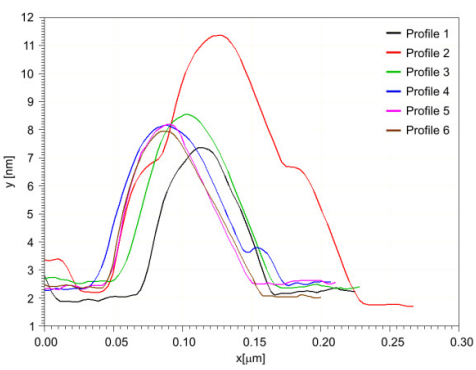
PHUE (165 500 g/mol) monolayers were prepared on water, sodium phosphate, and phosphate buffered saline (PBS) subphases. Monolayers were compressed until the surface pressure reached 12 mN/m, equilibrated for 5 minutes, and then transferred (at 0.5 mm/min) on solid surfaces (mica- freshly cleaved, or Si wafer- cleaned in piranha solution) using Langmuir-Blodgett upstroke transfer.

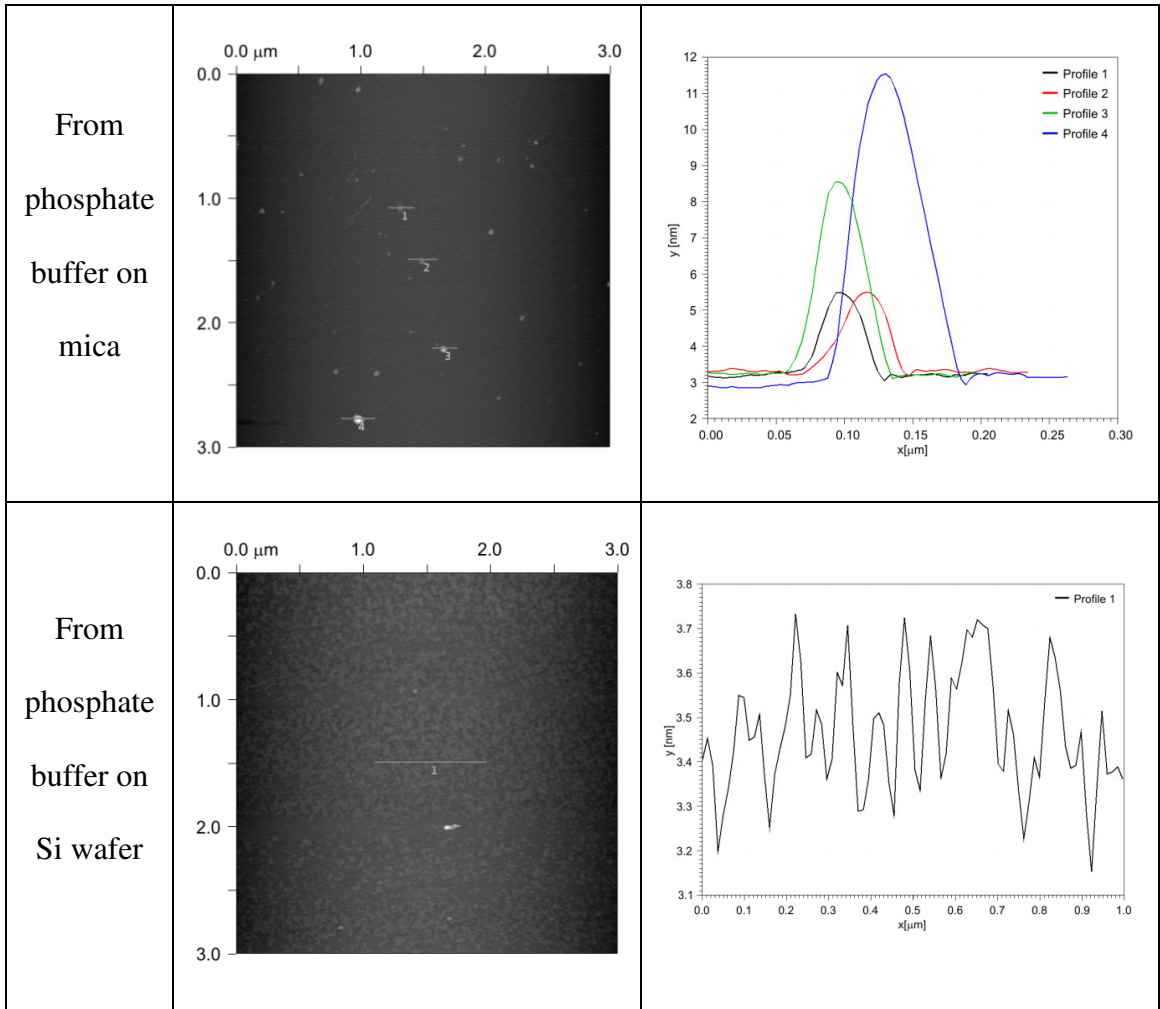
Transfer ratio (TR; a ratio between a decrease in the monolayer surface area during the film deposition, and the area of the solid support) provides the first approximate information if the transfer is successful ($TR \approx 1$ for good deposition). For samples studied here, TR was in the range of 2 to 10, and varied between the samples. It means that the monolayer area decreased 2 to 10 times comparing with the area of solid surfaces, to which the transfer was performed. It may suggest that during the transfer the molecular packing density changed and PHUE formed multilayers or aggregates. Together with poor transfer reproducibility, it was an indication that it is not possible to transfer defect-free PHUE monolayers on mica and silicon supports. Previously, Nobes et al. reported that scl- and mcl-PHAs (P(3HB), P(3HV), P(3HH), P(3HO), and P(3HN)) were easily deposited on mica, glass, and silicon wafers surfaces [Nobes *et al.*, In *From Annual Technical Conference - Society of Plastics Engineers 1999* (57), 2185]. This may suggest that 9 carbon atoms in the monomer unit constitute a threshold for the efficient transfer of PHAs to solid surfaces. However, the authors did not report the polymer molar mass, solid support preparation and characterization, and the transfer conditions (e.g. surface pressure, transfer rate). For that reason, the different observations made here

could result from large differences in the polymer masses, solid surface preparation, or experimental conditions.

Nevertheless, solid-supported PHUE films were examined using Atomic Force Microscopy (AFM), the images are collected in Table 5. It is clear that it was not feasible to transfer the polymer monolayers. Instead of homogeneous film, in most cases, we observed non-homogeneously distributed aggregates of a few to several nanometers in height.

Table 4. AFM images and height profile for PHUE transferred on solid surfaces.

| Transfer conditions | AFM image | Height profile |
|-------------------------|---|--|
| From water on mica |  |  |
| From PBS buffer on mica |  |  |



Curriculum vitae

PERSONAL DATA:

Agnieszka M. Jagoda

born in Tychy, Poland

on 29.12.1983

EDUCATION:

07.2009 – 11.2012 **PhD**, University of Basel, **Department of Chemistry**, Basel, Switzerland; specialization: Physical Chemistry/ Polymers, with Prof. Dr. Wolfgang Meier and Dr. Katarzyna Kita-Tokarczyk

“Polyhydroxyalkanoate-based thin films: characterization and optimization for calcium phosphate crystallization”

02.2009 – 01.2010 Postgraduate studies in Human Resources Management in Modern Organizations, Polish Open University- Higher School of Management, Cracow, Poland

10.2002 – 05.2007 **M.Sc.**, Jagiellonian University, **Faculty of Chemistry**, Cracow, Poland with Prof. Dr. Patrycja Dynarowicz-Łątka and Dr. Katarzyna Hąc-Wydro

“The study on the influence of the plant sterols on the molecular organization of the lipids monolayer”

WORK EXPERIENCE:

03.2009 – 06.2009 Chemist- laboratory technician, SGS EKO-PROJEKT LTD, Pszczyna, Poland

10.2007 – 10.2008 Chemist- laboratory technician, Premier Laboratory Inc., Dayville, USA

08.2007 Office worker (internship), Manpower Inc, Gliwice, Poland

09.2006 Chemistry teacher (pedagogical practice), V Secondary School, Cracow, Poland

09.2005 Chemistry teacher (pedagogical practice), II Gymnasium, Bieruń, Poland

COURSES:

03.2012 Project management for research (Organizer: University of Basel)

11.2011 Electron microscopy course (Organizer: The Center for Microscopy of the University of Basel- ZMB)

10.2010 Rational approaches towards materials and polymers with nanoscale order and improved properties, with Prof. Helmut Cölfen (Organizer: CUSO, EPFL, Lausanne)

SCHOLARSHIPS, GRANTS & AWARDS:

- SCNAT/SCS Chemistry Travel Award, 2011
- 3rd place in the C&EN's Photo Contest- Beauty at the Lab Bench, 2011
- Poster Prize Award - P2M Precision Polymer Materials, ESF Conference, Obernai (Strasbourg), France, 2011

SKILLS:

Experimental skills: thin films, surface analysis, self-assembly of colloids and polymers, crystallization

Experimental methods: Langmuir monolayers, Langmuir-Blodgett transfers, Brewster angle microscopy (BAM), transmission electron microscopy (TEM), scanning electron microscopy (SEM), energy-dispersive X-ray spectroscopy (EDX), atomic force microscopy (AFM), infrared spectroscopy (IR), contact angle

Languages: Polish: native
English: fluent (C1)
German: basic (A2/B1)

Computer skills: MS Windows, MS Office, data analysis and visualization (Origin), website administration, HTML (Macromedia Dreamweaver)

PUBLICATIONS:

1. **A. Jagoda**, M. Zinn, E. Bieler, W. Meier, K. Kita-Tokarczyk, “*Biodegradable polymer-lipid monolayers as templates for calcium phosphate mineralization*”, *J. Mater. Chem. B*, 1 (2013), 368-378
2. **A. Jagoda**, M. Zinn, W. Meier, K. Kita-Tokarczyk, “*Head group influence on lipid interactions with a polyhydroxyalkanoate biopolymer*”, *Macromol. Chem. Phys.*, 213 (2012), 1922-1932
3. **A. Jagoda**, J. Kowal, M. Delcea, C. G. Palivan, W. Meier, (2012). Polymer Vesicles on Surfaces. In J. Mano, J. C. Rodriguez-Cabello, A. Taubert (Eds.), *Biomaterials Surface Science*. Wiley. (submitted)
4. **A. Jagoda**, P. Ketikidis, M. Zinn, W. Meier, K. Kita-Tokarczyk, “*Interactions of biodegradable poly([R]-3-hydroxy-10-undecenoate) with DOPC lipid: a monolayer study*”, *Langmuir*, 27 (2011), 10878-10885
5. K. Hąc-Wydro, P. Wydro, **A. Jagoda**, J. Kapusta, “*The study on the interaction between phytosterols and phospholipids in model membranes*”, *Chem. Phys. Lipids*, 150 (2007) 22-34
6. K. Hąc-Wydro, J. Kapusta, **A. Jagoda**, P. Wydro, P. Dynarowicz-Łątka, “*The influence of phospholipid structure on the interactions with nystatin, a polyene antifungal antibiotic A Langmuir monolayer study*”, *Chem. Phys. Lipids*, 150 (2007) 125-135

POSTER PRESENTATIONS:

1. **A. Jagoda**, R. Hany, M. Zinn, W. Meier, K. Kita-Tokarczyk, “*Calcium phosphate growth induced by a polyester biopolymer*”, Materials Research Society Fall Meeting, Boston, USA, 2012
2. **A. Jagoda**, R. Hany, M. Zinn, W. Meier, K. Kita-Tokarczyk, “*Calcium phosphate growth induced by a polyester biopolymer*”, Biomineralization Gordon Research Conference, New London, USA, 2012
3. **A. Jagoda**, S. Winkler, R. Hany, M. Zinn, W. Meier, K. Kita-Tokarczyk, “*Controlling inorganic crystallization by organized polymer films*”, 1st P2M Networking Conference- Precision Polymer Materials (European Science Foundation), Obernai (Strasbourg), France, 2011, **POSTER PRIZE AWARD**
4. **A. Jagoda**, S. Winkler, R. Hany, M. Zinn, W. Meier, K. Kita-Tokarczyk, “*Calcium phosphate mineralization beneath medium-chain-length polyhydroxyalkanoates monolayers*”; DCH- Dorothy Crowfoot Hodgkin Symposium, Zurich, Switzerland, 2011

5. **A. Jagoda**, M. Zinn, W. Meier, K. Kita-Tokarczyk, “*Interactions between medium-chain-length polyhydroxyalkanoates and lipids: a monolayer study*”, ESBP, European Symposium on Biopolymers, Dublin, Ireland, 2011
6. **A. Jagoda**, M. Zinn, W. Meier, K. Kita-Tokarczyk, “*Interactions between medium-chain-length polyhydroxyalkanoates and lipids: a monolayer study*”, Syngenta-Basel Symposium: Syngenta Crop Protection Research Chemistry- Department of Chemistry of the University of Basel, Basel, Switzerland, 2011
7. **A. Jagoda**, P. Ketikidis, M. Zinn, W. Meier, K. Kita-Tokarczyk, “*Polymer-inorganic composite materials for bone tissue engineering*”, ESF-EMBO Symposium: Biological Surfaces and Interfaces, Sant Feliu de Guixols, Spain, 2011
8. **A. Jagoda**, P. Ketikidis, M. Zinn, W. Meier, K. Kita-Tokarczyk, “*Polyhydroxyalkanoate monolayers as scaffolds for biomimetic mineralization*”, LB13, 13th International Conference on Organized Films, Quebec, Canada, 2010
9. **A. Jagoda**, J. Kapusta, K. Hac-Wydro, P. Wydro, “*The study of the interaction between plant sterols and phospholipid in mixed Langmuir monolayers*”, COST D43 Workshop Functional Interfaces- Theory and Experiment and SURUZ Workshop Surfactants and Dispersed Systems, Cracow, Poland, 2007
10. J. Kapusta, **A. Jagoda**, K. Hac-Wydro, “*The influence of a phospholipid structure on the interaction with nystatin in mixed Langmuir monolayers*”, COST D43 Workshop Functional Interfaces-Theory and Experiment and SURUZ Workshop Surfactants and Dispersed Systems, Cracow, Poland, 2007